Terrestrial Laser Scanning for Quantifying Uncertainty in Fluvial Applications

by

Jonathan P. Resop

Dissertation submitted to the faculty of the
Virginia Polytechnic Institute and State University
in partial fulfillment of the requirements for the degree of

Doctor of Philosophy

in

Biological Systems Engineering

W. Cully Hession, Chair
Conrad D. Heatwole
Phil J. Radtke
Teresa M. Wynn

June 18, 2010
Blacksburg, VA

Keywords: Terrestrial laser scanning, Uncertainty analysis, Streambank retreat, Habitat complexity, Stream restoration

Terrestrial Laser Scanning for Quantifying Uncertainty in Fluvial Applications
Jonathan P. Resop

Abstract

Stream morphology is an important aspect of many hydrological and ecological applications such as stream restoration design (SRD) and estimating sediment loads for total maximum daily load (TMDL) development. Surveying of stream morphology traditionally involves point measurement tools, such as total stations, or remote sensing technologies, such as aerial laser scanning (ALS), which have limitations in spatial resolution. Terrestrial laser scanning (TLS) can potentially offer improvements over other surveying methods by providing greater resolution and accuracy. The first two objectives were to quantify the measurement and interpolation errors from total station surveying using TLS as a reference dataset for two fluvial applications: 1) measuring streambank retreat (SBR) for sediment load calculations; and 2) measuring topography for habitat complexity quantification. The third objective was to apply knowledge uncertainties and stochastic variability to the application of SRD.

A streambank on Stroubles Creek in Blacksburg, VA was surveyed six times over two years to measure SBR. Both total station surveying and erosion pins overestimated total volumetric retreat compared to TLS by 32% and 17%, respectively. The error in SBR using traditional methods would be significant when extrapolating to reach-scale estimates of sediment load. TLS allowed for collecting topographic data over the entire streambank surface and provides small-scale measurements on the spatial variability of SBR.

The topography of a reach on the Staunton River in Shenandoah National Park, VA was measured to quantify habitat complexity. Total station surveying underestimated the volume of in-stream rocks by 55% compared to TLS. An algorithm was developed for delineating in-stream rocks from the TLS dataset. Complexity metrics, such as percent in-stream rock cover and cross-sectional heterogeneity, were derived and compared between both methods. TLS quantified habitat complexity in an automated, unbiased manner at a high spatial resolution.

Finally, a two-phase uncertainty analysis was performed with Monte Carlo Simulation (MCS) on a two-stage channel SRD for Stroubles Creek. Both knowledge errors (Manning's n and Shield's number) and natural stochasticity (bankfull discharge and grain size) were incorporated into the analysis. The uncertainty design solutions for possible channel dimensions varied over a range of one to four times the magnitude of the deterministic solution. The uncertainty inherent in SRD should be quantified and used to provide a range of design options and to quantify the level of risk in selected design outcomes.

Acknowledgements

My advisor, Cully

My committee, Tess, Phil, and Conrad

My graduate student peers, colleagues, and friends, Andrea, Jess, Candice, Leslie, Mike, etc.

My parents

My sister, Mary

My fiancée, Shannon

Myself, since I wrote this darn thing

All photos have been taken by the author, Jonathan Resop, except when noted otherwise.

Table of Contents

Abstract..... ii
Acknowledgements..... iii
Table of Contents..... iv
List of Figures..... v
List of Tables..... vii

1. Background..... 1
    Introduction and Problem Description..... 1
    Research Objectives..... 3
    Literature Review..... 4
    Summary..... 24
    Organization of the Dissertation..... 25
    References..... 26

2. Terrestrial Laser Scanning for Monitoring Streambank Retreat: A Comparison with Traditional Surveying Techniques..... 40

3. Terrestrial Laser Scanning for Quantifying Habitat and Hydraulic Complexity Measures: A Comparison with Traditional Surveying Techniques..... 53

4. Quantifying and Utilizing Uncertainty in Stream Restoration Design..... 78

5. Conclusions and Future Research..... 99

Appendices
A. Erosion Pin Streambank Retreat Measurements..... 103
B. MATLAB Code..... 105
C. Stream Restoration Design Input Parameter Distributions..... 121
D. Terrestrial Laser Scanning Streambank Retreat Measurements..... 127

List of Figures

1.1. Sources of uncertainty, adapted from Hession and Storm (2000)..... 11
1.2. Overview of the main factors that influence streambank retreat, adapted from VT Center for TMDL and Watershed Studies (2006)..... 16
2.1. Image of streambank showing locations of scan targets (T's) and cross sections (X's).... 43
2.2. Cross section 4 of the streambank measured by both total station surveying and TLS.... 46
2.3. TLS measured lateral change over the bank surface from 05/07 to 12/08 (the gap in the data at 8 m upstream is a result of the way the data was projected). (Note: Additional TLS-derived SBR images not included in publication are shown in Appendix D.)..... 48
3.1. The 100-m forested stream reach of the Staunton River in Virginia, USA. Photo by Jess Kozarek, used with permission..... 56
3.2. a) An example section of the Staunton River and b) the same section represented by a TLS point cloud. Photo by Jess Kozarek, used with permission..... 58
3.3. Flow chart summarizing the processes used for delineating in-stream rocks..... 61
3.4. An example rock represented by a) a TIN derived from total station data and b) a 2-cm TLS DEM..... 64
3.5. Overhead maps of HC 2 showing a) the 2-cm TLS DEM and b) individual delineated in-stream rocks. The white space in both figures represents the water surface..... 65
3.6. a) 2-D projected areas of example rocks measured from the both the total station survey and TLS delineation and b) comparison between projected rock areas for 34 individual rocks measured by both total station measurements and TLS delineation..... 66
3.7. Examples of various errors that occurred when delineating rock boundaries from TLS data: a) measurement error due to gaps in the dataset, b) false positives caused by too much delineation and c) false negatives caused by not enough delineation..... 67
3.8. The exponential distribution of in-stream rock size determined from the TLS delineation algorithm for the entire stream reach..... 70
3.9. Plan-view showing the spatial distribution of individual in-stream rocks (represented by different colors) delineated within each Habitat Complex (HC)..... 70
3.10. Example cross-section from HC 6 showing both the total station and TLS data..... 71
4.1. Site of stream restoration project at Stroubles Creek in Blacksburg, VA. Image taken from Virginia state orthophotos in 2006..... 81
4.2. Cross-section diagram illustrating the general layout of the two-stage channel design, adapted from NRCS (2007b)..... 82
4.3. Flowchart of the stream restoration design process, culminating with the design outcomes: width and depth. This process was applied to both channel stages in the two-stage design..... 84
4.4. The two-phase MCS uncertainty process separating stochastic variability and knowledge error resulting in a distribution of complementary cumulative distribution functions (CCDFs), adapted from Hession et al. (1996)..... 85
4.5. Distribution of CCDFs for the Qbfn channel dimensions of a) width and b) depth..... 89
4.6. Combined CCDFs for the Qbfn channel dimensions of a) width and b) depth..... 89
4.7. Histogram of median values from each CCDF curve, representing the uncertainty in stochastic variability, for the Qbfn channel dimensions of a) width and b) depth..... 90
4.8. Distribution of CCDFs for the Qbfu channel dimensions of a) bench width and b) bench flow depth. (Note: These results include only 10,000 simulations of MCS.)..... 91

4.9. Combined CCDFs for the Qbfu channel dimensions of a) bench width and b) bench flow depth..... 91
4.10. Histogram of median values from each CCDF curve, representing the uncertainty in stochastic variability, for the Qbfu channel dimensions of a) bench width and b) bench flow depth..... 92
C.1. Channel forming discharge distribution for the first stage..... 121
C.2. Manning's roughness n distribution for the first stage..... 122
C.3. Stream bed grain size distribution..... 123
C.4. Critical Shield's number or dimensionless shear stress number distribution..... 124
C.5. Floodplain discharge distribution for the second stage..... 125
C.6. Manning's roughness n distribution for the second stage..... 126
D.1. Streambank retreat measured with TLS from May 2007 to August 2007..... 127
D.2. Streambank retreat measured with TLS from August 2007 to December 2007..... 127
D.3. Streambank retreat measured with TLS from December 2007 to May 2008..... 127
D.4. Streambank retreat measured with TLS from May 2008 to December 2008..... 128
D.5. Streambank retreat measured with TLS from December 2008 to May 2009..... 128

List of Tables

1.1. Independent and dependent variables involved with stream restoration design (NRCS 2007a)..... 22
2.1. Number of topographic points measured by each method and the mean absolute point differences..... 45
2.2. Median SBR (m) at each cross section and overall volume change (m3) by both methods (Negative = Retreat)..... 47
3.1. Results of the sensitivity analysis showing the effect of the local minima filter on the rock delineation algorithm..... 68
3.2. Summary of the habitat complexity measures for each in-stream HC..... 69
3.3. Average cross-sectional measures of complexity within each HC calculated by both methods..... 71
4.1. Input parameters and associated distributions used for Monte Carlo Simulations. Histograms for each distribution can be found in Appendix C..... 87
4.2. The design solutions for channel dimensions based on the expected value of the input parameters..... 88
A.1. Measured SBR and volume change over the entire stream bank between May 2007 and May 2009 (Negative = Retreat)..... 104

Introduction and Problem Description

Computer modeling is a necessary tool for many hydrological, ecological, and geomorphological applications. Such applications include streambank erosion modeling for sediment loading calculations, hydraulic modeling for in-stream habitat characterization, water quality modeling for Total Maximum Daily Load (TMDL) development, and hydrologic, hydraulic, and geomorphic modeling for stream restoration design. Modeling is a general term that includes a wide variety of types, including analytical, empirical, numerical, and spatial. Conceptually most models can be described as a set of input data that is sent through the model structure and a set of parameters to produce a set of output values. This can be a powerful instrument for engineers for analyzing trends in data, comparing different scenarios, or making projections for a system's performance. For any model the output is an approximation of reality and there will be a magnitude of error in the prediction. When this error cannot be easily calculated due to the lack of observed data in the field, uncertainty analysis can be performed to quantify how unsure one is with the model results.

For many hydrological and ecological applications topography and stream morphology are influential factors to consider. It is common practice for many studies to use surveyed data for creating topographic surface models. With most surveying methods, such as total station surveying or aerial laser scanning (ALS), there is a limitation in the resolution and often an inadequate number of points are measured to represent the spatial variability of the surface. Interpolation is commonly used to generate complete digital surface models (DSMs) or digital elevation models (DEMs), leading to a degree of interpolation error. The combination of measurement error from the surveying device, as well as interpolation error from the DSM or DEM, can lead to a high amount of total error and a propagation of that error through the various models, creating uncertainty. If this uncertainty can be quantified, it could contribute to the overall effectiveness of hydrological and ecological models.

Due to the limitations of field point measurements and remote sensing, terrestrial laser scanning (TLS), also known as ground-based lidar, has been researched recently for topographic applications. This research will focus on applying TLS for the measurement of stream morphology. TLS is a form of active remote sensing that is portable and easily used in the field. The application of TLS is a rapidly growing area of research in the fields of forestry, natural

resources, and geomorphology. While the processing and analysis of TLS data can be complex and time intensive due to its large output dataset size, TLS provides a unique opportunity for high-resolution, accurate measurements of topography. The topographic measurements taken with TLS and the resulting DSMs or DEMs derived using TLS data have the potential to be used as reference datasets for quantifying the measurement and interpolation errors resulting from other surveying methods.

Research Objectives

The overall focus of this research is to apply TLS to measure stream morphology and to compare the technology with existing topographic surveying techniques. TLS has been utilized for two different fluvial applications: 1) measuring streambank retreat (SBR) for sediment load calculations; and 2) measuring complex stream topography for fish habitat modeling. In both studies, point measurements were taken using traditional total station surveying and TLS. The measurement and interpolation errors from the total station data were determined based on using TLS as a reference dataset. The propagation of these errors through calculations and models to estimate the uncertainty associated with reach-level sediment load calculations and habitat quantification was then explored. The final objective of this study was to apply knowledge uncertainties and stochastic variability to the engineering application of stream restoration design. In summary, the specific research objectives include:

1. Compare total station surveying and TLS for measuring streambank retreat, and quantify the resulting uncertainty in sediment load calculations due to errors in SBR measurements.

2. Compare total station surveying and TLS for measuring complex stream topography, and quantify the resulting uncertainty in habitat complexity measures due to errors in topographic modeling or measurements.

3. Apply knowledge errors and stochastic variability to a real stream restoration design problem to quantify uncertainty inherent in restoration design computations.

1.0 Literature Review

1.1 Topographic Surveying Technology

The ability to create DEMs from topographic surveys is an invaluable tool for most geomorphological, hydrological, and ecological applications involving fluvial systems. For example, measurements of stream reach topography can be used as input to hydraulic models for use in habitat analyses (Crowder and Diplas 2000; Kozarek In Press). Topographic measurements are also used in repeated surveys over time to detect changes in channel morphology and calculate sediment loading (Brasington et al. 2000; Chandler et al. 2002). There are many surveying tools and technologies that are commonly used in geomorphologic research. In general, these surveying technologies can be divided into two categories: 1) field-based point measurements; and 2) aerial-based remote sensing. Each method has strengths and limitations, mostly related to the balance between spatial coverage and resolution (Heritage and Hetherington 2007; Hetherington et al. 2007).

Field-based Surveying Methods

Point measurements taken in the field have long been the traditional method of surveying technology. Simple tools such as laser levels and electronic total stations have been used in fluvial studies for performing simple measurements such as longitudinal and cross-sectional stream profiles. For higher-density point measurements, newer technologies such as survey-grade global positioning systems (GPS) can be implemented (Brasington et al. 2000). For engineering applications requiring only a general measurement of the topography, point measurements can be an effective method. However, when small-scale measurements are needed, point measurements can be time consuming to collect in the field and can be affected by human bias (Heritage and Hetherington 2007). Due to the time commitment, individual point measurements of topography are generally limited in spatial resolution (Chandler et al. 2001). The combination of measurement errors from the surveying tool and interpolation errors from creating DEMs can lead to uncertainty when applying the topographic data to hydraulic models and fluvial applications (Milan et al. 2007).

Aerial-based Surveying Methods

Aerial surveying methods rely on a variety of remote sensing techniques. There are a wide range of technologies that fall under the category of remote sensing, generally classified as either passive systems (instruments that use reflected or emitted light, such as photography and multispectral imagery) or active systems (images that use their own source of light, such as radar or lidar) (Campbell 2007). When measuring topography, the end result for many of these surveying methods is a DEM or digital terrain model (DTM), although a degree of data post-processing is required. Remotely-sensed images from airplanes or satellites can cover a large area of interest, which makes them ideal tools for large-scale studies. However, the resolution of aerial-based remote sensing is generally limiting, making it difficult to detect small-scale changes in topography (Heritage and Hetherington 2007). Aerial photographs, processed with methods such as photogrammetry, have trouble deriving surface topography from densely vegetated areas (Campbell 2007). The scanning angle and distance above the earth make it difficult for aerial surveying to measure steep slopes and stream channels and in general the accuracy and precision of the instrument decreases as the complexity of the surface increases (Ruiz et al. 2004; Rosser et al. 2005; Campbell 2007).

1.2 Terrestrial Laser Scanning

TLS Remote Sensing Technology

TLS is a form of active remote sensing that uses similar technology as ALS. Both the aerial and terrestrial systems are also referred to as "light detection and ranging," or lidar (Campbell 2007). TLS works similarly to sonar or radar in that it emits a specific electromagnetic pulse wavelength and measures the time it takes that pulse to reflect off of a surface and return to the scanner, also known as the "time of flight," calculating the distance (Bellian et al. 2005). For the Optech ILRIS-3D used for this study, the wavelength is 1535 nm, located in the near-infrared (NIR) part of the spectrum (Optech 2010). The spatial resolution of the scanner is mostly based on two properties of the system: the step-spacing between pulses and the laser beamwidth, or footprint, of individual pulses (Lichti and Jamtsho 2006). The Optech scanner used for this study has a step-spacing of 0.026 * D mm and a laser beamwidth of 0.17 * D + 12 mm, where D is the distance from the scanner to the target in meters (Lichti 2004).

Since the laser scanner emits multiple light particles for each pulse, it can theoretically record multiple distances, or returns, for each pulse (Large and Heritage 2009). Depending on the scanner, it can either record many returns at equal time spacing and at a large scale (large-footprint, full waveform) or only a few returns at a small scale (small-footprint, discrete return) (Means 1999; Campbell 2007). While full waveform lidar provides a distribution of returns over a large area, small-footprint, discrete return lidar can produce a high-resolution topographic image (Means 1999). For example, in the area of forest resources, large-footprint ALS is used for calculating large-scale vertical canopy distribution (Lim et al. 2003) while small-footprint ALS is better suited for measuring individual trees (Clark et al. 2004). The Optech used for this study has a discrete return scanner, as are all current TLS systems, which returns either the first or last return (Heritage and Large 2009). The resulting output from TLS is a high-resolution 3-D point cloud of x-y-z spatial coordinates (Buckley et al. 2008).

Although based on similar technologies, the scanning methods used by ALS and TLS (scanning from an airplane and scanning from a tripod in the field, respectively) yield differences in the resulting topographic point cloud in terms of spatial coverage, accuracy, and precision. ALS is capable of spatial resolutions ranging from 10 to 200 points/m^2 with elevation errors between ±0.15 m (Charlton et al. 2009; Devereux and Amable 2009). While TLS is more limited than ALS in terms of scope, it can provide more accurate and more precise measurements, with resolutions ranging from 1,000 to 10,000 points/m^2 and errors less than ±0.02 m (Milan et al. 2007; Entwistle and Fuller 2009). TLS has the capability to create true 3-D DEMs, compared to the 2.5-D surface models commonly created from ALS (only one elevation per x-y coordinate) (Bellian et al. 2005; Buckley et al. 2008). The resolution of TLS has the potential to allow us to explore and measure micro-scale topography and habitat complexity that are important when studying ecological dynamics (Large and Heritage 2009).

TLS Applications in Geomorphology, Natural Resources and Fluvial Systems

Due to the potential for creating high-resolution topographic maps, TLS has been increasingly used in research for areas such as geomorphology, natural resources assessment, and fluvial morphology. In geomorphology, TLS has been utilized as a method of generating high-resolution surface models. TLS has been shown to be an objective tool for monitoring and quantifying landslides using repeated scanning (Rowlands et al. 2003; Bitelli et al. 2004; Teza et

al. 2008). Individual rock surfaces have been measured with TLS with resolutions ranging from 0.0004 m to 0.1 m (Alba et al. 2005; Bourke et al. 2008; Olariu et al. 2008). Nagihara et al. (2004) used TLS to map the topography a 50-m long sand dune with an average resolution of 0.01 m, reporting an accuracy of 0.006 m and noted the potential of using TLS for calculating erosion and deposition volume. Bellian et al. (2005) discussed the potential of using TLS for creating digital outcrop models (DOMs) from triangulated irregular networks (TINs) and the advantages the technology provided for geologists to quantify features in a reproducible manner.

In the fields of forestry and natural resources TLS has been increasingly utilized as a method for measuring and describing forest structure and canopy cover. After using TLS in the field, the data can be processed to create surface models such as DTMs and canopy height models (CHMs) (Henning and Radtke 2006b). TLS can be used to calculate features of natural environment, such as tree location, tree height, tree diameter, canopy gap fraction, and foliage-height profiles, which are normally difficult to measure manually in the field (Radtke and Bolstad 2001; Aschoff et al. 2004; Danson et al. 2007). The main potential advantage of TLS is its ability to capture a large amount of spatial data in an automatic, objective manner with minimal disturbance to the environment, although more work is needed to develop methodology for processing raw TLS data (Hopkinson et al. 2004; Van der Zande et al. 2006).

There has been increasing interest in applying TLS technology to fluvial systems, such as measuring streambanks, streambed composition, and stream morphology. The ability of TLS to produce mm-scale resolution topography has been recognized for its potential to measure complex stream morphology (Brasington and Richards 2007; Smith et al. 2007; Hodge 2010), although there has been limited research applying TLS to fluvial studies. The most expansive work so far has been performed by Heritage and Hetherington (2007) who surveyed a 150 m x 15 m gravel-cobble bed stream in North Yorkshire, England. The researchers used 21 scans taken over 2 days during a dry summer period to collect a total of 17 million points at 0.01 m resolution. They noted the possibility of using the resulting TLS surface model for advancing research in surface roughness calculation, channel hydraulic modeling, and stream morphology change measurement. At a smaller scale, Entwistle and Fuller (2009) and Milan (2009) have explored the use of TLS data for measuring dry streambed gravel size distribution and roughness for ecological and hydraulic applications, concluding the potential of TLS for making automatic

high-resolution topographic measurements while noting that more research still needs to be done on data mining and data processing.

TLS Limitations and Sources of Error

Although the strengths of TLS provide a great amount of potential for fluvial research, limitations for this technology have been noted in the literature. The limitations of TLS can be generally classified as field-based issues or data post-processing issues. A goal of any future research involving TLS should involve learning more about how one can minimize these limitations to increase the effectiveness of the technology for geomorphological applications.

In the field, ground-based laser scanners are instruments placed on a stationary device like a tripod and aimed towards the area of interest (Buckley et al. 2008). When scanning a large area that requires multiple scans, the location and angle of the scanner around the study site becomes an issue of concern. Many studies recommend taking multiple scans of each area of interest to reduce random errors from the scanner and increase accuracy by averaging values during processing (Heritage and Hetherington 2007; Hodge 2010). However, a balance is necessary because too many scans can increase the point cloud file size and make the data difficult to manage (Alba et al. 2005).

Since TLS relies on a direct line of site to measure surfaces, obstructions can create gaps in the point cloud, known as a shadowing effect (Heritage and Hetherington 2007). The best way to avoid shadowing effects is to take many scans from different angles around the area of interest and allow for data overlap (Iavarone and Vagners 2003; Hodge et al. 2009). In particular, vegetation can be a significant cause of shadowing, which can be an issue of concern for applications requiring "bare earth" surface models (Charlton et al. 2009). If it is not too dense, vegetation can generally be removed from the dataset manually or by using minimum elevations or last returns when creating surface models (Campbell 2007).

Surface reflectivity is another source for concern that arises when scanning natural environments, particularly water surfaces (Charlton et al. 2009; Hetherington 2009). TLS relies on electromagnetic radiation and it dependant on the reflectance properties of NIR wavelengths and the surfaces measured in the field. Highly reflective surfaces as well as atmospheric conditions can both adversely affect distance measurements (Hodge 2010). This is an important factor for fluvial applications due to the fact that TLS does not measure water-covered surfaces,

forcing most researchers to wait for dry conditions to measure complete stream topography (Heritage and Hetherington 2007). The issues with shadowing due to vegetation and water surfaces will likely continue to be a problem for fluvial environments with current TLS technology. Recent studies have implemented blue-green wavelength scanners for performing bathymetric surveys, although this technology is currently limited to ALS (Wedding et al. 2008).

Post-processing difficulties have been noted by several researchers (Heritage and Hetherington 2007; Buckley et al. 2008). Data size is commonly listed as an issue during processing, as TLS data files can get large and analysis can be limited to high-processing power computers (Iavarone and Vagners 2003; Bellian et al. 2005; Hodge et al. 2009). Editing datasets to remove extraneous points is typically performed manually, which can be time consuming and introduce bias. As a result, researchers tend to look for automated methods for converting raw data to DEMs.

If multiple scans are taken for a particular site, alignment or registration of all the scans into the same coordinate system is another issue of concern. Two common methods for aligning individual TLS scans include the use of targets, or ground control points (GCPs), in the field or the use of a best-fit or surface matching algorithm (Scaioni 2005). Using GCPs for aligning datasets can be effective as long as at least three GCPs are used in multiple planes (Schaefer and Inkpen 2010), although they add to the total field time and need careful placement consideration. Best-fit algorithms built-in to software such as PolyWorks (InnovMetric 2008) can accurately align scans as long as there is significant overlap between scans (10% overlap is recommended) (Bellian et al. 2005). However, the issue of propagation of error from aligning multiple scans together can be an issue and should be taken into consideration (Bellian et al. 2005). A combination of both methods is likely the best strategy to use for optimal accuracy.

Common methods for converting raw point clouds into DEMs involve interpolating the data to form complete surfaces. It would be ideal for more applications to convert TLS data into TINs can take advantage of the data's 3-D properties instead of relying on the 2.5-D nature of DEMs (Buckley et al. 2008). At this point, however, 2.5-D surface models are likely good enough for most ecological applications (Hodge et al. 2009). In general, methods need to be optimized for converting the massive amount of TLS data from raw point clouds to DEMs as well as analyzing the resulting surface models for various applications, particularly for applications involving fluvial systems (Campbell 2007; Large and Heritage 2009).

1.3 Uncertainty Analysis

Models play a large role in ability of engineers to make predictions, establish trends, or to create designs. In general, most models are deterministic, or mechanistic, in nature: a single set of input variables will produce a single output variable. However, many processes in nature tend to be more stochastic than deterministic, so that any number of values, based on a statistical distribution function, could be the outcome (Laurenson 1974; Tyagi and Haan 2001). Generalization, such as taking the average value for a system or parameter, is commonly performed in modeling to simplify stochastic processes to deterministic ones (Sohrabi et al. 2003; Shirmohammadi et al. 2006). Prediction error is defined as the difference between the output value of the model and the value observed in the field. Observed data is typically difficult to collect for many applications at the desired spatial and temporal resolution, making validation of model results challenging (Johnston 2003). It is inevitable that errors and generalizations from many different sources will propagate through the model, especially when many calculations and iterations are performed, increasing the uncertainty in the output (Kennard et al. 2009). Uncertainty analysis is a way to quantify a model's limitations and the level of confidence one has with a model's predictions. It has been described as a form of "intellectual honesty" (Sohrabi et al. 2002) or "modeling honesty" (Rejeski 1993).

Even though uncertainty analysis is not performed for many hydrological and ecological applications, there are many reasons why it is important to study. Uncertainty analysis can provide scientists a better understanding of the system being studied with a more accurate representation of reality. Once the sources of uncertainty for the model have been identified and quantified, researchers can investigate ways of reducing or managing the level of uncertainty in the model predictions. Another important outcome of uncertainty analysis is that it can aid in management practices such as decision making and risk assessment (Hession et al. 1996b; Sohrabi et al. 2003). Ultimately, uncertainty analysis can increase the value of a model's output values by providing the user with a range of values, or a confidence interval, rather than a single deterministic answer (Gertner 1987).

Sources of Uncertainty

Sources of model uncertainty can be divided into two main categories: 1) natural stochasticity; and 2) knowledge uncertainty (Fig. 1.1) (MacIntosh et al. 1994). Natural stochasticity is the variation, or heterogeneity, that exists for natural attributes in environmental systems. It includes the unexplained variation in both the spatial and temporal domain. For example, stream discharge may have a general trend or average value over a long period of time (baseflow), but the daily values of streamflow vary in a way that is difficult to explain with a model. Looking at natural stochasticity spatially, a parameter such as surface roughness can vary in all three spatial dimensions over the length of a stream reach. For this study, the focus will be on spatial variability rather than temporal variability.

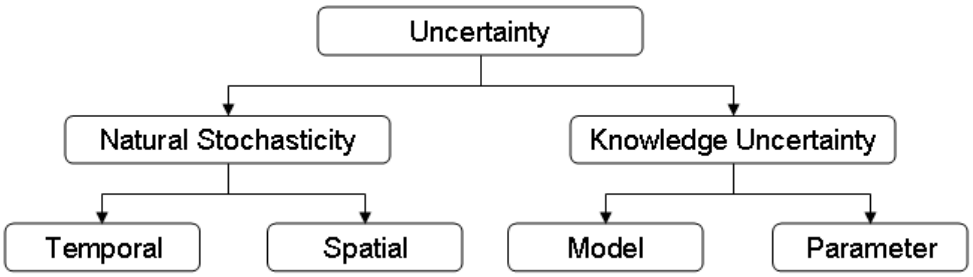

Figure 1.1. Sources of uncertainty, adapted from Hession and Storm (2000).

The other main type of model uncertainty is knowledge uncertainty. While natural stochasticity is a property of the system, knowledge uncertainty is a result of incomplete understanding of the system, and is produced by the modeler or analyst (Hession and Storm 2000). This type of uncertainty can be divided further into two main groups: error in the model structure and error in the measurement of parameters (Hession and Storm 2000). Model error is a result of the conceptual structure of the model and is due to our incomplete assumptions of the system or process being simulated. Parameter error is affected by many different factors in the field, such as sensor error, human error, measurement error, and interpolation error, and as a result can be difficult to estimate completely.

Methods of Uncertainty Analysis

Two common methods of uncertainty analysis are first-order approximation and Monte Carlo Simulation (MCS) (Tyagi and Haan 2001; Shirmohammadi et al. 2006). First-order

approximation involves defining uncertainty in terms of the variances of the input parameters (Haan and Zhang 1996). The input variances are propagated through to the output parameters using a first order Taylor series expansion of the model (Tyagi and Haan 2001). First-order approximation is useful for providing an estimate of output variance, although it is limited by assuming linearity in the system and is not practical for non-linear systems (Gardner et al. 1981).

MCS has been implemented for many hydrological, water quality and watershed models (Hession et al. 1996a; Shirmohammadi et al. 2006). MCS is a stochastic approach for estimating uncertainty that involves repeated simulations of randomly generated input values. First, the probability distribution functions (PDFs) of the input variables of interest are identified. Then, a specified number of random values are selected from these PDFs and the model is simulated for each set of inputs. Finally, the output values generated from the model iterations form the statistical distribution of the output variables. Many different variations of MCS have been studied and implemented. A two-stage MCS involves dividing the input variables into the two main categories of uncertainty (stochastic variability and knowledge error), whereby one can test the uncertainty of each type individually, one nested in the other (Hession et al. 1996a; Hession et al. 1996b). Another variation is latin hypercube sampling (LHS) (Shirmohammadi et al. 2006). This method is similar to traditional MCS, except instead of selecting n random value from the input variable PDF, the distribution is divided into n, equally-probability, non-overlapping intervals. Once divided, a random value is selected from each interval for simulation.

1.4 Spatial Analysis

In general, the connected structure of natural surfaces leads to inevitable correlation between spatial variables such as elevation. The level of autocorrelation is typically higher between close locations, due to the phenomenon of Waldo Tobler's First Law of Geography that states, "Everything is related to everything else, but near things are more related than distant things" (Longley et al. 2005). To quantify the amount of autocorrelation in a spatial area, a correlogram or semivariogram is often used, measuring the degree to which nearby spatial variables have similar values (O'Sullivan and Unwin 2003). In this way one can estimate the heterogeneity, or the level of complexity, of the surface that one wishes to represent. A common step for most research studies and projects is to use the measured data, along with a method of

interpolation, to create surface models to represent the study area, from which further analysis can be performed.

Spatial Interpolation

Interpolation is a method of defining a surface based on a set of measured data points, providing information in gap areas where no measured data are available. The result is a complete representation of the spatial variable over the study region, typically in the form of a DSM. The interpolated surface model can be used to provide a level of spatial detail necessary for many spatial models, such as estimating the topography of a watershed for calculating overland flow or predicting landslides. Interpolation methods can also be used to estimate the general trend and curves in a surface, which may not normally be apparent from the simple point data. In general, there are two main sources of uncertainty for DSMs: 1) the accuracy and resolution of the measured points used to create the surface model; and 2) the interpolation method implemented (Brasington et al. 2000; Wechsler 2007; Heritage et al. 2009). It is important for the modeler to understand the limitations of interpolation before applying DSMs to geomorphological applications. Ideally, one should calculate some measure of the uncertainty in the interpolated values generated to quantify the potential error that exists between the approximation and the true surface.

Uncertainty in Surface Models

An important step when using DSMs is evaluating the accuracy of the method, since each surveying and interpolation method has advantages and disadvantages. Interpolation error is highly dependent on the accuracy and resolution of the measured data (Heritage et al. 2009). The accuracy of the surface representation can also have dramatic effects on the output from any geomorphological models using the data as input, since errors from the DSM will propagate through topographic calculations to model outputs (Haile and Rientjes 2007; Wechsler 2007; Darnell et al. 2008). There are two methods used for quantifying interpolation error: 1) comparison to a higher-accuracy, independent dataset; and 2) the use of a cross-validation technique (Anderson et al. 2005).

One option is to compare the interpolated DSMs to a more accurate dataset. Darnell et al. (2008) tested the accuracy of DEMs created using interferometric synthetic aperture radar

(InSAR) data with ALS data as the "true" reference surface. The elevation difference between the interpolation method and the reference surface can be used to calculate an average error for the surface such as the root mean square error (RMSE). By comparing the RMSE value for multiple interpolation methods, one can determine which method produced the surface that most accurately matched the "true" surface. However, the task of assessing an interpolated grid using this method is made difficult due to the lack of accurate, "true-value" data to compare with the interpolation. There is promise in using TLS, a high-resolution and high-accuracy device, as a method for quantifying interpolation error (Heritage et al. 2009). Once laser scanning techniques become more mainstream, they will be invaluable for reducing the amount of uncertainty linked with coarse-resolution datasets (Shirmohammadi et al. 2006).

Another method for evaluating the accuracy of DSMs, particularly when accurate data for comparison are unavailable, is cross-validation (similar to another method known as jackknifing). Cross-validation involves omitting a subset of data from the measured dataset before performing interpolation on the remaining data to produce a DSM (Philips and Marks 1996). The omitted subset is then used as the reference data to evaluate the interpolation error. This method has been successfully used with ALS (Anderson et al. 2005; Smith et al. 2005), but has not yet been used for TLS-generated surface models. Since this method does not rely on a more accurate dataset, it is easy to apply for most applications. Another application of this method is to scale down the input data at multiple levels and evaluate the relationship between point density and DSM accuracy (Anderson et al. 2005; Smith et al. 2005).

Spatial Complexity, Variability, and Autocorrelation

Aside from using DSMs for representing spatial data, one can also investigate the degree of complexity or variability. Spatial complexity is a way to represent the heterogeneity or nonlinearity of a system (O'Sullivan and Unwin 2003). A measure of complexity is important when measuring topography, since the number of point measurements required to adequately define the surface is in general inversely proportional to the homogeneity of the surface (Fortin et al. 1989). Fractal dimensions can be used to quantify surface roughness and heterogeneity and measure spatial complexity, however, the results are difficult to verify and involve a degree of uncertainty depending on the method (Frost et al. 2005; Kostylev et al. 2005).

The variability of a system, in terms of the spatial patterns and relationships, can be quantified with spatial autocorrelation parameter (O'Sullivan and Unwin 2003). Correlation can be positive, indicating that there is high correlation between distance and similar values; negative, indicating that there is a pattern but close objects are usually dissimilar; or zero, indicating that there is no pattern and the data is essentially randomly distributed. Two metrics for calculating spatial autocorrelation are Moran's I and Geary's C (O'Sullivan and Unwin 2003). Moran's I ranges from -1 (negative correlation) to +1 (positive correlation), while Geary's C ranges from 0 (positive correlation) to 2 (negative correlation) (Fortin et al. 2002). These parameters can either be calculated as a scalar value for an entire area or as a function of distance to create a correlogram relating distance to correlation.

A semivariogram (also sometimes known as simply a variogram) is a measure of the difference (or variance) between spatial values at a series of distances (also known as lags) (O'Sullivan and Unwin 2003). The calculation for semivariance is similar to Geary's C value, in that both methods use the square of the differences, except that the semivariance is not bounded (Fortin et al. 2002). Plotting semivariance with respect to time yields a plot of points, known as a variogram cloud (O'Sullivan and Unwin 2003). The plot can then be generalized by fitting the data to a theoretical variogram equation, commonly represented by either a linear, exponential, or spherical model (Longley et al. 2005). Components of this graph include the nugget (the variance at distance equals zero), the sill (the maximum variance for the area) and the range (the distance at which maximum variance has been reached).

1.5 Streambank Retreat Measurement

A component of many geomorphological projects is measuring streambank retreat (SBR) and quantifying sediment transport. In fluvial applications, interest exists in being able to quantitatively measure these events with a high amount of both spatial and temporal resolution, as well as study the processes behind these phenomena (Lawler 2005; Milan et al. 2007; Bartley et al. 2008). SBR is a process that is affected by many different factors, including subaerial processes (climate-related events), fluvial entrainment (direct transport of soil material by stream flow) and mass failure caused by bank instability (Fig. 1.2) (Lawler 1992). The phenomenon of SBR is dependent on many complex processes in both the stream system and the watershed and so it is difficult to predict accurately (Evans et al. 2003). SBR rates are also challenging to

quantify with traditional methods, with measurements scarce and highly variable, ranging from 0 to 1100 m/yr (Simon et al. 2000). The measurement of SBR is used for applications such as developing sediment budgets for TMDLs and so it is important to quantify the uncertainties involved with sediment load calculations.

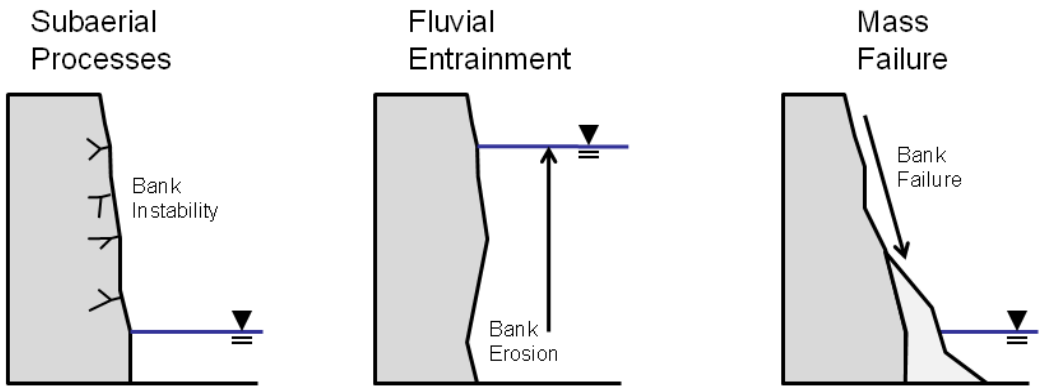

Figure 1.2. Overview of the main factors that influence streambank retreat, adapted from VT Center for TMDL and Watershed Studies (2006).

Traditional SBR Monitoring Methods

Traditional methods for monitoring SBR include erosion pin measurements or total station surveying (Lawler 1993). Both of these methods have qualities that are advantageous for researchers. Erosion pins can provide some spatial detail on streambank erosion and deposition and can also be installed relatively easily to long stream reaches, such as the 250-pin, 400-m reach of Stroubles Creek studied in Blacksburg, VA (Utley and Wynn 2008). Total station surveying can potentially collect topographic data on the streambed and opposing streambank, which can convey more information about local erosion and deposition dynamics (Bartley et al. 2008). Overall, both of these methods are simple and have well established methodologies, which make them ideal for many projects.

While point measurements from erosion pins or total station surveying are traditionally used, they have many limitations. Measuring topography with both methods can be time consuming, with large stream reaches potentially requiring days to measure (Heritage and Hetherington 2007). Not only is there a large amount of field time necessary, but the point spacing, or spatial resolution, of the measurements can be limiting for many applications (Nasermoaddeli and Pasche 2008). The installation of erosion pins and surveying with a total

station both involve direct physical measurement of the streambank, which can potentially disturb the streambank being studied and contribute to measurement error (Pyle et al. 1997). Another source of error is the fact that human judgment is needed when taking measurements, which can add bias to results (Lawler 1993). Erosion pins can also be lost in the field during long-term studies, negating any results from that pin during the study (Couper et al. 2002; DeWolfe et al. 2004). Point measurement techniques are also difficult to implement when measuring complex physical structures, such as undercut streambanks and boulder-filled streams. Due to the spatial limitations of erosion pins and total station surveying, many studies of SBR and erosion processes are only able to generalize an average retreat rate value for an entire streambank (Knighton 1973; Davis and Gregory 1994). Another method commonly used is to create a DEM with measured points and calculate the difference in DEMs (Brasington et al. 2003), which introduces interpolation error and is sensitive to the "quality" of the DEM (Brasington et al. 2000). Although these simple point measurement methods are commonly used, it is important to quantify the uncertainty associated with SBR and sediment load calculations due to measurement and interpolation errors.

Remote sensing technology is being applied more frequently for SBR measurement applications, particularly for large-scale studies. Rhoades et al. (2009) implemented aerial photography and ALS for estimating streambank erosion over a long time period (1937 to 2005), although such studies are limited by assumptions such as vertical banks. Thoma et al. (2005) used ALS for quantifying streambank erosion at a resolution of 1 to 3.3 points per m^2. However, ALS is still bound to the limitations discussed earlier, such as point density, vertical accuracy, and difficulties with measuring steep banks.

TLS for Monitoring SBR

As discussed previously, much of the literature in the area of landscape change detection involves calculating differences in DEMs over time to locate areas of erosion and deposition on a surface (Bitelli et al. 2004; Milan et al. 2007; Morche et al. 2008). A similar methodology has been applied to the study of SBR (Brasington et al. 2000; Lane et al. 2003), however most research has implemented surveying methods such as point measurements, photogrammetry, or ALS. Only recently has TLS been explored as a possible tool for measuring SBR, although so far most research has been at a relatively large scale, with average bank height ranging from 14 to

65 m and average spatial resolution between 0.03 and 0.1 m (Lim et al. 2005; Rosser et al. 2005; Collins and Sitar 2008). Rosser et al. (2005) and Nasermoaddeli and Pasche (2008) noted the potential for using TLS for recording undercut streambank surfaces and small-scale changes, which are difficult to measure with ALS. Pizzuto (2010) implemented TLS for monitoring SBR on smaller banks (2.5 m bank heights) with 0.05 m spatial resolution, and observed the potential of using TLS for measuring the spatial variability of SBR.

There are two main issues to overcome with TLS when measuring SBR: 1) the limitation of TLS for penetrating water surfaces and dense vegetation; and 2) transforming complex TLS point clouds of the streambank surface into DEMs (the method commonly used for topographic change detection). As a result of these issues, new methods must be investigated and evaluated for accurately monitoring SBR with TLS, particularly at small-scale resolutions. If TLS processing methodology can be established, then it has the potential to open up new areas of research, such as quantifying the uncertainty involved with traditional point measurement techniques by using TLS as a higher accuracy dataset.

Uncertainty in Sediment Load Calculations

In the United States, sediment is the second leading pollutant for impaired streams (USEPA 2002). As a result, it is critical to calculate sediment load accurately for TMDL development. The mass of sediment load into the stream due to SBR has been estimated from 31% to as high as 70 to 85% of total sediment loads (Trimble 1997; Simon et al. 2000; DeWolfe et al. 2004). Streambank sediment load can be calculated from various models, as well as from calculations combining SBR rates, stream dimensions and soil bulk density (Staley 2006). It is also possible to calculate sediment load as the change in volume from interpolated surfaces created with measured data (Thoma et al. 2005). Measurement and interpolation errors in streambank surface models can propagate through to calculations of volume change, adding uncertainty to the estimation of reach-scale sediment budgets (Brasington et al. 2000; Rumsby et al. 2008). TLS has been recognized for its potential for calculating highly accurate sediment load calculations and sediment budgets (Morche et al. 2008). Lane et al. (2003) demonstrated a method of estimating the propagated error from volume changes calculated from the difference in DEMs based on aerial photogrammetry and ALS and showed how this error compared with cross-section measurements taken at various longitudinal spacings. This method has the potential

to be applied to quantifying the uncertainty in TLS measurements of SBR and the comparison of this error to the spacing of point measurements from erosion pins or total station surveying.

1.6 Quantifying Habitat Complexity

Habitat complexity, based on the heterogeneity of the topography and vegetation in the system, has been recognized as an important factor for predicting species diversity in aquatic ecosystems (Gorman and Karr 1978). The term habitat complexity involves a wide range of phenomena important for aquatic organism dynamics and ecological processes, such as rock and vegetation cover providing habitat for fish (Marzolf 1978; Rankin 1989; Warren and Kraft 2003) and in-stream boulders influencing stream hydraulic complexity (Crowder and Diplas 2000; Shen and Diplas 2008). The importance of habitat complexity for species dynamics has be studied at multiple scales, ranging from macroinvertebrates, to amphibians such as salamanders, to larger organisms such as fish (Davic and Orr 1987; Beisel et al. 2000; Peckarsky et al. 2000; Venter et al. 2008).

One of the primary issues that researchers have had with studying habitat complexity is that it is difficult to measure quantitatively (Sanson et al. 1995; Downes et al. 2000). Ecological metrics such as the percent of the in-stream area covered by cobbles and boulders are typically estimated visually in the field (Wang et al. 1996; Kaufmann and Robison 1998; Willis et al. 2005) or only the dominant substrate type is recorded for an entire reach (Pearsons et al. 1992; Klaar et al. 2009). While hydraulic complexity measures, such as the flow vorticity around rocks and in-stream eddies, are important for characterizing habitat complexity at multiple scales (Crowder and Diplas 2006; Kozarek In Press), the hydraulic modeling and computational fluid dynamics (CFD) used to calculate these metrics can be challenging to perform and verify. Quantitative measures for habitat complexity metrics based on high-resolution spatial data have the potential to reduce the uncertainty associated with habitat modeling and would be useful for better understanding appropriate protocol for ecological and stream restoration designs.

Measures of Habitat Complexity

Indices that have been developed for evaluating habitat complexity typically include many different attributes of the fluvial system, such as cover from boulders and large woody debris (LWD), flow dynamics, and substrate diversity (Gorman and Karr 1978; Kaufmann and

Robison 1998; Kaufmann et al. 1999; Willis et al. 2005). In-stream boulders have been speculated to be a more dominant factor in aquatic species abundance compared to LWD, particularly for high-gradient streams (Hilderbrand et al. 1997; Warren and Kraft 2003). Peckarsky et al. (2000) found a positive relationship between protruding rocks and mayfly population dynamics. Crowder and Diplas (2000) showed that the presence of in-stream obstructions such as boulders can significantly influence hydraulic complexity, which affects habitat conditions. Most measures of in-stream boulders and structural complexity are quantified visually and generally the accuracy of visual estimates decreases as the heterogeneity of the system increases (Wang et al. 1996). Hydraulic complexity and CFD studies can be useful tools for characterizing habitat, however, currently most research is limited to topographic surveys generated from point measurements using only a few points to define each in-stream rock (Crowder and Diplas 2000; Shen and Diplas 2008).

Other metrics that have been shown to be important for habitat complexity characterization include surface roughness and structural heterogeneity. For example, Downes et al. (2000) studied the effect of rock surface roughness on macroinvertebrate species diversity, noting that species richness increased with roughness. In this study rock roughness was measured qualitatively. Lepori et al. (2005) related in-stream structural heterogeneity, based on a moving window of the topography, to species richness when comparing channelized to restored stream reaches. The researchers speculated that structural heterogeneity is an important and relevant factor for aquatic species diversity at multiple scales not directly studied, depending on the species. Another measure that has been studied with regards to structural complexity is the spatial autocorrelation of bed elevation (Madej 1999; Madej 2001).

Recently, researchers have been investigating the use of TLS for measuring stream complexity. Entwistle and Fuller (2009) used a 2-cm DEM of a dry stream bed to measure grain size distribution based on the standard deviation of elevations within a moving window. Milan (2009) estimated bed roughness with TLS data, using a similar moving window method, for input to hydraulic models. Hodge (2010) implemented TLS for measuring stream bed sediment with mm-scale resolution and explored the use of semivariograms for calculating spatial variability. More research is needed, however, to further develop methods of processing TLS data for quantifying complexity and explore the potential of high-resolution data for uncertainty analysis.

Delineating Natural Features from TLS Topographic Data

While there has not been much research in the area of extracting habitat complexity metrics from high-resolution topographic data for fluvial systems, there has been work done in the fields of forestry and natural resources. TLS has been used to automatically measure information such as individual tree location, height, and stem diameter (Hopkinson et al. 2004; Henning and Radtke 2006a). Another area of research has been in tree stand delineation, which has been performed using a variety of remote sensing techniques such as aerial photography and aerial lidar. Many different methods have been studied including image edge detection and local maxima to define tree tops (Wang et al. 2004), local minima to define valleys in between tree tops (Culvenor 2002), and image processing tools such as top-hat transformation (Andersen et al. 2001). The application of tree stand delineation can be viewed as similar to the task of delineating in-stream rocks from TLS-based surface models and could potentially be used to derive measures such as in-stream substrate distribution and rock cover from TLS data.

1.7 Stream Restoration Design and Uncertainty

Stream restoration is a growing field of research and application, with approximately $1 billion spent on various projects nationally (Bernhardt et al. 2005). The term "stream restoration" has been used, often incorrectly, to cover a wide variety of different types of project goals, ranging from ecological restoration and returning a stream to a natural state, to streambank stabilization and stream morphology manipulation (Kauffman et al. 1997; Shields et al. 2003). Once the goal of the stream restoration project has been defined, there are many methods for determining the restoration design, including regime, analogy, hydraulic geometry, extremal hypothesis, and analytical (NRCS 2007a). This research will focus on a two-stage stream restoration design using analytical methods and the associated uncertainty. A two-stage channel design is defined as one containing both a main channel as well as a floodplain channel, and is viewed to be more stable and ecologically beneficial than a traditional trapezoidal channel (NRCS 2007b).

Stream Restoration Design Variables and Equations

The basic principles of designing a stream channel stem from Lane's Balance, which relates stream discharge and longitudinal slope to sediment discharge (or bed material load) and median bed particle size (Lane 1955). These parameters work together to create a stream system that exists in a form of dynamic equilibrium, where a stream maintains its natural morphology over time (Shields et al. 2003). When looking at stream restoration for alluvial channels from the approach of a two-stage channel design, four dependant design variables must be determined: width, depth, longitudinal slope and planform (Table 1) (NRCS 2007a). The independent variables include the inflows of water and sediment and the composition of the streambed and streambanks (Table 1) (NRCS 2007a). To solve for the dependant variables, two equations commonly used are a hydraulic resistance equation, such as Manning's Equation, and a sediment transport equation, such as Shield's Equation (NRCS 2007a). The analytical design equations are then solved using the independent variables of the fluvial system measured in the field as well as the assumptions or criteria defined by the project goals.

Table 1.1. Independent and dependent variables involved with stream restoration design (NRCS 2007a).

Dependent Variables	Independent Variables
Width	Sediment Flow
Depth	Water Inflow
Slope	Bank Composition
Planform	Bed Composition

Sources of Uncertainty in Stream Restoration Design

When conducting a stream restoration design, there are many possible sources of error and uncertainty. Uncertainty exists even at the start of the restoration process, as many stream restoration projects have objectives that are poorly defined or that are qualitatively based, such as improving the ecological health of a fluvial system (Kondolf 1995; Kondolf 1996; Johnson and Brown 2001; Lemons and Victor 2008). All phases of the design process can be affected by uncertainty, including design implementation and long-term monitoring (Johnson and Brown 2001). Other general sources of uncertainty that can occur throughout a restoration project include communication between scientists and management, scientific bias, uncertainty in the restoration theory, and uncertainty in the research and design process (Graf 2008).

Uncertainty in stream restoration design can be classified (using the hierarchy from Fig. 1.1) into natural stochasticity (both spatial and temporal) and knowledge uncertainty (measurement error and model error) (Montgomery and Bolton 2003; Stewardson and Rutherfurd 2008; Wheaton et al. 2008). Similarly, Johnson and Brown (2001) characterize uncertainty as model uncertainty, parameter uncertainty, randomness and human error. Stewardson and Rutherfurd (2008) identified specific sources of error in the analytical design process, including sources of measurement error (cross section surveys, grain size measurement and determining the stage-discharge rating curve) and model error (values for Manning's n and Shield's parameter). Measurement errors, such as the variability in grain size measurements, arise during surveying and sampling in the field. Manning's n can be a difficult parameter to estimate since it varies depending on the stream discharge (Stewardson and Rutherfurd 2008). Likewise, Shield's parameter is dependent on many variables, such as armoring of the stream surface (Wilcock 2004).

One of the primary sources of measurement error in stream restoration design is determining the channel-forming discharge, one of the most important independent variables of channel design (NRCS 2007a). Channel-forming discharge is defined as the magnitude of discharge that dominates the natural channel morphology and processes (Shields et al. 2003). However, this phenomenon is difficult to measure quantitatively in the field. As a result, other similar measures of discharge are often used as surrogates for channel-forming discharge, such as effective discharge, bankfull discharge, and the discharge of some recurrence interval (such as two years) (Doyle et al. 2007). Measuring all of these values for a stream system will likely provide the user with a wide range of channel-forming discharge estimates. This variability, as well as the other uncertainties that have been identified for stream restoration design, need to be included in design equations to produce honest ranges of design variables. Such knowledge is critical for engineers to better understand what it means to create a natural channel and the variability that must be considered during design.

Summary

Based on a review of the literature, there are two main areas of research that need to be explored involving the use of terrestrial laser scanning in hydrological and ecological applications. First, more research is needed to optimize methodology and protocol for using TLS. This includes both methods in the field, and more importantly, automated processing algorithms to use once the data are collected. A new way of thinking is required for geomorphological, hydrological, and ecological applications to use the high-resolution, 3-D data provided by TLS in ways that maximize the advantages of the technology. Second, further research is needed to explore the use of TLS data as a potential high-accuracy, reference dataset. Surface data measured by TLS are as close to "real-life" measurements as currently possible with today's technology. The point clouds and DEMs generated by TLS could potentially be used to quantify the uncertainty associated with the measurement and interpolation errors from various topographic models and calculations used in the fields of hydrology and ecology. It is important for these errors, as well as others, to be further researched to quantify the uncertainty associated with engineering applications such as stream restoration design.

Organization of the Dissertation

This dissertation follows the journal article format. Three articles for publication in peer-reviewed journals follow the comprehensive literature review. Each article contains its own abstract, literature review, results, discussion and conclusion sections. The article contained in Chapter 2 has been submitted and accepted by the Journal of Hydraulic Engineering. Chapter 3 will be submitted to Ecohydrology, and Chapter 4 will be submitted to the Journal of the American Water Resources Association. The dissertation citation format follows that of the Journal of Hydraulic Engineering. Each article can stand alone on its own merit; however, when viewed together they provide a more complete picture of the role that uncertainty, due to sources such as measurement error, interpolation error, parameter error, model error, and spatial variability, plays in the outcome of hydrologic and ecologic modeling for fluvial applications.

Ch. 2 - Resop, J. P. and W. C. Hession. "Terrestrial Laser Scanning for Monitoring Streambank Retreat: A Comparison with Traditional Surveying Techniques." Journal of Hydraulic Engineering. (In Press). This manuscript is reused with permission from ASCE.

Ch. 3 - Resop, J. P., J. L. Kozarek, and W. C. Hession. "Terrestrial Laser Scanning for Quantifying Habitat and Hydraulic Complexity Measures: A Comparison with Traditional Surveying Techniques." Ecohydrology. (To Be Submitted).

Ch. 4 - Resop, J. P., W. C. Hession, and T. M. Wynn. "Quantifying and Utilizing Uncertainty in Stream Restoration Design." Journal of the American Water Resources Association. (To Be Submitted).

References

Alba, M., Longoni, L., Papini, M., Roncoroni, F., and Scaioni, M. (2005). "Feasibility and Problems of TLS in Modeling Rock Faces for Hazard Mapping." *ISPRS Workshop, Laser Scanning 2005*, Enschede, the Netherlands.

Andersen, H.-E., Reutebuch, S. E., and Schreuder, G. F. (2001). "Automated Individual Tree Measurement through Morphological Analysis of a LIDAR-based Canopy Surface Model." *Proceedings of the First International Precision Forestry Cooperative Symposium*, Seattle, WA, 11-22.

Anderson, E. S., Thompson, J. A., and Austin, R. E. (2005). "LIDAR Density and Linear Interpolator Effects on Elevation Estimates." *International Journal of Remote Sensing*, 26(18), 3889-3900.

Aschoff, T., Thies, M., and Spiecker, H. (2004). "Describing Forest Stands Using Terrestrial Laser-scanning." *International Archives of Photogrammetry, Remote Sensing and Spatial Information Sciences*, 35(B), 237-241.

Bartley, R., Keen, R. J., Hawdon, A. A., Hairsine, P. B., Disher, M. G., and Kinsey-Henderson, A. E. (2008). "Bank Erosion and Channel Width Change in a Tropical Catchment." *Earth Surface Processes and Landforms*, 33, 2174-2200.

Beisel, J.-N., Usseglio-Polatera, P., and Moreteau, J.-C. (2000). "The Spatial Heterogeneity of a River Bottom: A Key Factor Determining Macroinvertebrate Communities." *Hydrobiologia*, 422/423, 163-171.

Bellian, J. A., Kerans, C., and Jennette, D. C. (2005). "Digital Outcrop Models: Applications of Terrestrial Scanning LIDAR Technology in Stratigraphic Modeling." *Journal of Sedimentary Research*, 75(2), 166-176.

Bernhardt, E. S., Palmer, M. A., Allan, J. D., Alexander, G., Barnas, K., Brooks, S., Carr, J., Clayton, S., Dahm, C., Follstad-Shah, J., Galat, D., Gloss, S., Goodwin, P., Hart, D., Hassett, B., Jenkinson, R., Katz, S., Kondolf, G. M., Lake, P. S., Lave, R., Meyer, J. L., and O'Don, T. K. (2005). "Synthesizing U. S. River Restoration Efforts." *Science*, 308, 636-637.

Bitelli, G., Dubbini, M., and Zanutta, A. (2004). "Terrestrial Laser Scanning and Digital Photogrammetry Techniques to Monitor Landslide Bodies." *Proceedings of the XXth ISPRS Congress*, Istanbul, Turkey.

Bourke, M., Viles, H., Nicoli, J., Lyew-Ayee, P., Ghent, R., and Holmlund, J. (2008). "Innovative Applications of Laser Scanning and Rapid Prototype Printing to Rock Breakdown Experiments." *Earth Surface Processes and Landforms*, 10.1002/esp.1631, Letters to ESEX.

Brasington, J., Langham, J., and Rumsby, B. (2003). "Methodological Sensitivity of Morphometric Estimates of Coarse Fluvial Sediment Transport." *Geomorphology*, 53, 299-316.

Brasington, J., and Richards, K. (2007). "Reduced-complexity, Physically-based Geomorphological Modelling for Catchment and River Management." *Geomorphology*, 90, 171-177.

Brasington, J., Rumsby, B. T., and McVey, R. A. (2000). "Monitoring and Modelling Morphological Change in a Braided Gravel-bed River Using High Resolution GPS-based Survey." *Earth Surface Processes and Landforms*, 25, 973-990.

Buckley, S. J., Howell, J. A., Enge, H. D., and Kurz, T. H. (2008). "Terrestrial Laser Scanning in Geology: Data Acquisition, Processing and Accuracy Considerations." *Journal of the Geological Society, London*, 165, 625-638.

Campbell, J. B. (2007). *Introduction to Remote Sensing*, The Guilford Press, New York.

Chandler, J., Ashmore, P., Paola, C., Gooch, M., and Varkaris, F. (2002). "Monitoring River Channel Change Using Terrestrial Oblique Digital Imagery and Automated Digital Photogrammetry." *Annals of the Association of American Geographers*, 92(4), 631-644.

Chandler, J. H., Shiono, K., Rameshwaren, P., and Lane, S. N. (2001). "Measuring Flume Surfaces for Hydraulics Research Using a Kodak DCS460." *Photogrammetric Record*, 17(97), 39-61.

Charlton, M. E., Coveney, S. J., and McCarthy, T. (2009). "Issues in Laser Scanning." Laser Scanning for the Environmental Sciences, G. L. Heritage and A. R. G. Large, eds., Wiley-Blackwell, Chichester, 35-48.

Clark, M. L., Clark, D. B., and Roberts, D. A. (2004). "Small-footprint Lidar Estimation of Sub-canopy Elevation and Tree Height in a Tropical Rain Forest Landscape." *Remote Sensing of Environment*, 91, 68-89.

Collins, B. D., and Sitar, N. (2008). "Processes of Coastal Bluff Erosion in Weakly Lithified Sands, Pacifica, California, USA." *Geomorphology*, 97, 483-501.

Couper, P., Stott, T., and Maddock, I. (2002). "Insights into River Bank Erosion Processes Derived from Analysis of Negative Erosion-pin Recordings: Observations from Three Recent UK Studies." *Earth Surface Processes and Landforms*, 27, 59-79.

Crowder, D. W., and Diplas, P. (2000). "Using Two-dimensional Hydrodynamic Models at Scales of Ecological Importance." *Journal of Hydrology*, 230, 172-191.

Crowder, D. W., and Diplas, P. (2006). "Applying Spatial Hydraulic Principles to Quantify Stream Habitat." *River Research and Applications*, 22, 79-89.

Culvenor, D. S. (2002). "TIDA: An Algorithm for Delineation of Tree Crowns in High Spatial Resolution Remotely Sensed Imagery." *Computers & Geosciences*, 28, 33-44.

Danson, F. M., Hetherington, D., Morsdorf, F., Koetz, B., and Allgower, B. (2007). "Forest Canopy Gap Fraction From Terrestrial Laser Scanning." *IEEE Geoscience and Remote Sensing Letters*, 4(1), 157-160.

Darnell, A. R., Tate, N. J., and Brunsdon, C. (2008). "Improving User Assessment of Error Implications in Digital Elevation Models." *Computers, Environment and Urban Systems*, (In Press).

Davic, R. D., and Orr, L. P. (1987). "The Relationship Between Rock Density and Salamander Density in a Mountain Stream." *Herpetologica*, 43(3), 357-361.

Davis, R. J., and Gregory, K. J. (1994). "A New Distinct Mechanism of River Bank Erosion in a Forested Catchment." *Journal of Hydrology*, 157, 1-11.

Devereux, B., and Amable, G. (2009). "Airborne LiDAR: Instrumentation, Data Acquisition and Handling." Laser Scanning for the Environmental Sciences, G. L. Heritage and A. R. G. Large, eds., Wiley-Blackwell, Chichester, 102-114.

DeWolfe, M. N., Hession, W. C., and Watzin, M. C. (2004). "Sediment and Phosphorus Loads from Streambank Erosion in Vermont, USA." *Proceedings of World Water and Environmental Resources Congress 2004*, Salt Lake City, UT.

Downes, B. J., Lake, P. S., Schreiber, E. S. G., and Glaister, A. (2000). "Habitat Structure, Resources, and Diversity: The Separate Effects of Surface Roughness and Macroalgae on Stream Invertebrates." *Oecologia*, 123, 569-581.

Doyle, M., Shields, D., Boyd, K. F., Skidmore, P. B., and Dominick, D. (2007). "Channel-forming Discharge Selection in River Restoration Design." *Journal of Hydraulic Engineering*, 133(7), 831-837.

Entwistle, N. S., and Fuller, I. C. (2009). "Terrestrial Laser Scanning to Derive Surface Grain Size Facies Character of Gravel Bars." Laser Scanning for the Environmental Sciences, G. L. Heritage and A. R. G. Large, eds., Wiley-Blackwell, Chichester, 102-114.

Evans, B. M., Sheeder, S. A., and Lehning, D. W. (2003). "A Spatial Technique for Estimating Streambank Erosion Based on Watershed Characteristics." *Journal of Spatial Hydrology*, 3(1), 1-13.

Fortin, M., Dale, M., and Hoef, J. (2002). "Spatial Analysis in Ecology." Encyclopedia of Environmetrics, A. H. El-Shaarawi and W. P. Piegorsch, eds., John Wiley & Sons, Inc., Chichester, 2051-2058.

Fortin, M., Drapeau, P., and Legendre, P. (1989). "Spatial Autocorrelation and Sampling Design in Plant Ecology." *Vegetation*, 83, 209-222.

Frost, N. J., Burrows, M. T., Johnson, M. P., Hanley, M. E., and Hawkins, S. J. (2005). "Measuring Surface Complexity in Ecological Studies." *Limnology and Oceanography: Methods*, 3, 203-210.

Gardner, R. H., O'Neill, R. V., Mankin, J. B., and Carney, J. H. (1981). "A Comparison of Sensitivity Analysis and Error Analysis Based on a Stream Ecosystem Model." *Ecological Modeling*, 12, 173-190.

Gertner, G. (1987). "Approximating Precision in Simulation Projections: An Efficient Alternative to Monte Carlo Methods." *Forest Science*, 33(1), 230-239.

Gorman, O. T., and Karr, J. R. (1978). "Habitat Structure and Stream Fish Communities." *Ecology*, 59(3), 507-515.

Graf, W. L. (2008). "Sources of Uncertainty in River Restoration Research." River Restoration: Managing the Uncertainty in Restoring Physical Habitat, S. Darby and D. Sear, eds., John Wiley & Sons, Ltd., Chichester, 15-19.

Haan, C. T., and Zhang, J. (1996). "Impact of Uncertain Knowledge of Model Parameters on Estimated Runoff and Phosphorus Loads in the Lake Okeechobee Basin." *Transactions of the ASAE*, 39(2), 511-516.

Haile, A. T., and Rientjes, T. H. M. (2007). "Uncertainty issues in hydrodynamic flood modeling." *Proceedings of the 5th International symposium on Spatial Data Quality SDQ 2007, Modelling Qualities in Space and Time*, Enschede, The Netherlands.

Henning, J. G., and Radtke, P. J. (2006a). "Detailed Stem Measurements of Standing Trees from Ground-based Scanning Lidar." *Forest Science*, 52(1), 67-80.

Henning, J. G., and Radtke, P. J. (2006b). "Ground-based Laser Imaging for Assessing Three-dimensional Forest Canopy Structure." *Photogrammetric Engineering and Remote Sensing*, 72(12), 1349-1358.

Heritage, G., and Hetherington, D. (2007). "Towards a Protocol for Laser Scanning in Fluvial Geomorphology." *Earth Surface Processes and Landforms*, 32(1), 66-74.

Heritage, G., and Large, A. R. G. (2009). "Principles of 3D Laser Scanning." Laser Scanning for the Environmental Sciences, G. L. Heritage and A. R. G. Large, eds., Wiley-Blackwell, Chichester, 21-34.

Heritage, G. L., Milan, D. J., Large, A. R. G., and Fuller, I. C. (2009). "Influence of Survey Strategy and Interpolation Model on DEM Quality." *Geomorphology*, 112, 334-344.

Hession, W. C., and Storm, D. E. (2000). "Watershed-level Uncertainties: Implications for Phosphorus Management and Eutrophication." *Journal of Environmental Quality*, 29(4), 1172-1179.

Hession, W. C., Storm, D. E., and Haan, C. T. (1996a). "Two-phase Uncertainty Analysis: An Example Using the Universal Soil Loss Equation." *The Transactions of the ASAE*, 39(4), 1309-1319.

Hession, W. C., Storm, D. E., Haan, C. T., Reckhow, K. H., and Smolen, M. D. (1996b). "Risk Analysis of Total Maximum Daily Loads in an Uncertain Environment using EUTROMOD." *Journal of Lake and Reservoir Management*, 12(3), 331-347.

Hetherington, D. (2009). "Laser Scanning: Data Quality, Protocols and General Issues." Laser Scanning for the Environmental Sciences, G. L. Heritage and A. R. G. Large, eds., Wiley-Blackwell, Chichester, 82-101.

Hetherington, D., German, S., Utteridge, M., Cannon, D., Chisholm, N., and Tegzes, T. (2007). "Accurately Representing a Complex Estuarine Environment Using Terrestrial Lidar." *Remote Sensing and Photogrammetry Society Annual Conference*.

Hilderbrand, R. H., Lemly, A. D., Dolloff, C. A., and Harpster, K. L. (1997). "Effects of Large Woody Debris Placement on Stream Channels and Benthic Macroinvertebrates." *Canadian Journal of Fisheries and Aquatic Sciences*, 54, 931-939.

Hodge, R., Brasington, J., and Richards, K. (2009). "In Situ Characterization of Grain-scale Fluvial Morphology using Terrestrial Laser Scanning." *Earth Surface Processes and Landforms*, 34, 954-968.

Hodge, R. A. (2010). "Using Simulated Terrestrial Laser Scanning to Analyse Errors in High-resolution Scan Data of Irregular Surfaces." *ISPRS Journal of Photogrammetry and Remote Sensing*, 65, 227-240.

Hopkinson, C., Chasmer, L., Young-Pow, C., and Treitz, P. (2004). "Assessing Forest Metrics with a Ground-based Scanning Lidar." *Canadian Journal of Forest Restoration* 34, 573-583.

Iavarone, A., and Vagners, D. (2003). "Sensor Fusion: Generating 3D by Combining Airborne and Tripod-Mounted LIDAR data." *International Archives of the Photogrammetry, Remote Sensing and Spatial Information Sciences*, 34(5).

InnovMetric. (2008). "PolyWorks." Ver. 10.1.6, Quebec, Canada.

Johnson, P. A., and Brown, E. R. (2001). "Incorporating Uncertainty in the Design of Stream Channel Modifications." *Journal of the American Water Resources Association*, 37(5), 1225-1236.

Johnston, S. (2003). "Uncertainty in Bathymetric Surveys." *US Army Corps of Engineers*, ERDC/CHL CHETN-IV-59, 1-22.

Kauffman, J. B., Beschta, R. L., Otting, N., and Lytjen, D. (1997). "An Ecological Perspective of Riparian and Stream Restoration in the Western United States." *Fisheries*, 22, 12-24.

Kaufmann, P. R., Levine, P., Robison, E. G., Seeliger, C., and Peck, D. V. (1999). "Quantifying Physical Habitat in Wadeable Streams." *Field and Lab Manuals*, United States Environmental Protection Agency.

Kaufmann, P. R., and Robison, E. G. (1998). "Physical Habitat Characterization." *Environmental Monitoring and Assessment Program-Surface Waters: Field Operations and Methods for*

Measuring the Ecological Condition of Wadeable Streams, United States Environmental Protection Agency, Washington, D.C.

Kennard, M. J., Mackay, S. J., Pusey, B. J., Olden, J. D., and Marsh, N. (2009). "Quantifying Uncertainty in Estimation of Hydrologic Metrics for Ecohydrological Studies." *River Research and Applications*, 26(2), 137-156.

Klaar, M. J., Maddoc, I., and Milner, A. M. (2009). "The Development of Hydraulic and Geomorphic Complexity in Recently Formed Streams in Glacier Bay National Park, Alaska." *River Research and Applications*, 25, 1331-1338.

Knighton, A. D. (1973). "Riverbank Erosion in Relation to Streamflow Conditions, River Bollin-Dean, Cheshire." *East Midland Geographer*, 5, 416-426.

Kondolf, G. M. (1995). "Five Elements for Effective Evaluation of Stream Restoration." *Restoration Ecology*, 3(2), 133-136.

Kondolf, G. M. (1996). "A Cross Section of Stream Channel Restoration." *Journal of Soil and Water Conservation*, 51(2), 119-125.

Kostylev, V. E., Erlandsson, J., Ming, M. Y., and Williams, G. A. (2005). "The Relative Importance of Habitat Complexity and Surface Area in Assessing Biodiversity: Fractal Application on Rocky Shores." *Ecological Complexity*, 2, 272-286.

Kozarek, J. L., W. C. Hession, C. A. Dolloff, P. Diplas. (In Press). "Hydraulic Complexity Metrics for Evaluating In-stream Brook Trout Habitat." *Journal of Hydraulic Engineering*.

Lane, E. W. (1955). "Design of Stable Channels." *Transactions of the American Society of Civil Engineers*, 20, 1234-1279.

Lane, S. N., Westaway, R. M., and Hicks, D. M. (2003). "Estimation of Erosion and Deposition Volumes in a Large, Gravel-bed, Braided River Using Synoptic Remote Sensing." *Earth Surface Processes and Landforms*, 28, 249-271.

Large, A. R. G., and Heritage, G. L. (2009). "Laser Scanning." Laser Scanning for the Environmental Sciences, G. L. Heritage and A. R. G. Large, eds., Wiley-Blackwell, Chichester, 1-20.

Laurenson, E. M. (1974). "Modeling of Stochastic-deterministic Hydrologic Systems." *Water Resources Research*, 10(5), 955-961.

Lawler, D. M. (1992). "Process Dominance in Bank Erosion Systems." Lowland Floodplain Rivers: Geomorphological Perspectives, P. A. Carling and G. E. Petts, eds., Wiley, Chichester, 119-141.

Lawler, D. M. (1993). "The Measurement of River Bank Erosion and Lateral Channel Change: A Review." *Earth Surface Processes and Landforms*, 18, 777-821.

Lawler, D. M. (2005). "The Importance of High-resolution Monitoring in Erosion and Deposition Dynamics Studies: Examples from Estuarine and Fluvial Systems." *Geomorphology*, 64, 1-23.

Lemons, J., and Victor, R. (2008). "Uncertainty in River Restoration." River Restoration: Managing the Uncertainty in Restoring Physical Habitat, S. Darby and D. Sear, eds., John Wiley & Sons, Ltd., Chichester, 3-13.

Lepori, F., Palm, D., Brannas, E., and Malmqvist, B. (2005). "Does Restoration of Stuctural Heterogeneity in Streams Enhance Fish and Macroinvertebrate Diversity?" *Ecological Applications*, 15(6), 2060-2071.

Lichti, D. D. (2004). "A Resolution Measure for Terrestrial Laser Scanners." *Proceedings of the XXth ISPRS Congress*, Istanbul, Turkey, 216-221.

Lichti, D. D., and Jamtsho, S. (2006). "Angular Resolution of Terrestrial Laser Scanners." *The Photogrammetric Record*, 21(114), 141-160.

Lim, K., Treitz, P., Wulder, M., St-Onge, B., and Flood., M. (2003). "LiDAR Remote Sensing of Forest Structure." *Progress in Physical Geography*, 27(1), 88-106.

Lim, M., Petley, D. N., Rosser, N. J., Allison, R. J., and Long, A. J. (2005). "Combined Digital Photogrammetry and Time-of-flight Laser Scanning for Monitoring Cliff Evolution." *The Photogrammetric Record*, 20(110), 109-129.

Longley, P. A., Goodchild, M. F., Maguire, D. J., and Rhind, D. W. (2005). *Geographic Information Systems and Science*, John Wiley & Sons, Inc, Hoboken.

MacIntosh, D. L., II, G. W. S., and Hoffman, F. O. (1994). "Uses of Probablistic Exposure Models in Ecological Risk Assessments of Contaminated Sites." *Risk Analysis*, 14, 405-419.

Madej, M. A. (1999). "Temporal and Spatial Variability in Thalweg Profiles of a Gravel-bed River." *Earth Surface Processes and Landforms*, 24, 1153-1169.

Madej, M. A. (2001). "Development of Channel Organization and Roughness Following Sediment Pulses in Single-thread, Gravel Bed Rivers." *Water Resources Research*, 37(8), 2259-2272.

Marzolf, G. R. (1978). "The Potential Effects of Clearing and Snagging on Stream Ecosystems." Fish and Wildlife Service, United States Department of the Interior, Washington, D.C.

Means, J. E. (1999). "Design, Capabilities and Uses of Large-footprint and Small-footprint Lidar Systems." *International Archives of Photogrammetry and Remote Sensing*, 32(3-W14), 201-207.

Milan, D. J. (2009). "Terrestrial Laser Scan-derived Topographic and Roughness Data for Hydraulic Modelling of Gravel-bed Rivers." Laser Scanning for the Environmental Sciences, G. L. Heritage and A. R. G. Large, eds., Wiley-Blackwell, Chichester, 133-146.

Milan, D. J., Heritage, G. L., and Hetherington, D. (2007). "Application of a 3D Laser Scanner in the Assessment of Erosion and Deposition Volumes and Channel Change in a Proglacial River." *Earth Surface Processes and Landforms*, 32, 1657-1674.

Montgomery, D. R., and Bolton, S. M. (2003). "Hydrogeometric Variability and River Restoration." *American Fisheries Society*, 39-80.

Morche, D., Schmidt, K.-H., Sahling, I., Herkommer, M., and Kutschera, J. (2008). "Volume Changes of Alpine Sediment Stores in a State of Post-event Disequilibrium and the Implications for Downstream Hydrology and Bed Load Transport." *Norwegian Journal of Geography*, 62, 89-101.

Nagihara, S., Mulligan, K. R., and Xiong, W. (2004). "Use of a Three-dimensional Laser Scanner to Digitally Capture the Topography of Sand Dunes in High Spatial Resolutions." *Earth Surface Processes and Landforms*, 29(3), 391-398.

Nasermoaddeli, M. H., and Pasche, E. (2008). "Application of Terrestrial 3D Laser Scanner in Quantification of the Riverbank Erosion and Deposition." *International Conference on Fluvial Hydraulics, Riverflow 2008*, Izmir, Turkey.

NRCS. (2007a). "Alluvial Channel Design." *Part 654 Stream Restoration Design National Engineering Handbook, 210-VI-NEH*, United States Department of Agriculture.

NRCS. (2007b). "Two-stage Channel Design." *Part 654 Stream Restoration Design National Engineering Handbook, 210-VI-NEH*, United States Department of Agriculture.

O'Sullivan, D., and Unwin, D. J. (2003). *Geographic Information Systems*, John Wiley & Sons, Inc., Hoboken.

Olariu, M. I., Ferguson, J. F., Aiken, C. L. V., and Xu, X. (2008). "Outcrop Fracture Characterization using Terrestrial Laser Scanners: Deep-water Jackfork Sandstone at Big Rock Quarry, Arkansas." *Geosphere*, 4(1), 247-259.

Optech. (2010). "Technical Overview - ILRIS-3D Specifications." <http://www.optech.ca/i3dtechoverview-ilris.htm> Accessed March 2010.

Pearsons, T. N., Li, H. W., and Lamberti, G. A. (1992). "Influence of Habitat Complexity on Resistance to Flooding and Resilience of Stream Fish Assemblages." *Transactions of the American Fisheries Society*, 121, 427-436.

Peckarsky, B. L., Taylor, B. W., and Caudill, C. C. (2000). "Hydrologic and Behavioral Constraints on Oviposition of Stream Insects: Implications for Adult Disperal." *Oecologia*, 125, 186-200.

Philips, D. L., and Marks, D. G. (1996). "Spatial Uncertainty Analysis: Propagation of Interpolation Errors in Spatially Distributed Models." *Ecological Modeling*, 91, 213-229.

Pizzuto, J., O'Neal, M., and Stotts, S. (2010). "On the Retreat of Forested, Cohesive Riverbanks." *Geomorphology*, 116, 341-352.

Pyle, C. J., Richards, K. S., and Chandler, J. H. (1997). "Digital Photogrammetric Monitoring of River Bank Erosion." *Photogrammetric Record* 15(89), 753-764.

Radtke, P. J., and Bolstad, P. V. (2001). "Laser Point-Quadrat Sampling for Estimating Foliage-height Profiles in Broad-leaved Forests." *Canadian Journal of Forest Restoration*, 31, 410-418.

Rankin, E. T. (1989). "The Qualitative Habitat Evaluation Index (QHEI): Rationale, Methods and Application." Environmental Protection Agency, State of Ohio.

Rejeski, D. (1993). "GIS and Risk: A Three-culture Problem." Environmental Modeling with GIS, M. F. Goodchild, B. O. Parks, and L. T. Steyaert, eds., Oxford University Press, New York.

Rhoades, E. L., O'Neal, M. A., and Pizzuto, J. E. (2009). "Quantifying Bank Erosion on the South River from 1937 to 2005, and its Importance in Assessing Hg Contamination." *Applied Geography*, 29, 125-134.

Rosser, N. J., Petley, D. N., Lim, M., Dunning, S. A., and Allison, R. J. (2005). "Terrestrial Laser Scanning for Monitoring the Process of Hard Rock Coastal Cliff Erosion." *Quarterly Journal of Engineering Geology and Hydrogeology*, 38, 363-375.

Rowlands, K. A., Jones, L. D., and Whitworth, M. (2003). "Landslide Laser Scanning: A New Look at an Old Problem." *Quarterly Journal of Engineering Geology and Hydrogeology*, 36, 155-157.

Ruiz, A., Kornus, W., Talaya, J., and Colomer, J. L. (2004). "Terrestrial Modeling in an Extremely Steep Mountain: A Combination of Airborne and Terrestrial Lidar." *Proceedings of the XXth ISPRS Congress on Geo-Imagery Bridging Continents*, Istanbul, Turkey.

Rumsby, B. T., Brasington, J., Langham, J. A., McLelland, S. J., Middleton, R., and Rollinson, G. (2008). "Monitoring and Modelling Particle and Reach-scale Morphological Change in Gravel-bed Rivers: Applications and Challenges." *Geomorphology*, 93, 40-54.

Sanson, G. D., Stolk, R., and Downes, B. J. (1995). "A New Method for Characterizing Surface Roughness and Available Space in Biological Systems." *Functional Ecology*, 9(1), 127-135.

Scaioni, M. (2005). "Direct Georeferencing of TLS in Surveying of Complex Sites." *International Archives of the Photogrammetry, Remote Sensing and Spatial Information Sciences*, 36(5-W17).

Schaefer, M., and Inkpen, R. (2010). "Towards a Protocol for Laser Scanning of Rock Surfaces." *Earth Surface Processes and Landforms*, 35(4), 417-423.

Shen, Y., and Diplas, P. (2008). "Application of Two- and Three-dimensional Computational Fluid Dynamics Models to Complex Ecological Stream Flows." *Journal of Hydrology*, 348(1-2), 195-214.

Shields, F. D., Copeland, R. R., Klingeman, P. C., Doyle, M. W., and Simon, A. (2003). "Design for Stream Restoration." *Journal of Hydraulic Engineering*, 129(8), 575-584.

Shirmohammadi, A., Chaubey, I., Harmel, R. D., Bosch, D. D., Munoz-Carpena, R., Dharmasri, C., Sexton, A., Arabi, M., Wolfe, M. L., Frankenberger, J., Graff, C., and Sohrabi, T. M. (2006). "Uncertainty in TMDL Models." *Transactions of the ASABE*, 49(4), 1033-1049.

Simon, A., Curini, A., Darby, S. E., and Langendoen, E. J. (2000). "Bank and Near-bank Processes in an Incised Channel." *Geomorphology*, 35, 193-217.

Smith, M. W., Cox, N. J., and Bracken, L. J. (2007). "Applying Flow Resistance Equations to Overland Flows." *Progress in Physical Geography*, 31(4), 363-387.

Smith, S. L., Holland, D. A., and Longley, P. A. (2005). "The Importance of Understanding Error in Lidar Digital Eleveation Models." *International Archives of the Photogrammetry, Remote Sensing and Spatial Information Sciences*, 35, 996-1001.

Sohrabi, T. M., Shirmohammadi, A., Chu, T. W., Montas, H., and Nejadhashemi, A. P. (2003). "Uncertainty Analysis of Hydrologic and Water Quality Predictions for a Small Watershed Using SWAT2000." *Environmental Forensics*, 4, 229-238.

Sohrabi, T. M., Shirmohammadi, A., and Montas, H. (2002). "Uncertainty in Nonpoint Source Pollution Models and Associated Risks." *Environmental Forensics*, 3, 179-189.

Staley, N. A. (2006). "Modeling Channel Erosion at the Watershed Scale: A Comparison of GWLF, SWAT and AGNPS/CONCEPTS." *ASABE Annual International Meeting*, Portland, Oregon.

Stewardson, G. M., and Rutherfurd, I. (2008). "Conceptual and Mathematical Modelling in River Restoration: Do We Have Unreasonable Confidence?" River Restoration: Managing the Uncertainty in Restoring Physical Habitat, S. Darby and D. Sear, eds., John Wiley & Sons, Ltd., Chichester, 61-78.

Teza, G., Pesci, A., Genevois, R., and Galgaro, A. (2008). "Characterization of Landslide Ground Surface Kinematics from Terrestrial Laser Scanning and Strain Field Computation." *Geomorphology*, 97(2008), 424-437.

Thoma, D. P., Gupta, S. C., Bauer, M. E., and Kirchoff, C. E. (2005). "Airborne Laser Scanning for Riverbank Erosion Assessment." *Remote Sensing of Environment*, 95, 493-501.

Trimble, S. W. (1997). "Contribution of Stream Channel Erosion to Sediment Yield from an Urbanizing Watershed." *Science*, 278, 1442-1444.

Tyagi, A., and Haan, C. T. (2001). "Uncertainty Analysis using Corrected First-order Approximation Method." *Water Resources Research*, 37(6), 1847-1858.

USEPA. (2002). "Rivers and Streams." *2000 National Water Quality Inventory, USEPA-841-F-02-003*, United States Environmental Protection Agency, Office of Water, Washington, D.C.

Utley, B. C., and Wynn, T. M. (2008). "Spatial and Temporal Changes in Bank Retreat Rates in a Small Headwater Stream." *American Geophysical Union*, Fall Meeting.

Van der Zande, D., Hoet, W., Jonckheer, I., Aardt, J. v., and Coppin, P. (2006). "Influence of Measurement Set-up of Ground-based LiDAR for Derivation of Tree Structure." *Agricultural and Forest Meteorology*, 141, 147-160.

Venter, O., Grant, J. W. A., Noel, M. V., and Kim, J. (2008). "Mechanisms Underlying the Increase in Young-of-the-year Atlantic Salmon (Salmo salar) Density with Habitat Complexity." *Canadian Journal of Fisheries and Aquatic Sciences*, 65, 1956-1964.

VT Center for TMDL and Watershed Studies. (2006). "Streambank Retreat." <http://www.tmdl.bse.vt.edu/stream_restoration/C117/> Accessed May 2010.

Wang, L., Gong, P., and Biging, G. S. (2004). "Individual Tree-crown Delineation and Treetop Detection in High-spatial-resolution Aerial Imagery." *Photogrammetric Engineering & Remote Sensing*, 70(3), 351-357.

Wang, L., Simonson, T. D., and Lyons, J. (1996). "Accuracy and Precision of Selected Stream Habitat Estimates." *North American Journal of Fisheries Management*, 16, 340-347.

Warren, D. R., and Kraft, C. E. (2003). "Brook Trout (Salvelinus fontinalis) Response to Wood Removal from High-gradient Streams of the Adirondack Mountains (NY, USA)." *Canadian Journal of Fisheries and Aquatic Sciences*, 60, 379-389.

Wechsler, S. P. (2007). "Uncertainties Associated with Digital Elevation Models for Hydrologic Applications: A Review." *Hydrology and Earth System Sciences*, 11, 1481-1500.

Wedding, L. M., Friedlander, A. M., McGranaghan, M., Yost, R. S., and Monaco, M. E. (2008). "Using Bathymetric Lidar to Define Nearshore Benthic Habitat Complexity: Implications for Management of Reef Fish Assemblages in Hawaii." *Remote Sensing of Environment*, 112, 4159-4165.

Wheaton, J. M., Darby, S. E., and Sear, D. A. (2008). "The Scope of Uncertainties in River Restoration." River Restoration: Managing the Uncertainty in Restoring Physical Habitat, S. Darby and D. Sear, eds., John Wiley & Sons, Ltd., Chichester, 21-39.

Wilcock, P. R. (2004). "Sediment Transport in the Restoration of Gravel-bed Rivers." *Proceedings of the 2004 ASCE-EWRI World Water and Environmental Resources Congress, Critical Transactions in Water and Environmental Resource Management*, Salt Lake City, Utah, 1-11.

Willis, S. C., Winemiller, K. O., and Lopez-Fernandez, H. (2005). "Habitat Structural Complexity and Morphological Diversity of Fish Assemblages in a Neotropical Floodplain River." *Oecologia*, 142, 284-295.

2.0 Terrestrial Laser Scanning for Monitoring Streambank Retreat: A Comparison with Traditional Surveying Techniques

Jonathan P. Resop and W. Cully Hession

Abstract

Data concerning streambank retreat (SBR) rates are important for many different engineering applications such as stream restoration and Total Maximum Daily Load (TMDL) development. However, measurement of SBR can be time consuming and is often characterized by large measurement and interpolation errors. These errors propagate into the calculation of sediment budgets for the development of TMDLs, creating uncertainty in source partitioning and overall load estimates. We compared two techniques for measuring SBR: 1) traditional surveying with a total station; and 2) terrestrial laser scanning (TLS). An 11-m streambank on Stroubles Creek in Blacksburg, VA was surveyed six times over a two-year period. The average SBR along the entire bank was estimated to be -0.15 m/yr with TLS and -0.18 m/yr with total station surveying. The resulting differences in median SBR estimates along five distinct cross sections between each of the survey dates ranged from -0.11 to +0.06 m. This error in SBR due to total station surveying would be significant when extrapolating to a reach- or watershed-scale estimate of sediment load due to SBR. In addition, TLS collects data across the entire streambank surface, rather than just at distinct cross sections, providing much more information concerning SBR volumes and spatial variability.

Keywords

Streambank retreat, Terrestrial laser scanning, Remote sensing, Bank retreat monitoring, Topographic surveys, Uncertainty principles

Manuscript Note

This manuscript is in press for the Journal of Hydraulic Engineering. This manuscript is reused with permission from ASCE.

The erosion pin analysis was not complete in time for publication. The results are included in Appendix A.

2.1 Introduction

Stream morphology is measured for many hydraulic applications such as flood routing, habitat modeling and sediment load estimation, as well as larger engineering projects such as stream restoration and Total Maximum Daily Load (TMDL) development. These projects have significant economic impacts, with approximately $1 billion spent annually on stream restoration (Bernhardt et al. 2005) and $16 billion spent on sediment damages (Osterkamp et al. 1998). Fluvial applications rely on effective surveying of stream morphology for engineers to produce cross-section profiles or 3-D topographic models. Traditionally, the measurement of topography is performed by manual point surveying with laser levels or electronic total stations. However, these methods are limited by time-intensive field surveys, spatial resolution restrictions, and difficulties in surveying complex morphology such as undercut banks.

We applied ground-based lidar (Light Detection and Ranging), also known as terrestrial laser scanning (TLS), to measure streambank retreat (SBR). SBR is a process affected by many different factors, including subaerial processes (climate-related events), fluvial entrainment (direct transport of soil material by stream flow), and mass failure (caused by bank instability) (Lawler 1992). Traditional methods for measuring this phenomenon, such as erosion pins and total station surveying, have limitations in point resolution and can be affected by sensor error and operator bias (Lawler 1993). In addition, both erosion pins and total station surveying can result in direct, physical disturbance of the streambanks being measured (Pyle et al. 1997). Aerial photography has also been used for measuring SBR (Winterbottom and Gilvear 2000; Rhoades et al. 2009), but is limited by photogrammetric errors and assumptions such as vertical banks.

Along with measurement error, interpolation and generalization influence how SBR data and erosion rates are represented. It is common for many applications to use point measurements for calculating an average SBR rate (Knighton 1973; Davis and Gregory 1994), which loses information pertaining to the spatial variability of SBR. Studies have calculated SBR using the difference in repeated stream cross-sectional surveys (Agouridis et al. 2005) and the change in 3-D surface models created from point measurements (Brasington et al. 2003). The combination of measurement error, interpolation error and spatial generalization can lead to a high amount of total error. Propagation of these errors can result in extensive output uncertainty in geomorphologic and hydraulic models. In most applications involving average SBR rates and

sediment load estimation, the amount of uncertainty and variability in estimates are not adequately quantified (Green et al. 1999; Laubel et al. 1999; Lawler et al. 1999).

The use of TLS for measuring stream morphology is still in its early stages of research. TLS for geomorphologic applications have ranged in scope from measuring individual rock breakdown (Bourke et al. 2008) to monitoring landslides (Bitelli et al. 2004; Hsiao et al. 2004; Teza et al. 2008). Most TLS research to date has involved calculating the difference in digital elevation models (DEMs) over time to detect change. There has been some research involving TLS for measuring erosion from streambanks and coastal cliffs at a relatively large scale (bank heights ranging from 14 to 65 m and resolutions ranging from 0.03 to 0.1 m) (Lim et al. 2005; Rosser et al. 2005; Collins and Sitar 2008). The potential, however, for using TLS for recording undercut banks and small-scale changes has been noted by Rosser et al. (2005). Heritage and Hetherington (2007) used TLS to scan a 150-m stream reach at 0.01 m resolution. When the data were compared to 257 independent survey points, they found a mean error of 0.004 m with a standard deviation of 0.17 m and 55% of the survey data within ±0.02 m of the TLS data.

The objectives of this study were: 1) to compare the measurements of traditional total station surveying and TLS for monitoring SBR in a small stream with little riparian vegetation and complex, undercut banks; and 2) to make observations about the measurement and interpolation error of traditional surveying. TLS provides a means of estimating the error associated with measuring SBR with point measurements by using it as a reference dataset.

2.2 Methods

Study Site

The study was conducted on a streambank along Stroubles Creek located downstream of Virginia Tech's main campus in Blacksburg, VA. Stroubles Creek has been identified as an impaired stream with both urban and agricultural impacts (Benham et al. 2003) and is currently undergoing a TMDL implementation plan for reducing sediment loads (Yagow et al. 2006). It is a gravel-bed stream with cohesive banks ranging in height from 1.0 to 1.3 m and an average baseflow depth of 0.2 m (Wynn et al. 2008). The stream reach has a watershed drainage area of approximately 17.1 km^2 and is located in a pasture with dairy cattle access. The bank face is bare with little vegetation and is undercut along much of its length (Fig. 2.1). Topographic measurements were taken along the 11-m streambank on six dates between May 2007 and May

2009. Two different surveying methods were used, surveying with an electronic total station and TLS. Both methods were used on the same day each time, first using TLS and then the total station.

Figure 2.1. Image of streambank showing locations of scan targets (T's) and cross sections (X's).

Field Methods

Total station surveying was performed using a Leica TC 307. Five cross sections were measured over the length of the streambank (Fig. 2.1). Points were surveyed on both sides of the stream focusing on slope breaks. On average, five points were measured at each cross section on the target eroding streambank, or one point every 0.25 m change in elevation over the 1-m tall streambank. Along each cross section, points were measured at the top of bank, the edge of water, and the location of existing erosion pins, which also acted to spatially align the repeated cross sections over time. The erosion pins were installed as part of a separate study.

The ground-based laser scanner used for this study was an Optech ILRIS-3D. This is a non-panning system with a 40° field of view. Three scans were taken of the target streambank from three different locations on the opposite bank ranging 6 to 10 m from the target bank. The average point spacing on the target bank was 1 cm. Both first and last returns were measured to limit the effect of shading due to vegetation on the streambanks. The scanner has a footprint diameter of 13.7 mm at a distance of 10 m (based on a beam divergence of 0.00974°) and an accuracy of 7 to 8 mm at 100 m (Lichti and Jamtsho 2006; Optech 2009).

Permanent references using 0.6-m rebar were placed into the ground for spatial alignment over time. For the total station measurements, the top of each rebar was surveyed. For TLS, 0.3-m square metal plates placed on the rebar were used as scanner targets (Fig. 2.1).

Data Analysis

The total station data were processed by converting the easting, northing, and elevation values to distance from the total station and elevation. The TLS scans for a particular study date were aligned together using the IMAlign tool in InnovMetric PolyWorks, which has an iterative algorithm that best-fits the point clouds to within a mean error of ±0.0001 m. The point clouds for different study dates were then aligned using reference points selected from the three scan targets (the stationary metal plates). After alignment, the data were manually edited to remove vegetation. The points between the top of bank and the edge of water were then exported into MATLAB for further analysis.

Three metrics were used to measure the differences between the total station and TLS data: 1) individual point differences; 2) median SBR at each cross section; and 3) volume change over the entire streambank surface. The first metric was calculated for each of the six survey dates by comparing the total station and TLS data from individual dates. The second and third metrics were calculated using differences in surveys between each of the six survey dates (where negative change represents SBR).

Individual point differences were determined by first aligning the survey and TLS data for each study date manually in IMAlign using the benchmarks and targets. The point differences between each of the survey points and the TLS point cloud were calculated using the IMInspect tool in PolyWorks that identified the closest point in the TLS data to each survey point and calculated the point-to-point distance.

For the total station surveys, median SBR was calculated by interpolating every 2 cm from the top of bank to the edge of water, and determining the lateral change between cross sections. Volume change was calculated from the total station datasets as the weighted average of cross-sectional area change multiplied by the overall bank length.

For TLS, the data were first divided into two sections (to minimize error due to the curvature of the stream). Both sections were projected to a plane behind the bank surface (parallel to streamflow). The points were then converted to a 2-cm DEM with respect to the two

planes by taking the minimum point-to-plane distance within each cell (to filter out vegetation). SBR was then calculated as the change in DEMs over time. Volume change was calculated numerically as the SBR at each 2-cm grid cell over the entire bank area.

2.3 Results

Individual Point Differences

Over the six study dates, a total of 152 points were measured with the total station compared with 755,709 points with TLS. Using TLS in the field was faster than the total station and did not physically disturb the topography of the bank. While post-processing the TLS data presented a challenge due to its size and complexity, with proper alignment software and high-speed computers the post-processing time of both datasets was comparable. The mean absolute point difference between the two methods was 0.018 m with a standard deviation of 0.020 m and 63% of survey points within ±0.02 m of the TLS data. The number of points for each method and the point differences for each study date are shown in Table 2.1.

Table 2.1. Number of topographic points measured by each method and the mean absolute point differences.

	05/07	08/07	12/07	05/08	12/08	05/09
Survey Points	23	24	25	27	28	25
TLS Points	360,042	40,339	52,328	96,175	105,806	101,019
Mean Abs. Diff. (m)	0.017	0.015	0.016	0.020	0.024	0.014

An example cross section is shown in Fig. 2.2 comparing the topographic measurements from both methods. The total station measurements were fairly accurate where points were surveyed and in general they captured the trend of the cross-section topography (Fig. 2.2). The higher-resolution TLS provided a more accurate and complete measurement of streambank topography. The difference between the cross sections measured by both methods illustrates the interpolation error inherent in taking limited point measurements.

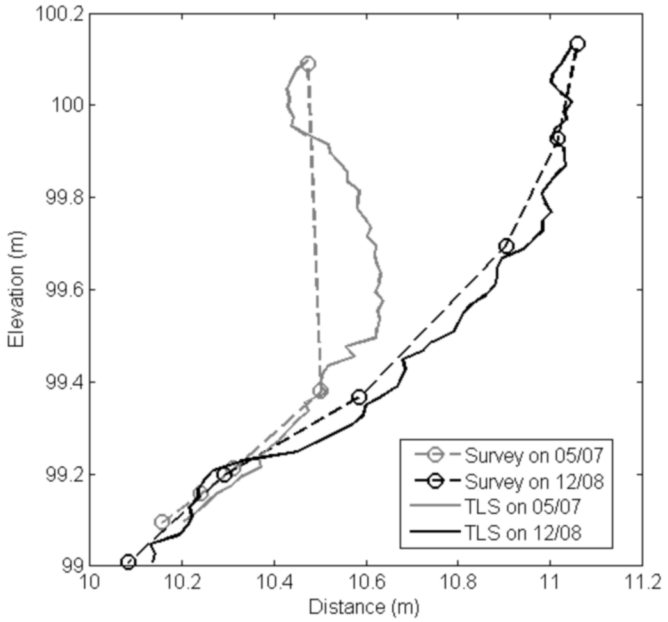

Figure 2.2. Cross section 4 of the streambank measured by both total station surveying and TLS.

Cross-sectional SBR

The median cross-sectional SBR values between each of the survey dates from both total station surveying and TLS are shown in Table 2.2. There was positive correlation between the median SBR for both methods (r = 0.81), indicating general agreement. The difference between surveying and TLS calculations of median SBR at individual cross sections ranged from -0.11 to +0.06 m or 0 to 3,000% relative to TLS with a mean relative error of 248%. Only 12 of the 25 median SBR measurements had relative errors less than 50%. Over the two-year study the relative error between surveying and TLS for measuring median SBR at each cross section ranged from 12 to 157% with a mean of 49%. The average SBR per year over the entire bank was -0.18 and -0.15 m/yr from surveying and TLS respectively, a relative error of 20% compared to TLS. The relative errors show that while there is a large variability of SBR error between two surveys, as expected the error decreases as the measurement time increases and more surveys are performed.

Table 2.2. Median SBR (m) at each cross section and overall volume change (m^3) by both methods (Negative = Retreat).

Cross Section	05/07 to 08/07		08/07 to 12/07		12/07 to 05/08		05/08 to 12/08		12/08 to 05/09	
	Median SBR (m)									
	Surv.	TLS	Surv.	TLS	Surv.	TLS	Surv.	TLS	Surv.	TLS
1	-0.03	0.00	-0.03	-0.07	-0.06	-0.12	0.00	0.02	-0.13	-0.12
2	0.01	0.02	-0.11	-0.13	-0.15	-0.13	0.03	0.01	-0.13	-0.17
3	-0.12	-0.02	0.04	-0.02	-0.13	-0.13	0.00	0.01	-0.19	-0.17
4	-0.11	0.00	-0.03	-0.05	-0.17	-0.16	0.00	0.00	-0.13	-0.11
5	-0.01	0.02	0.00	-0.02	-0.15	-0.11	-0.03	-0.03	-0.01	0.06
	Volume Change (m^3)									
	Surv.	TLS	Surv.	TLS	Surv.	TLS	Surv.	TLS	Surv.	TLS
	-0.71	0.26	-0.33	-0.42	-1.71	-1.92	-0.06	0.17	-1.38	-1.29

Volume Change

The volume changes for each method between the six study dates are provided in Table 2.2 (negative represents erosion). The difference between surveying and TLS ranged from 7 to 373% of the total erosion measured by TLS with a mean of 109%. The average yearly erosion rate was measured to be -2.1 and -1.6 m^3/yr by surveying and TLS respectively, a relative error of 31% compared to TLS. The relative error in volume was slightly more than the relative error for average SBR (20%), likely since errors are added over the bank face when calculating volumes rather than averaged as in the case with cross-sectional SBR rates. The largest error occurred during the first two survey dates, likely due to the total station being unable to measure a section of the bank that was deeply undercut during the first survey date (Fig. 2.2), resulting in an overestimation of erosion. Aside from cases such as this where an undercut bank results in less erosion measured by TLS, there does not seem to be a systematic difference between the results of the two methods. The rest of the difference between the two methods was likely the result of the higher spatial resolution of TLS (about 4,400 times that of surveying in this study).

2.4 Discussion

One of the advantages of TLS data over total station point data is that much more information can be learned about the spatial variability of SBR. Total station surveying is limited to calculating the average SBR value for an entire bank or looking at erosion and deposition along stream cross sections. TLS on the other hand is capable of creating a change map over the entire bank surface allowing for the identification of areas of erosion and deposition (Fig. 2.3).

This type of information could be invaluable for studies where the spatial variability of erosion is critical, such as studying micro-scale streambank erosion processes.

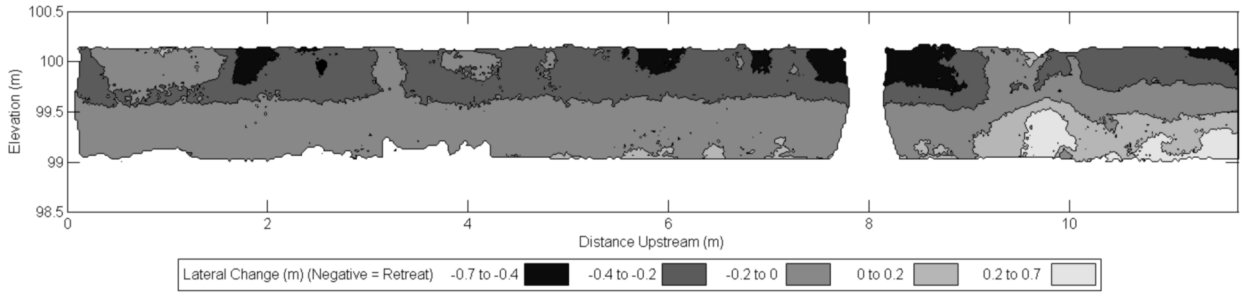

Figure 2.3. TLS measured lateral change over the bank surface from 05/07 to 12/08 (the gap in the data at 8 m upstream is a result of the way the data was projected). (Note: Additional TLS-derived SBR images not included in publication are shown in Appendix D.)

The high accuracy of TLS allows for measuring topography of streambanks nondestructively at a previously unattainable resolution. However, there are many improvements that must be made to the scanning and data-processing methodology before TLS can be an effective tool for many stream applications. The analysis of TLS data can be complex and time intensive due to the size of the datasets. There are also limitations such as the inability to scan underwater topography and difficulties with measuring heavily vegetated surfaces.

Most applications involving measuring fluvial topography rely on total station surveys due to their familiarity and cost effectiveness. Our future research efforts will focus on the propagation of surveying error to larger-scale analyses such as reach- and watershed-scale sediment load estimates. Until TLS technology is more readily available and post-processing techniques more accessible, research and management projects will continue to rely on total station surveys. In the meantime, TLS can help us estimate the error in topographic measurements from more standard techniques so that uncertainty can be quantified for TMDL sediment load estimates and other geomorphologic applications.

2.5 Summary and Conclusions

In this technical note we discussed the methodology of using TLS in the field to collect high-resolution streambank topography data, and then processed that data to calculate SBR and erosion volume. The differences in these calculations were then found between total station data

and TLS data. While total station surveying can be accurate for measuring single points, the error is much greater when looking at interpolated SBR values and overall erosion volume, particularly when measuring undercut banks and other complex topographies. TLS also has an advantage over point measurements in the ability to quantify the spatial variability of erosion and deposition over the entire streambank surface.

Acknowledgements

Thanks to Bethany Bezak, Kristen Bronnenkant, Leslie Hopkinson, Jess Kozarek, Andrea Ludwig, Sara Morris, Mike Nassry, Sheila Ranganath, Matt Smith, Barb Utley and Dr. Tess Wynn.

2.6 References

Agouridis, C. T., Edwards, D. R., Workman, S. R., Bicudo, J. R., Koostra, B. K., Vanzant, E. S., and Taraba, J. L. (2005). "Streambank Erosion Associated with Grazing Practices in the Humid Region." *Trans. ASAE*, 48(1), 181-190.

Benham, B., Brannan, K., Dillaha, T., Mostaghimi, S., Wagner, R., Wynn, J., Yagow, G., and Zeckoski, R. (2003). "Benthic TMDL for Stroubles Creek in Montgomery County, Virginia." *Submitted October 16, 2003 to the Virginia Departments of Environmental Quality, and Conservation and Recreation. Richmond, Virginia.* <http://www.deq.virginia.gov/tmdl/apptmdls/newrvr/stroub.pdf> (September 2009).

Bernhardt, E. S., Palmer, M. A., Allan, J. D., Alexander, G., Barnas, K., Brooks, S., Carr, J., Clayton, S., Dahm, C., Follstad-Shah, J., Galat, D., Gloss, S., Goodwin, P., Hart, D., Hassett, B., Jenkinson, R., Katz, S., Kondolf, G. M., Lake, P. S., Lave, R., Meyer, J. L., and O'Don, T. K. (2005). "Synthesizing U. S. River Restoration Efforts." *Science,* 308, 636-637.

Bitelli, G., Dubbini, M., and Zanutta, A. (2004). "Terrestrial Laser Scanning and Digital Photogrammetry Techniques to Monitor Landslide Bodies." *Proceedings of the XXth ISPRS Congress*.

Bourke, M., Viles, H., Nicoli, J., Lyew-Ayee, P., Ghent, R., and Holmlund, J. (2008). "Innovative Applications of Laser Scanning and Rapid Prototype Printing to Rock Breakdown Experiments." *Earth Surf. Processes and Landforms,* Letters to ESEX.

Brasington, J., Langham, J., and Rumsby, B. (2003). "Methodological Sensitivity of Morphometric Estimates of Coarse Fluvial Sediment Transport." *Geomorphology*, 53, 299-316.

Collins, B. D., and Sitar, N. (2008). "Processes of Coastal Bluff Erosion in Weakly Lithified Sands, Pacifica, California, USA." *Geomorphology,* 97, 483-501.

Davis, R. J., and Gregory, K. J. (1994). "A New Distinct Mechanism of River Bank Erosion in a Forested Catchment." *J. Hydrol.*, 157, 1-11.

Green, T. R., Beavis, S. G., Dietrich, C. R., and Jakeman, A. J. (1999). "Relating Stream-bank Erosion to In-stream Transport of Suspended Sediment." *Hydrol. Process.*, 13, 777-787.

Heritage, G., and Hetherington, D. (2007). "Towards a Protocol for Laser Scanning in Fluvial Geomorphology." *Earth Surf. Processes and Landforms,* 32(1), 66-74.

Hsiao, K. H., Liu, J. K., Yu, M. F., and Tseng, Y. H. (2004). "Change Detection of Landslide Terrains Using Ground-based Lidar Data." *Int. Arch. Photogramm., Rem. Sens. Spatial Inform. Sci.,* 35(B7), 617-621.

Knighton, A. D. (1973). "Riverbank Erosion in Relation to Streamflow Conditions, River Bollin-Dean, Cheshire." *East Midland Geographer*, 5, 416-426.

Laubel, A., Svendsen, L. M., Kronvang, B., and Larsen, S. E. (1999). "Bank Erosion in a Danish Lowland Stream System." *Hydrobiologia*, 410, 279-285.

Lawler, D. M. (1992). "Process Dominance in Bank Erosion Systems." *Lowland Floodplain Rivers: Geomorphological Perspectives,* Carling, P. A. and Petts G. E., eds., Wiley, Chichester, 119-141.

Lawler, D. M. (1993). "The Measurement of River Bank Erosion and Lateral Channel Change: A Review." *Earth Surf. Processes and Landforms*, 18, 777-821.

Lawler, D. M., Grove, J. R., Couperthwaite, J. S., and Leeks, G. J. L. (1999). "Downstream Change in River Bank Erosion Rates in the Swale-Ouse System, Northern England." *Hydrol. Process.*, 13, 977-992.

Lichti, D. D. and Jamtsho, S. (2006). "Angular Resolution of Terrestrial Laser Scanners." *Photogramm. Rec.*, 21(114), 141-160.

Lim, M., Petley, D. N., Rosser, N. J., Allison, R. J., and Long, A. J. (2005). "Combined Digital Photogrammetry and Time-of-flight Laser Scanning for Monitoring Cliff Evolution." *Photogramm. Rec.,* 20(110), 109-129.

Optech. (2009). "Technical Overview - ILRIS-3D Specifications." <http://www.optech.ca/i3dtechoverview-ilris.htm> (September 2009).

Osterkamp, W. R., Heilman, P., and Lane, L. J. (1998). "Economic consideration of a continental sediment-monitoring program." *Intl. J. Sediment Res.,* 13(4), 12-24.

Pyle, C. J., Richards, K. S., and Chandler, J. H. (1997). "Digital Photogrammetric Monitoring of River Bank Erosion." *Photogramm. Rec.*, 15(89), 753-764.

Rhoades, E. L., O'Neal, M. A., and Pizzuto, J. E. (2009). "Quantifying Bank Erosion on the South River from 1937 to 2005, and its Importance in Assessing Hg Contamination." *Appl. Geogr.*, 29, 125-134.

Rosser, N. J., Petley, D. N., Lim, M., Dunning, S. A., and Allison, R. J. (2005). "Terrestrial Laser Scanning for Monitoring the Process of Hard Rock Coastal Cliff Erosion." *Q. J. Eng. Geol. Hydrogeol.,* 38, 363-375.

Teza, G., Pesci, A., Genevois, R., and Galgaro, A. (2008). "Characterization of Landslide Ground Surface Kinematics from Terrestrial Laser Scanning and Strain Field Computation." *Geomorphology,* 97(3-4), 424-437.

Winterbottom, S. J., and Gilvear, D. J. (2000). "A GIS-based Approach to Mapping Probabilities of River Bank Erosion: Regulated River Tummel, Scotland." *Regul. Rivers: Res. Mgmt.*, 16, 127-140.

Wynn, T. M., Henderson, M. B., and Vaughan, D. H. (2008). "Changes in Streambank Erodibility and Critical Shear Stress due to Subaerial Processes along a Headwater Stream, Southwestern Virginia, USA." *Geomorphology*, 97, 260-273.

Yagow, G., Benham, B., Wynn, T., and Younos, T. (2006). "Upper Stroubles Creek Watershed Draft TMDL Implementation Plan, Montgomery County, Virginia." *VT-BSE Document No. 2005-0013. Submitted February 17, 2006 to the Virginia Department of Environmental Quality and the Virginia Department of Conservation and Recreation. Richmond, Virginia.* <http://www.deq.virginia.gov/tmdl/implans/stroubip.pdf> (September 2009).

3.0 Terrestrial Laser Scanning for Quantifying Habitat and Hydraulic Complexity Measures: A Comparison with Traditional Surveying Techniques

Jonathan P. Resop, Jessica L. Kozarek, and W. Cully Hession

Abstract

Accurate stream topography measurement is important for many ecological applications such as hydraulic modeling and habitat characterization. Measures of habitat complexity are often difficult to quantify or are performed qualitatively. Traditional surveying with a total station can be time intensive and limited by poor spatial resolution. These problems lead to measurement and interpolation errors, which propagate to model uncertainty. Terrestrial laser scanning (TLS) has the potential to measure topography at a high resolution and accuracy. Two methods, total station surveying and TLS, were used to measure a 100-m forested reach on the Staunton River in Shenandoah National Park, VA, USA. The TLS dataset was post-processed to remove vegetation and create a 2-cm digital elevation model (DEM). The position and size of ten rocks were compared for each method. An algorithm was developed for delineating rocks within the stream channel from the TLS DEM. Ecological metrics based on the structural complexity of the stream, such as percent in-stream rock cover and cross-sectional heterogeneity, were derived from the TLS dataset for six habitat areas and compared with the estimates from traditional methods. Compared to TLS, total station surveying underestimated rock volume and cross-sectional heterogeneity by 55% and 41%, respectively. TLS has the potential to quantify habitat complexity measures in an automated, unbiased manner.

Keywords

Terrestrial laser scanning, Stream morphology, Habitat complexity, Remote sensing, Topographic surveys, Uncertainty principles

Manuscript Note

This manuscript will be submitted to Ecohydrology.

3.1 Introduction

The complexity of stream habitat plays an important role in ecological issues such as species diversity and population dynamics for aquatic organisms (Gorman and Karr 1978). Habitat complexity is difficult to quantify objectively (Downes et al. 2000), particularly at small scales (Sanson et al. 1995), creating the need for improved, high-resolution techniques for measuring stream morphology (Legleiter et al. 2004). The size and location of in-stream obstructions such as boulders have been shown to be important habitat factors influencing hydraulic complexity (Crowder and Diplas 2000; Shen and Diplas 2008). However, boulder shape is typically defined using only a few measured points. In-stream rock cover and substrate composition, such as cobble and boulder, have been associated with population dynamics at various scales, ranging from macroinvertebrate to fish (Wesche et al. 1987; Beisel et al. 2000; Peckarsky et al. 2000; Venter et al. 2008). However, percent rock cover is typically measured qualitatively in the field or estimated visually (Kaufmann and Robison 1998; Willis et al. 2005). Accuracy and precision of rock cover measures decrease as the substrate heterogeneity of the site increases (Wang et al. 1996). The lack of accurate and precise spatial data has the potential to increase the uncertainty associated with habitat assessments and hydraulic models.

One potential strategy for quantifying habitat complexity is by measuring the structural complexity of the stream topography (Bartley and Rutherfurd 2005). Two categories of methods are traditionally used for surveying topography: 1) point measurements in the field; and 2) remote sensing from above. Field-based point measurements are commonly surveyed with tools such as electronic total stations or global positioning systems (GPS). While these methods can provide accurate measurements where points are taken, they can be time intensive, be affected by user bias, and have limitations in spatial resolution and scope (Heritage and Hetherington 2007). Remote sensing can be performed by methods such as aerial photography, satellites, or aerial laser scanning (ALS), also known as aerial lidar. ALS has been used in many geomorphology and natural resources studies to generate digital terrain models (DTMs) or canopy height models (CHMs) with typical resolutions ranging from 10 to 200 points/m^2 and elevation errors ranging from ±0.15 m (Charlton et al. 2009; Devereux and Amable 2009). Marchamalo (2007) implemented ALS to perform 2-D hydraulic modeling for trout habitat characterization and noted the advantage of ALS for large-scale studies. While aerial remote sensing has the ability to

provide greater spatial coverage, it is limited in its resolution and precision for measuring small-scale stream complexity, such as boulders and undercut banks (Heritage and Hetherington 2007).

Terrestrial laser scanning (TLS), or ground-based lidar, offers the potential of generating high-resolution topographic point clouds over a fairly large area. TLS can create surface models with typical resolutions ranging from 1,000 to 10,000 points/m^2 with absolute errors less than ±0.02 m (Entwistle and Fuller 2009). There is great potential for using TLS to measure small-scale changes and spatial features in fluvial systems (Rosser et al. 2005; Hetherington et al. 2007). TLS has been utilized in a range of fluvial applications from measuring 1 m^2 gravel stream surface patches at 1 mm resolution (Hodge et al. 2009) to measuring a 150 m x 15 m stream reach at 1 cm resolution (Heritage and Hetherington 2007).

Researchers have recently been investigating the potential for TLS to measure parameters that are difficult to estimate for hydraulic models, such as surface roughness (Smith et al. 2007). Milan (2009) calculated bed roughness using TLS-derived stream topography and a moving window method. Similarly, Entwistle and Fuller (2009) derived grain size from a DEM created using TLS on a dry stream bed. A major advantage of lidar is its ability to take multiple measurements within each grid space of a DEM, providing small-scale measures of roughness and variability (Glenn 2006). TLS has also been utilized for measuring vegetation density as a roughness factor for hydrodynamic floodplain flow models (Straatsma et al. 2008).

The objectives of this study were to: 1) compare stream topography measured by two methods (total station surveying and TLS) in terms of point measurements and individual rock locations and volumes; 2) delineate the location and size of individual rocks within the stream channel from high-resolution digital elevation models (DEMs) created from TLS data; and 3) compare traditional methods (total station surveying and visual estimates) with TLS for deriving measures of habitat and hydraulic complexity, including in-stream rock cover and cross-sectional heterogeneity, for six habitat complex (HC) areas within a brook trout stream in Virginia.

3.2 Methods

Study Site

The study site was a 100-m forested stream reach on the Staunton River located in Shenandoah National Park, VA (Fig. 3.1). The second-order stream is classified as a combination of step pool and cascade morphology with an average stream width of 3.5 m (Roghair et al. 2002). The site is characterized by many cobbles and boulders, a large section of undercut bank, and extensive vegetation (trees, bushes, and large woody debris [LWD]). Kozarek et al. (In Press) studied this stream reach to model 2-D hydraulic complexity for characterizing brook trout habitat and found a positive correlation between trout population and percent rock cover. The reach has been divided into six HCs for measuring brook trout population, defined as continuous 10 to 40 m sub-reaches with several pools and riffles (Roghair et al. 2002). Brook trout were measured using single-pass electrofishing within each HC.

Figure 3.1. The 100-m forested stream reach of the Staunton River in Virginia, USA. Photo by Jess Kozarek, used with permission.

Field Methods

The stream reach was surveyed with a Topcon GTS 230W total station in May 2007. The total station survey was completed over four days with approximately 10 hours of field work per day for a total of 40 hours. In addition, an Optech ILRIS-3D portable TLS was used to survey the reach over three days in July 2007 with approximately six hours of field work per day for a total of 18 hours. Six benchmarks were used for aligning the TLS data to the survey data.

The total station survey resulted in 2,701 points for characterizing the complex topography of the streambed, banks, and boulders. Mean point density was approximately two points per square meter; however, point density was higher in complex areas and less dense in relatively uniform topography. The reported accuracy of the scanner is ±(3.2 mm + 2 ppm * D), where D is the measuring distance in mm (Topcon 2010). To characterize individual boulders points were taken at the apexes and around the bottom. Because of vegetation, benchmarks were

used over the course of the stream on specific rocks to align the data from different stations. Additional details for the total station data collection can be found in Kozarek et al. (In Press).

TLS was used to survey the stream during baseflow conditions. The scanner was moved to multiple places on both sides of the bank to collect data from different angles and minimize shadowing effects of the laser. A total of 89 scans were taken of the entire reach with an average of approximately 1 cm point spacing or 10,000 points per square meter (Fig. 3.2). Overlap was allowed between scans to aid in the iterative alignment process implemented later. A combination of both first and last pulse returns was used during measurement. The average distance of the scanner to the stream was 12 m, with scan distances ranging from 5 to 20 m. Based on the beam divergence of the laser system (0.00974°), the scanner has a footprint of 14 mm at the average distance and has an accuracy of 7 to 8 mm at a distance of 100 m (Lichti and Jamtsho 2006; Optech 2010). Large triangular targets were placed over the location of the six benchmarks used in the total station survey to align the two datasets.

Figure 3.2. a) An example section of the Staunton River and b) the same section represented by a TLS point cloud. Photo by Jess Kozarek, used with permission.

Data Alignment and Processing

Once the total station data were aligned using the benchmarks, the dataset was converted to a triangulated irregular network (TIN) for further analysis. The TLS data were imported into PolyWorks (InnovMetric 2008) one scan at a time and aligned into the same coordinate system

using the IMAlign tool. Starting with the first two scans, similar identifiable features in the point clouds, such as rocks and fallen logs, were used to provide control points for a manual alignment. An automatic alignment algorithm within IMAlign was then used to best-fit the data to within a mean error of ±0.0001 m. The rest of the scans were aligned in a similar manner until all of the TLS data were in the same coordinate system, at which point the entire TLS point cloud was aligned to the total station survey data using the benchmarks and the best-fit algorithm was used to minimize the error of rock peaks.

After the raw TLS data were aligned, the data were further processed to remove unwanted vegetation. Manual inspection in PolyWorks was performed to remove large sections of data representing trees, bushes and excess data beyond the streambank. There were 9.5 million points remaining in the dataset after cleaning. The data were imported into MATLAB (MathWorks 2009) and converted into a 2-cm DEM. The minimum elevation was selected for each 2-cm grid cell to increase the probability of using ground points for the DEM. Pixels in the DEM with a "no data" value were assumed to represent the water surface. Image filters were then used to fill in small data holes in the DEM (isolated water pixels located within the rock surface area) or remove isolated surface pixels from the water surface area. For "no data" pixels that were determined to be part of the rock surface area, an elevation value was interpolated using the mean value of pixels within a 3 x 3 neighborhood. A binary grid was then created from the DEM representing either water surface or rock surface.

Data Comparison

Once the data points for each method were aligned and the surface models were created, two metrics were used to compare the two methods in terms of their ability to measure stream topography for ecological applications: 1) individual point differences and; 2) the differences between individual rock locations, peak elevations, plan-view areas, and volumes.

Individual point differences between the total station and TLS data were measured as the point-to-point distances. The survey point elevations were compared to the closest TLS data point within a 5-cm square grid around the point. Survey points on the streambed under the water surface, not scanned by TLS, were not included.

For the analysis of individual rocks, ten in-stream rocks were selected from the stream reach. The pixels representing these ten rocks were then manually selected from the TLS DEM.

Rock location was defined as the x-y position of the center of mass for the 2-D plan-view area. For the total station data, rock volume was calculated based on the 3-D TIN polygon created from the points surveyed at the top and around the sides of the rock. For the TLS data, rock volume was calculated numerically from the 2-cm DEM by subtracting the elevation of each pixel by the minimum elevation of the rock and multiplying by the grid size. The peak, or maximum, elevation was also determined and compared for both datasets.

Delineating In-stream Rocks

The rock delineation algorithm developed for this dataset consisted of multiple image-processing functions designed to filter the TLS DEM and to define boundaries between rocks and the water surface and between rocks and other rocks, as summarized in Fig. 3.3. Similar algorithms have been developed in the field of forestry for delineating tree stands from remotely sensed data (Andersen et al. 2001; Culvenor 2002). DEM pixels located within the stream channel were selected based on the stream surface boundary defined by the water-edge locations measured by the total station. Using the rock/water binary grid, a continuous boundary was created between the water surface and the rock areas.

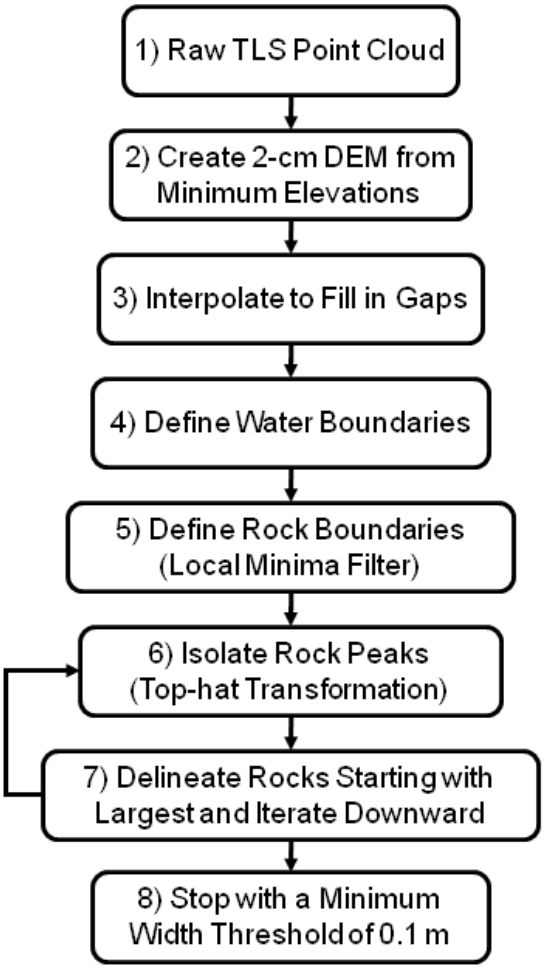

Figure 3.3. Flow chart summarizing the processes used for delineating in-stream rocks.

The next step was to define the boundaries between individual rocks. A 5 x 5 cell low-pass (mean) filter was performed over the entire DEM to smooth the surface of irregularities. A 7 x 7 cell local minima filter was then used to determine the valley in the DEM and define the boundaries between rocks, similar to a method used by Culvenor (2002) to delineate tree boundaries. The rock-boundary layer was then merged with the water-boundary layer to create a single boundary layer. The boundary layer was processed with multiple filters to remove dead ends and connect small gaps, resulting in continuous, well-defined boundaries representing the areas of one or more rocks (Culvenor 2002). An image-processing skeleton function was then used to reduce the width of the boundary to one pixel.

A sensitivity analysis was performed to evaluate the effect of the minima filter size on the balance between Type I (false positives) and Type II (false negatives) errors in the rock

delineation process. Type I errors occur when rock delineation boundaries are created that do not really exist in reality, for example, when a large rock is divided into many smaller rocks. Type II errors occur when the algorithm fails to delineate a cluster of rocks, leaving them as a single object. Minima filters of increasing size (3 x 3, 5 x 5, 7 x 7, and 9 x 9) were used in the algorithm and the resulting rock size distributions were compared for each filter size.

The final step was to identify individual rocks in each area using a top-hat transformation, similar to a method used by Andersen et al. (2001) to identify tree crowns. A top-hat filter with a disc size of radius 15 pixels was used to identify the largest rocks in the DEM. A threshold and morphological open filter were then used to isolate the rock boundaries. Starting with the largest rock in the stream channel, the area defined by that rock was removed from the DEM. This process was then repeated with smaller morphological filter sizes until all of the rocks were defined, using a 0.1 m minimum rock width threshold (a disc size of radius 3 pixels). The end result was a database of rock size (area and volume) and location within the stream generated for the entire reach.

The results of the rock delineation algorithm were compared to the locations and 2-D plan-view in-stream area of 34 rocks measured from the total station survey. The number of survey points used to define the measured rock surfaces ranged from four to nine. The rocks in the total station dataset were matched to the nearest rock from the delineated TLS dataset based on the center of mass. Due to the fact that the field measurements with the total station are of much lower resolution than the TLS dataset, they were primarily used to compare the general size and location of the delineated rocks. Another limitation of the survey dataset is that the boundaries of smaller rocks (those with diameters approaching 0.1 m) were not defined by the total station point measurements and as a result could not be compared with the TLS delineation results.

Ecological Metrics

The TLS data, 2-cm DEM, and database of delineated in-stream rocks were then used to derive four habitat complexity measures: 1) percent in-stream rock cover; 2) distribution of rock size; 3) cross-sectional unobstructed area; and 4) cross-sectional heterogeneity. These measures were compared between traditional methods and TLS for six HCs within the stream channel.

In-stream rock cover was measured in the field through visual approximation. For each HC, two surveyors at the time of the total station survey estimated the percent of the channel area covered by protruding boulders. For the TLS data, rock cover was calculated using the pixels in the 2-cm DEM within the in-stream boundary layer. The area of the 2-cm rock/water binary grid, discussed earlier, that was classified as "rock" was then calculated numerically and compared with the total area of the HC to get a percentage. The values derived from the TLS dataset were then compared to visual estimates of percent rock cover made in the field. Rocks were divided into two size categories based on their diameter (estimated by taking the square root of the plan-view area): cobbles (greater than 0.1 m and less than 0.256 m) and boulders (greater than 0.256 m). Within each HC the distribution of rocks was determined based on the mean, standard deviation, and maximum of 2-D plan-view rock areas as well as the number of rocks.

Three cross-sections from each HC were extracted from both the total station TIN and the TLS DEM. Each cross-section was interpolated at 2-cm increments for both datasets. For each cross-section two measures were calculated: unobstructed flow area and heterogeneity. Unobstructed flow area was defined as the area above the cross-section elevation below the water surface (assumed to be an arbitrary maximum depth of 2 m). This measure is inversely proportional to in-stream obstruction density, which is similar to hydrodynamic vegetation density used by other studies (Straatsma et al. 2008). Heterogeneity was calculated as the standard deviation of elevation within a 1 m moving window. For each cross-section the average heterogeneity was then determined as a measure of roughness.

3.3 Results and Discussion

Data Comparison

Out of the 2,701 points measured with the total station, 596 were either located in the streambed (topography not scanned by TLS) or in small gaps in the TLS dataset. The other 2,105 total station points had a mean absolute elevation difference with the TLS data of 0.111 m and a standard deviation of 0.361 m. The point differences are comparable to the results found by similar studies, with 82.3% of the total station data within ±0.1 m of the TLS data (Heritage and Hetherington 2007). The differences between the raw points measured by both methods are most likely due to the measurement error of the total station or any vegetation or LWD that was not

removed from the TLS data. Other potential minor errors include the measurement error of the laser scanner and the error from aligning the two datasets to the same coordinate system.

For the ten rocks selected from within the stream channel, in general, both datasets characterize the overall shape and location. The absolute difference in peak elevation measured by both methods was on average 0.04 m. There was an average difference of 0.08 m between the plan-view centers of mass identified by both the total station survey and TLS. The differences in peak elevation and center of mass are likely a result of errors in the total station survey and alignment errors between the two datasets, as discussed previously. The total station survey underestimated the 2-D plan-view area of each rock by on average 31% compared to TLS.

Based on the individual rock volumes, the points surveyed using the total station consistently underestimated volume compared to TLS, on average 55% smaller. The difference in volume is expected due to the difference in resolution between the two datasets. On average, six points were measured by the total station to define the boundary of each individual rock compared to the approximately 14,000 points on average surveyed by TLS. These results show how topographic surveying with a total station can oversimplify the shape of rocks, which can potentially result in significant uncertainty when using this information for hydraulic models (Fig. 3.4).

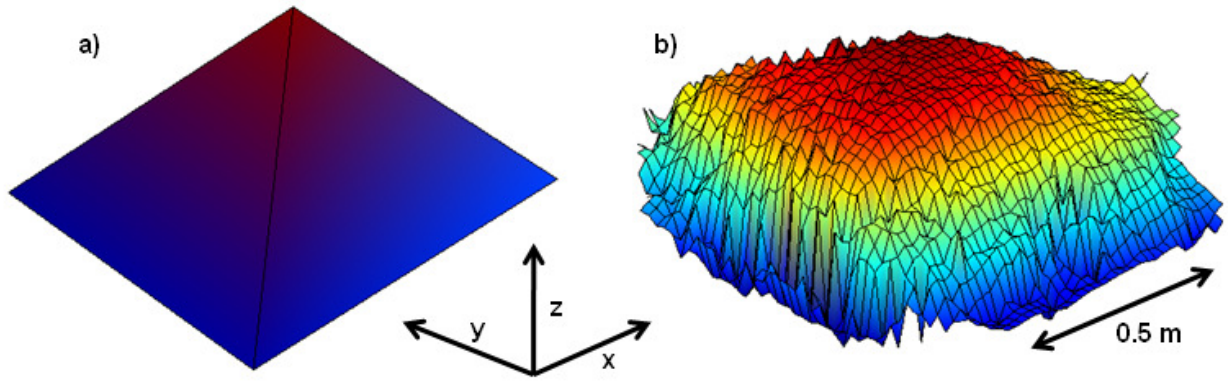

Figure 3.4. An example rock represented by a) a TIN derived from total station data and b) a 2-cm TLS DEM.

Delineating In-stream Rocks

The delineation algorithm performed fairly well in terms of identifying and isolating individual cobble and boulders within the stream reach in an automated manner, based on comparing the TLS DEM to the delineation results (Fig. 3.5). The in-stream rock delineation

method used for this study shows how relatively simple image-processing algorithms based on similar studies of tree canopy delineation can be used with high-resolution stream topography data. The results generated can be used for precise and accurate measures of rock size and location, which has been shown to be valuable information for hydraulic modeling due to the significant effect that boulders have on flow complexity as shown by Crowder and Diplas (2000).

It is difficult to fully validate the results without a higher resolution total station survey or detailed field measurements, although some comparisons can be made with the existing total station data. The algorithm is not perfect, as there are obvious errors in the results, such as rock clusters that were not fully delineated and other objects in the stream, such as LWD, which were delineated and classified as rocks. More discussion on the sources of error within the data and algorithm are discussed at the end of this section.

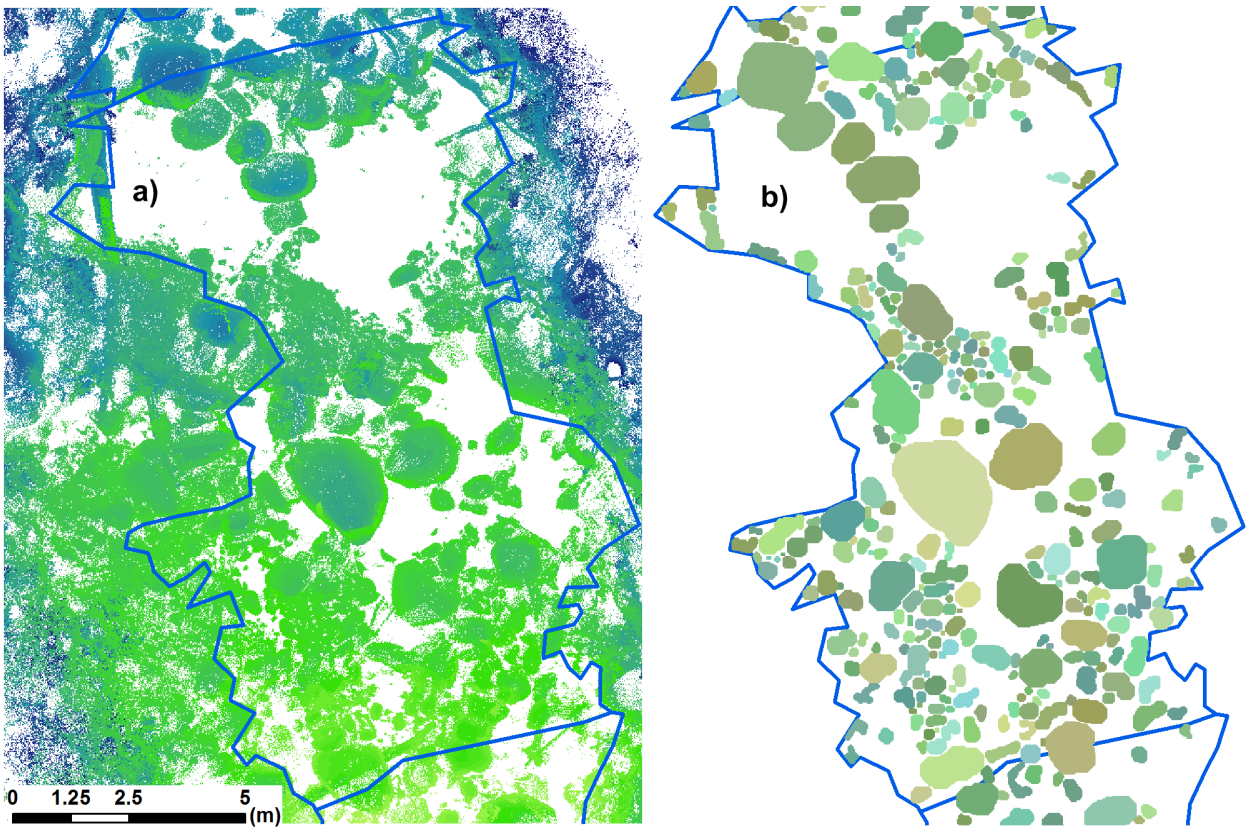

Figure 3.5. Plan-view maps of HC 2 showing a) the 2-cm TLS DEM with white space representing the water surface and b) individual delineated in-stream rocks represented by different colors to emphasize boundaries.

A comparison was made between the total station point measurements and the TLS delineation algorithm using 34 rocks selected from the stream reach (Fig. 3.6a). The algorithm performed well at identifying the boundaries of rocks measured in the field, based on the 2-D plan-view in-stream rock areas. This process also served to perform a rough validation of the general size and location of rocks delineated from the TLS data. There was general agreement (r = 0.91) between the rocks areas measured in the field with the total station and the rocks delineated from the TLS data (Fig. 3.6b). The root mean square error (RMSE) was 0.27 m^2, or 55% with respect to the average delineated rock area and 74% of the delineated rocks had a center of mass within 0.2 m of the measured rock center of mass. Similar to the manual rock volume comparisons discussed previously, in general, the total station data underestimated the size of individual rocks compared to TLS. While small differences in area between the two datasets can be attributed to the difference in resolution, larger differences are likely a result of errors within the TLS dataset and the delineation algorithm.

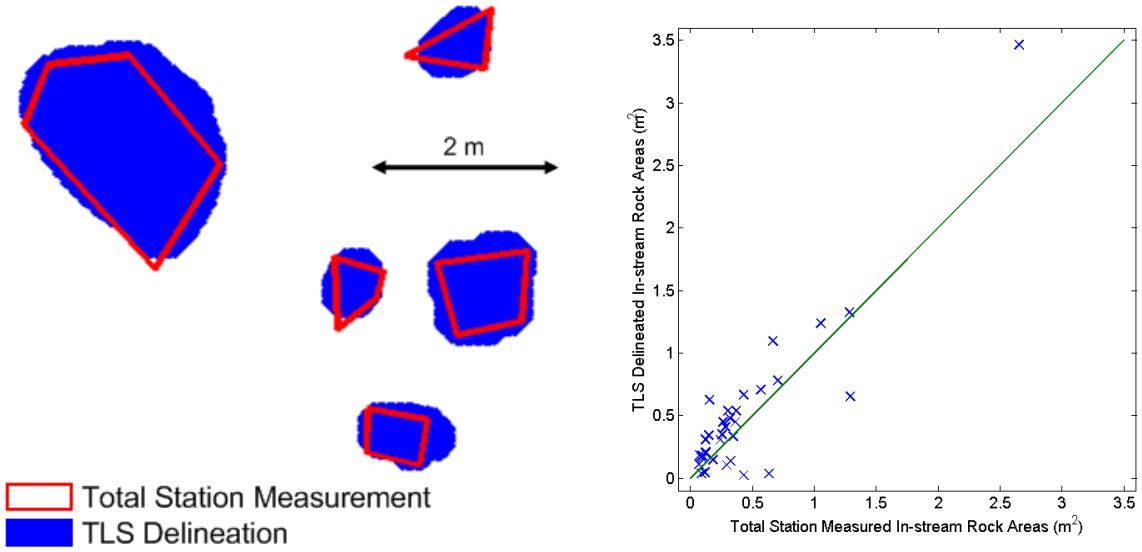

Figure 3.6. a) 2-D plan-view areas of example rocks measured from the both the total station survey and TLS delineation and b) comparison between plan-view rock areas for 34 individual rocks measured by both total station measurements and TLS delineation.

Sources of uncertainty in the rock delineation process include both spatial variability (due to the complexity of the surface being scanned) and knowledge uncertainty (due to both parameter and model error). Parameter error consists primarily of measurement errors that

occurred during the scanning process, such as gaps in the TLS data caused by shadowing and the presence of vegetation and LWD in the data (Fig. 3.7a). Modeling error can be described as a variation of Type I/Type II errors inherent to the delineation process. Type I errors, or false positives, occur when a rock is delineated that doesn't really exist. Examples of false positives include when a large rock is broken into many smaller rocks by the algorithm (which happened rarely, see Fig. 3.7b) or when other in-stream objects were identified as rocks (such as LWD, which was not identified separately by the algorithm and would be more difficult to determine). Type II errors, or false negatives, occur when the algorithm fails to delineate a cluster of rocks. During this type of error, the algorithm fails to delineate the boundary between two or more rocks, identifying the cluster as a single, large rock (Fig. 3.7c).

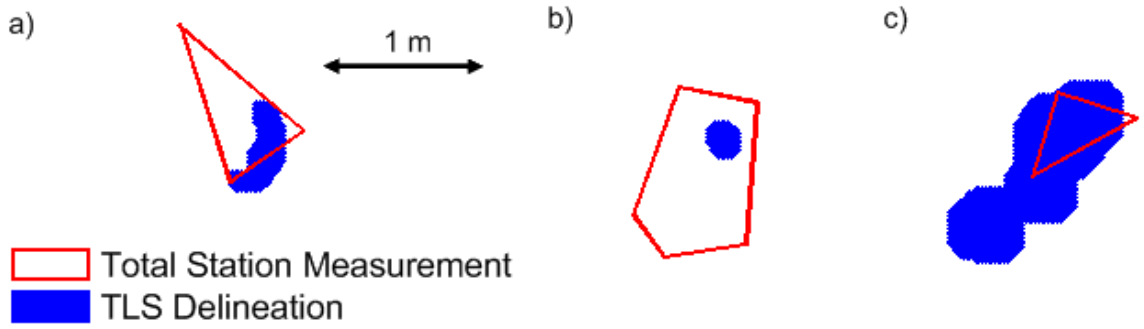

Figure 3.7. Examples of various errors that occurred when delineating rock boundaries from TLS data: a) measurement error due to gaps in the dataset, b) false positives caused by too much delineation, and c) false negatives caused by not enough delineation.

A sensitivity analysis was performed to explore the relationship between Type I and Type II errors in the delineation algorithm. Specifically, the size of the local minima filter used for defining rock boundaries was varied. Pixels identified by the filter as being a local minimum were used for defining the valleys that create the boundaries between individual rocks. As the size of the filter increases, it becomes less likely that a pixel is classified as a local minimum, fewer boundary pixels are identified over the entire reach in general, and as a result the number of delineated rocks decreases and the average rock size increases (Table 3.1). Fewer individual rocks identified can potentially lead to more Type II errors occurring. As the local minima filter size decreases, pixels are more likely to be local minima. In this situation, the number of rocks increases and the average size decreases, making Type I errors more likely. The large range in

the number of rocks and average size shows how sensitive the delineation algorithm is to the size of the local minima filter. The sensitivity analysis demonstrates that more work is needed to optimize the algorithm.

Table 3.1. Results of the sensitivity analysis showing the effect of the local minima filter on the rock delineation algorithm.

Size of Local Minima Filter	Number of Rocks	Mean Rock Area (m^2)
3 x 3	1445	0.074
5 x 5	1358	0.112
7 x 7	1088	0.155
9 x 9	878	0.200

The sensitivity analysis shown here is just one example of how the algorithm parameters can affect the occurrence of Type I and Type II errors in delineating rocks from the TLS dataset. There are other factors that affect the delineation error, such the spatial heterogeneity or complexity of the surface being surveyed and the accuracy of the TLS point cloud. Noise in the dataset that is a result of small vegetation or scanner errors can adversely affect the delineation process. Aside from these notes of uncertainty, the in-stream rocks delineated from the TLS data have been shown to agree favorably with the crude total station measurements taken in the field and the results can be used to derive quantitative measures of the structural complexity within the stream reach.

Ecological Metrics

The visual estimates for percent rock cover and the values derived from TLS are summarized in Table 3.2. For the six HCs, the percent of in-stream rock cover estimated in the field ranged from 10 to 65%, while the calculations made from the TLS data ranged from 24 to 42%. In general, the visual estimates in the field overestimated the percent rock cover with a percent mean absolute difference of 41% relative to TLS. The smaller range of values computed from the TLS data indicates the possibility that there is not as much difference in percent rock cover between the HC areas as estimated visually. Both methods of measurement have a degree of uncertainty and so it is difficult to determine which result is the "true" value of percent rock cover. More research needs to be done to further evaluate the measurements and calculations made using TLS.

From the TLS data it was determined that 63% of the delineated rocks in the entire stream reach were classified as boulders (an approximate diameter of 0.256 m) with the rest classified as cobble. The main limitation with this method is that the smaller substrate, particles most likely to lie below the water surface on the streambed, were not measured by TLS. The algorithm was also limited to identifying rocks with a minimum diameter of 0.1 m due to the resolution of the data. As a result, we are only able to get a partial, larger-scale picture of the substrate composition.

Table 3.2. Summary of the habitat complexity measures for each in-stream HC.

Habitat Complex	Rock Cover (%)		TLS Derived Individual Rock Area (m^2)			
	Visual	TLS	Mean	St. Dev.	Max	Number of Rocks
1	10	31.0	0.159	0.151	0.789	124
2	44	42.3	0.169	0.334	3.462	304
3	40	30.9	0.158	0.282	3.064	182
4	55	34.1	0.133	0.194	2.358	230
5	65	41.5	0.158	0.271	2.416	173
6	30	24.2	0.144	0.116	0.705	75

The in-stream rocks delineated from TLS had a negative exponential distribution in regards to rock size (Fig. 3.8). The rocks within each of the six individual HCs had similar negative distributions. Table 3.2 and Fig. 3.9 show how the distribution and density of rocks vary between the different HC areas. From this information, we can observe in-stream areas defined by fewer, smaller rocks (HCs 1 and 6) as well as areas that are more densely covered (HC 2). These results are similar to the visual estimates of rock cover made in the field. However, with the TLS data, much more information can be quantified about the structural complexity of the stream, such as the size, location, and distribution of in-stream rocks. Measures such as these could potentially be used to improve habitat characterization indices and hydraulic models by providing automated, unbiased information.

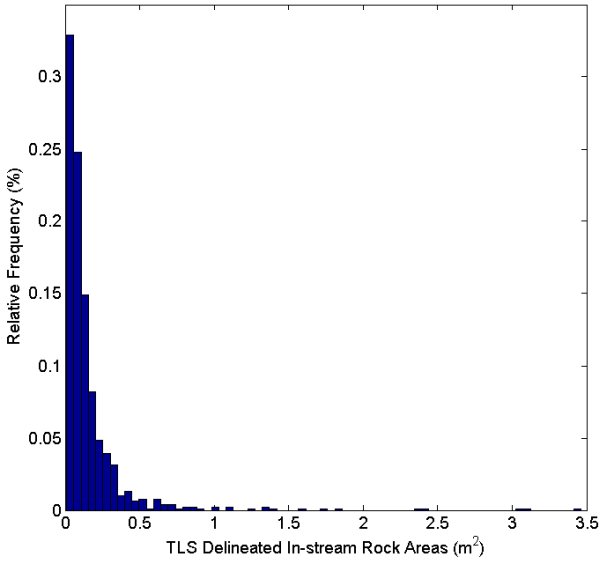

Figure 3.8. The exponential distribution of in-stream rock size determined from the TLS delineation algorithm for the entire stream reach.

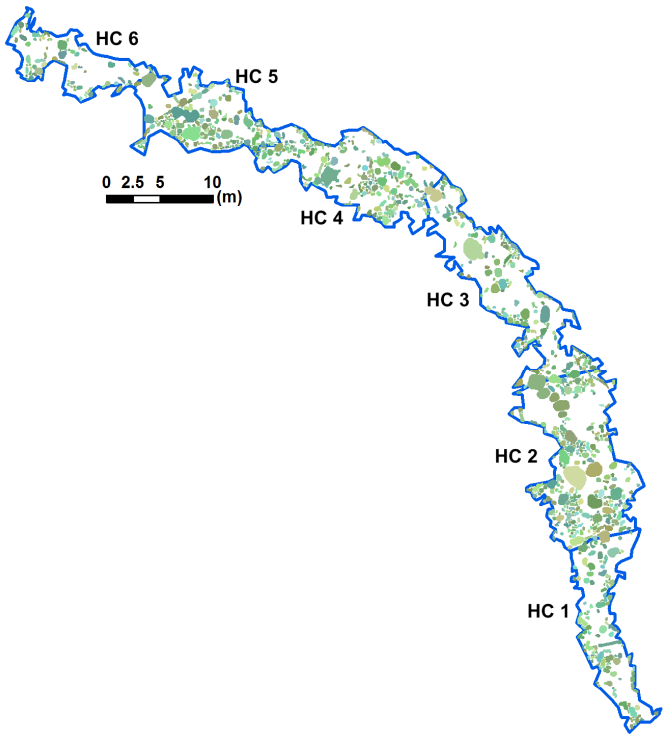

Figure 3.9. Plan-view showing the spatial distribution of individual in-stream rocks (represented by different colors) delineated within each Habitat Complex (HC).

For both cross-sectional unobstructed flow area and spatial heterogeneity, the average value between the three cross-sections was calculated for both total station surveying and TLS (Table 3.3). In general, the total station data overestimated the flow area within each cross-section, thereby underestimating the hydrodynamic obstruction density. As expected, the total station greatly underestimated the amount of heterogeneity within each cross-section compared to TLS due to the lower point density of the total station survey (Fig. 3.10). The TLS is able to capture much more of the spatial variability within the channel. Comparing both methods at each cross-section, the total station data had a relative error of 9% compared to the TLS for measuring unobstructed flow area and 41% for measuring heterogeneity. These errors illustrate the loss of information and uncertainty associated with limited point measurements.

Table 3.3. Average cross-sectional measures of complexity within each HC calculated by both methods.

Habitat Complex	Unobstructed Flow Area (m^2)		Spatial Heterogeneity (m)	
	Total Station	TLS	Total Station	TLS
1	16.9	14.1	0.09	0.31
2	21.3	20.2	0.12	0.18
3	15.4	15.1	0.13	0.21
4	13.6	12.5	0.12	0.24
5	16.0	15.8	0.13	0.19
6	13.1	11.9	0.14	0.23

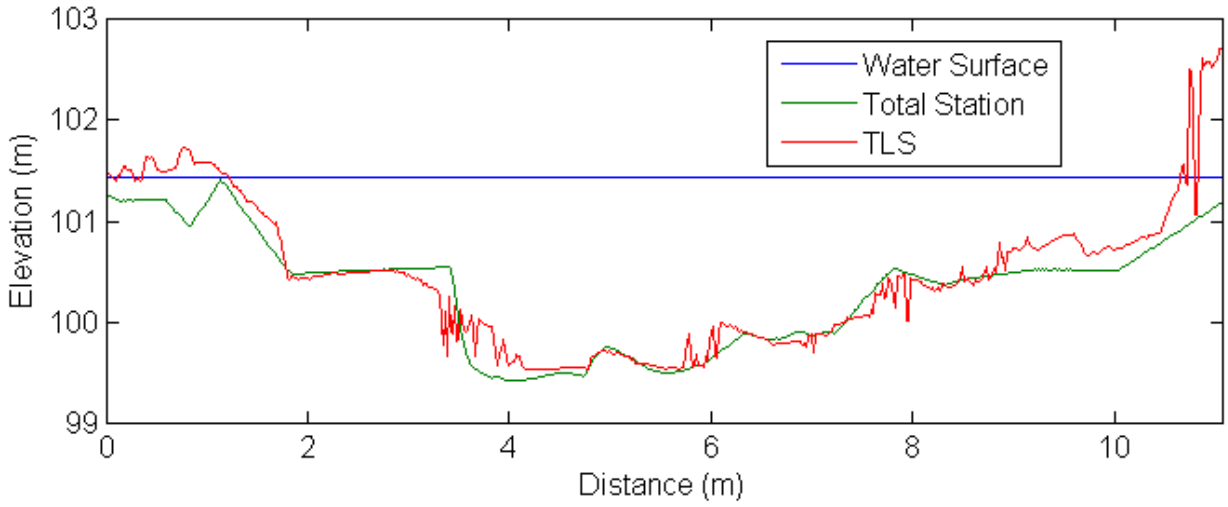

Figure 3.10. Example cross-section from HC 6 showing both the total station and TLS data.

3.4 Summary and Conclusions

TLS has the potential for producing high-resolution, quantitative values for habitat complexity. The measures of topographic and structural complexity generated from TLS data could be used for further investigations involving habitat characterization and modeling. Measurements can be generated from TLS data for habitat metrics, such as in-stream rock cover, in an unbiased and automated manner, thereby reducing the amount of uncertainty generated from qualitative assessments. The high-resolution topography measured by TLS can potentially improve the accuracy of 2-D and 3-D hydraulic models and reduce the uncertainty associated with measurement and interpolation errors. The results generated from this study also have the potential to be used for quantifying the uncertainty in reach-wide measures for habitat assessment and hydraulic modeling and reduce the need for qualitative habitat complexity metrics.

This paper shows the potential of applying the tree crown delineation algorithms used in forestry for processing TLS-generated DEMs for stream topography. However, more work needs to be done to fine-tune the data processing and rock delineation algorithms to optimize the balance between Type I and Type II errors. The primary problem with optimization will be finding accurate, high-resolution data for validating the results generated from processed TLS data. In the same vein, more research should be done in quantifying the uncertainty in TLS.

One of the main limitations of TLS is its inability to survey topography under water surfaces. This factor is less of an issue when quantifying certain habitat complexity parameters, such as percent rock cover as demonstrated in this study. However, the water surface phenomenon due to the reflectivity of the laser can be a disadvantage when studying other characterizations of channel morphology, such as substrate composition. Some TLS research has been performed on dry stream beds (Entwistle and Fuller 2009; Milan 2009), although this may not be a feasible option for many systems. Blue-green wavelength laser scanners have been implemented for bathymetric surveys, although this technology is currently only available for ALS (Wedding et al. 2008). Ideally, TLS should be combined with a high-resolution bathymetric surveying tool to garner a more complete picture of the stream topography. A DEM created using both technologies could be used to perform more involved calculations of habitat complexity, such as structural heterogeneity and spatial autocorrelation, at both a high resolution and accuracy.

Acknowledgements

Special thanks to Dr. Phil Radtke from the Forestry department at Virginia Tech for his assistance.

3.5 References

Andersen, H.-E., Reutebuch, S. E., and Schreuder, G. F. (2001). "Automated Individual Tree Measurement through Morphological Analysis of a LIDAR-based Canopy Surface Model." *Proceedings of the First International Precision Forestry Cooperative Symposium*, Seattle, WA, 11-22.

Bartley, R., and Rutherfurd, I. (2005). "Measuring the Reach-scale Geomorphic Diversity of Streams: Application to a Stream Disturbed by a Sediment Slug." *River Research and Applications*, 21, 39-59.

Beisel, J.-N., Usseglio-Polatera, P., and Moreteau, J.-C. (2000). "The Spatial Heterogeneity of a River Bottom: A Key Factor Determining Macroinvertebrate Communities." *Hydrobiologia*, 422/423, 163-171.

Charlton, M. E., Coveney, S. J., and McCarthy, T. (2009). "Issues in Laser Scanning." Laser Scanning for the Environmental Sciences, G. L. Heritage and A. R. G. Large, eds., Wiley-Blackwell, Chichester, 35-48.

Crowder, D. W., and Diplas, P. (2000). "Using Two-dimensional Hydrodynamic Models at Scales of Ecological Importance." *Journal of Hydrology*, 230, 172-191.

Culvenor, D. S. (2002). "TIDA: An Algorithm for Delineation of Tree Crowns in High Spatial Resolution Remotely Sensed Imagery." *Computers & Geosciences*, 28, 33-44.

Devereux, B., and Amable, G. (2009). "Airborne LiDAR: Instrumentation, Data Acquisition and Handling." Laser Scanning for the Environmental Sciences, G. L. Heritage and A. R. G. Large, eds., Wiley-Blackwell, Chichester, 102-114.

Downes, B. J., Lake, P. S., Schreiber, E. S. G., and Glaister, A. (2000). "Habitat Structure, Resources, and Diversity: The Separate Effects of Surface Roughness and Macroalgae on Stream Invertebrates." *Oecologia*, 123, 569-581.

Entwistle, N. S., and Fuller, I. C. (2009). "Terrestrial Laser Scanning to Derive Surface Grain Size Facies Character of Gravel Bars." Laser Scanning for the Environmental Sciences, G. L. Heritage and A. R. G. Large, eds., Wiley-Blackwell, Chichester, 102-114.

Glenn, N. F., D. R. Streutker, D. J. Chadwick, G. D. Thackray, and S. J. Dorsch. (2006). "Analysis of LiDAR-derived Topographic Information for Characterizing and Differentiating Landslide Morphology and Activity." *Geomorphology*, 73, 131-148.

Gorman, O. T., and Karr, J. R. (1978). "Habitat Structure and Stream Fish Communities." *Ecology*, 59(3), 507-515.

Heritage, G., and Hetherington, D. (2007). "Towards a Protocol for Laser Scanning in Fluvial Geomorphology." *Earth Surface Processes and Landforms*, 32(1), 66-74.

Hetherington, D., German, S., Utteridge, M., Cannon, D., Chisholm, N., and Tegzes, T. (2007). "Accurately Representing a Complex Estuarine Environment Using Terrestrial Lidar." *Remote Sensing and Photogrammetry Society Annual Conference*.

Hodge, R., Brasington, J., and Richards, K. (2009). "In Situ Characterization of Grain-scale Fluvial Morphology using Terrestrial Laser Scanning." *Earth Surface Processes and Landforms*, 34, 954-968.

InnovMetric. (2008). "PolyWorks." Ver. 10.1.6, Quebec, Canada.

Kaufmann, P. R., and Robison, E. G. (1998). "Physical Habitat Characterization." *Environmental Monitoring and Assessment Program-Surface Waters: Field Operations and Methods for Measuring the Ecological Condition of Wadeable Streams*, United States Environmental Protection Agency, Washington, D.C.

Kozarek, J. L., W. C. Hession, C. A. Dolloff, P. Diplas. (In Press). "Hydraulic Complexity Metrics for Evaluating In-stream Brook Trout Habitat." *Journal of Hydraulic Engineering*.

Legleiter, C. J., Roberts, D. A., Marcus, W. A., and Fonstad, M. A. (2004). "Passive Optical Remote Sensing of River Channel Morphology and In-stream Habitat: Physical Basis and Feasibility." *Remote Sensing of Environment*, 93, 493-510.

Lichti, D. D., and Jamtsho, S. (2006). "Angular Resolution of Terrestrial Laser Scanners." *The Photogrammetric Record*, 21(114), 141-160.

Marchamalo, M., Bejarano, M.-D., Jalon, D. G., and Marin, R. M. (2007). "Fish Habitat Characterization and Quantification using LIDAR and Conventional Topographic Information in River Survey." *Remote Sensing for Agriculture, Ecosystems, and Hydrology IX, Proceedings of SPIE*, 6742, 1-12.

MathWorks. (2009). "MATLAB." Ver. R2009b, Natick, MA.

Milan, D. J. (2009). "Terrestrial Laser Scan-derived Topographic and Roughness Data for Hydraulic Modelling of Gravel-bed Rivers." Laser Scanning for the Environmental Sciences, G. L. Heritage and A. R. G. Large, eds., Wiley-Blackwell, Chichester, 133-146.

Optech. (2010). "Technical Overview - ILRIS-3D Specifications." <http://www.optech.ca/i3dtechoverview-ilris.htm> Accessed March 2010.

Peckarsky, B. L., Taylor, B. W., and Caudill, C. C. (2000). "Hydrologic and Behavioral Constraints on Oviposition of Stream Insects: Implications for Adult Disperal." *Oecologia*, 125, 186-200.

Roghair, C. N., Dolloff, C. A., and Underwood, M. K. (2002). "Response of a Brook Trout Population and Instream Habitat to a Catastrophic Flood and Debris Flow." *Transactions of the American Fisheries Society*, 131, 718-730.

Rosser, N. J., Petley, D. N., Lim, M., Dunning, S. A., and Allison, R. J. (2005). "Terrestrial Laser Scanning for Monitoring the Process of Hard Rock Coastal Cliff Erosion." *Quarterly Journal of Engineering Geology and Hydrogeology*, 38, 363-375.

Sanson, G. D., Stolk, R., and Downes, B. J. (1995). "A New Method for Characterizing Surface Roughness and Available Space in Biological Systems." *Functional Ecology*, 9(1), 127-135.

Shen, Y., and Diplas, P. (2008). "Application of Two- and Three-dimensional Computational Fluid Dynamics Models to Complex Ecological Stream Flows." *Journal of Hydrology*, 348(1-2), 195-214.

Smith, M. W., Cox, N. J., and Bracken, L. J. (2007). "Applying Flow Resistance Equations to Overland Flows." *Progress in Physical Geography*, 31(4), 363-387.

Straatsma, M. W., Warmink, J. J., and Middelkoop, H. (2008). "Two Novel Methods for Field Measurements of Hydrodynamic Density of Floodplain Vegetation using Terrestrial Laser Scanning and Digital Parallel Photography." *International Journal of Remote Sensing*, 29(5), 1595-1617.

Topcon. (2010). "Topcon: GTS-230W Specifications." <http://www.topconpositioning.com/applications/forensic-mapping/optical-products/gts-230w.html> Accessed March 2010.

Venter, O., Grant, J. W. A., Noel, M. V., and Kim, J. (2008). "Mechanisms Underlying the Increase in Young-of-the-year Atlantic Salmon (Salmo salar) Density with Habitat Complexity." *Canadian Journal of Fisheries and Aquatic Sciences*, 65, 1956-1964.

Wang, L., Simonson, T. D., and Lyons, J. (1996). "Accuracy and Precision of Selected Stream Habitat Estimates." *North American Journal of Fisheries Management*, 16, 340-347.

Wedding, L. M., Friedlander, A. M., McGranaghan, M., Yost, R. S., and Monaco, M. E. (2008). "Using Bathymetric Lidar to Define Nearshore Benthic Habitat Complexity: Implications for Management of Reef Fish Assemblages in Hawaii." *Remote Sensing of Environment*, 112, 4159-4165.

Wesche, T. A., Goertler, C. M., and Frye, C. B. (1987). "Contribution of Riparian Vegetation to Trout Cover in Small Streams." *North American Journal of Fisheries Management*, 7(1), 151-153.

Willis, S. C., Winemiller, K. O., and Lopez-Fernandez, H. (2005). "Habitat Structural Complexity and Morphological Diversity of Fish Assemblages in a Neotropical Floodplain River." *Oecologia*, 142, 284-295.

4.0 Quantifying and Utilizing Uncertainty in Stream Restoration Design

Jonathan P. Resop, W. Cully Hession, and Teresa M. Wynn

Abstract

Public agencies spend significant funds on stream restoration projects to improve the quality of impaired stream reaches. Many sources of uncertainty can potentially influence the final design, such as the natural stochasticity of input variables, the measurement of variables in the field, and the uncertainties inherent to the parameters and conceptualizations of the equations used for the design model. For this study, a two-phase uncertainty analysis was performed on a two-stage channel stream restoration design for Stroubles Creek in Blacksburg, VA, USA. Monte Carlo Simulation was used to calculate a range of channel dimensions including channel width, channel depth, bench width and bench flow depth from stochastic variables, such as bankfull discharge and grain size distribution, and calculated parameters, such as Manning's n and critical Shield's number. Results of this research indicate the final stream restoration design outcomes can vary over one to four orders of magnitude with respect to the deterministic solution, reinforcing the high uncertainty and risk associated with stream restoration.

Keywords

Stream restoration design, Uncertainty analysis, Stochastic variability, Knowledge errors, Monte carlo simulation

Manuscript Note

This manuscript will be submitted to the Journal of the American Water Resources Association.

4.1 Introduction

As the public has become more aware of the declining ecological health of impaired and channelized streams as a result of agricultural and urban impacts, there has been increased interested in stream restoration. In the United States, approximately one billion dollars is spent each year on various restoration projects (Bernhardt et al. 2005). These projects can be defined by goals ranging from bank stabilization to water quality management to ecological restoration (Kauffman et al. 1997; Shields et al. 2003; Wheaton et al. 2008). Many restoration goals are qualitative in nature, which makes it difficult to set quantitative measures of design effectiveness (Kondolf 1995; Kondolf 1996; Johnson and Brown 2001; Lemons and Victor 2008). Restoration projects are also affected by multiple sources of error and variability that create uncertainty in the final design, most of which is not fully incorporated or quantified (Wilcock 2004). Ineffective stream restoration design can lead to severe consequences, such as excessive costs and design failure (Niezgoda and Johnson 2007).

The qualitative nature of many stream restoration projects has the potential for many different sources of uncertainty. Graf (2008) classified uncertainty into four general categories: uncertainty in restoration theory, uncertainty in the research process, uncertainty in the communication of results, and scientific bias. Johnson and Brown (2001) characterized uncertainties in stream restoration as either model uncertainty, parameter uncertainty, randomness, and human error. In general, uncertainty in any modeling project or engineering design can be grouped into two classes: natural stochasticity (both spatial and temporal variability) and knowledge uncertainty (MacIntosh et al. 1994; Hession and Storm 2000). Knowledge uncertainty can be further divided into model error (resulting from our assumptions and representation of the system) and parameter error (resulting from measurement and interpolation errors). Due to the many different types of uncertainty, it is difficult for designers to determine how much each uncertainty contributes to the overall project.

Many sources of uncertainty exist when designing and implementing stream restoration projects. When looking at a engineered stream restoration project, the input variables used for calculating dependant design variables such as channel width and height experience a degree of variability. One of the most important parameters for channel design is the channel-forming discharge, however this discharge is difficult to measure directly and is commonly estimated using similar discharge analogs such as bankfull discharge, effective discharge, or discharge at

some recurring time interval (Shields et al. 2003; Doyle et al. 2007). The rating curve relating discharge to stage is also affected by natural variability and measurement error (Stewardson and Rutherfurd 2008). Other uncertainties in the independent design parameters include measurement errors (cross-section, slope and grain size distribution) and model errors (Manning's n and Shield's number) (Wilcock 2004; Stewardson and Rutherfurd 2008).

Uncertainty analysis provides a method for quantifying the amount of variability in model results and project outcomes. One method of uncertainty analysis commonly used is Monte Carlo Simulation (MCS). MCS is a technique where many different iterations of a model are performed using different values for the input variables (taken from a distribution of values) to derive a distribution of possible output values. The result is a range of possible values or confidence interval (CI) instead of a single deterministic output. MCS has been applied successfully for many hydrological and ecological applications, such as watershed modeling (Hession and Storm 2000; Shirmohammadi et al. 2006) and population dynamics modeling (Skarpaas et al. 2005). Recently, Stewardson and Rutherfurd (2008) applied MCS to stream restoration project designed to quantify the volume of water needed to flush fine sediment. The authors looked at the uncertainty associated with design parameters, noted a large amount of uncertainty due to hydraulic modeling, and recommended using larger measurement sample sizes as a way to reduce uncertainty. However, more research is needed to further expand the knowledge of how different variables and errors affect stream restoration design.

The objective of this research is to investigate the uncertainty associated with two-stage channel stream restoration design. Specifically, the uncertainty in design parameters such as bench width and bench flow depth will be quantified using a two-phase MCS. The two-phase MCS will allow for the separate classes of uncertainty (stochastic variability and knowledge error) to be analyzed individually. Finally, this paper will explore the implications of uncertainty in management and design practices.

4.2 Methods

Study Site

The study site for the stream restoration design uncertainty analysis was a reach of Stroubles Creek in Blacksburg, VA (Fig. 4.1). Stroubles Creek is on the USEPA's 303(d) list of impaired streams due to bacterial contamination (Benham et al. 2003). The stream reach is also

currently undergoing a TMDL implementation plan for reducing sediment load due to streambank erosion by 77% (Yagow et al. 2006). In 2009, a stream restoration project was designed and implemented to restore a 0.5 km section of the stream (Smith 2009). The restored section has a drainage area of approximately 17.1 km^2. Stroubles Creek is located downstream of the town of Blacksburg and Virginia Tech's main campus, and is influenced by both agricultural and urban impacts. Stroubles Creek has also been the site of other hydraulic research, such as measuring streambank retreat with erosion pins (Utley and Wynn 2008) and terrestrial laser scanning (TLS) (Resop and Hession In Press), and calculating streambank erodibility and critical shear stress (Wynn et al. 2008). In addition, a stage-discharge curve over the past five years has been developed, and suspended sediment concentration and flow have been sampled for various storm events.

Figure 4.1. Site of stream restoration project at Stroubles Creek in Blacksburg, VA. Image taken from Virginia state orthophotos in 2006.

Stream Restoration Design

The primary goals of the restoration project were to improve the ecological integrity of Stroubles Creek and to remove it from the list of impaired waters using a two-stage channel design. The two-stage design incorporates two levels of streamflow: the first level for channel-forming discharge and the second level for floodplain discharge (Fig. 4.2) (NRCS 2007b). Separating the two channels are benches that serve to stabilize the main channel during baseflow conditions and provide a surface for when flow enters the floodplain. In our case, the first stage was designed to handle the "natural" bankfull flows expected in a watershed this size within the Valley and Ridge Physiographic province (Keaton et al. 2005) and the second stage was designed to handle what we have observed to be the existing "urban" bankfull flow. The design assumed a 3:1 (horizontal to vertical) bank slope. Grass and brush vegetation were planted on the bank and bench surfaces to provide stability and habitat.

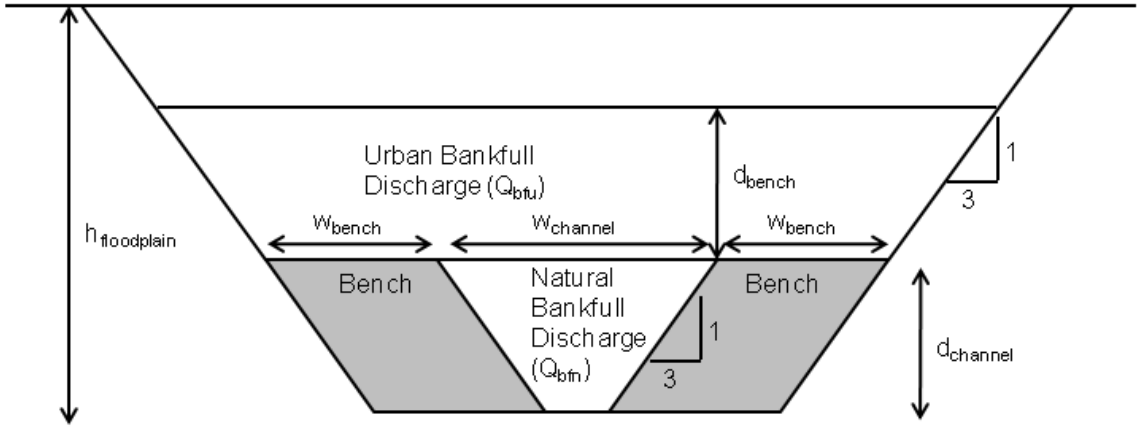

Figure 4.2. Cross-section diagram illustrating the general layout of the two-stage channel design, adapted from NRCS (2007b).

The design outcomes for stream restoration typically include width, depth, slope, and planform (NRCS 2007a). For this study, slope and planform were held constant to minimize impact to floodplain wetlands and because the sinuosity was similar to a reference reach. Design variables of width and depth are generally solved for using independent parameters such as water discharge, sediment discharge, bank composition, and bed composition (NRCS 2007a). Sediment discharge was unknown for this study and so the methodology relied on measures and estimates of the other three parameters. In relation to the two-stage channel design, the design variables

were defined as channel width ($w_{channel}$), channel depth ($d_{channel}$), bench width (w_{bench}), and bench flow depth (d_{bench}) (Fig. 4.2). For this restoration design, floodplain elevation ($h_{floodplain}$) was held constant based on site topography.

The specific design objectives for this stream restoration project were:

1. The "natural" bankfull discharge (Q_{bfn}) defines the stage one channel dimensions.
2. The "altered" or "urban" bankfull discharge (Q_{bfu}) inundates the stage two benches.
3. Bed particle sizes larger than D_{84} are not transported by either discharge (Q_{bfn} and Q_{bfu}).
4. The sum of channel depth and bench flow depth is less than or equal to floodplain height.

When using analytical methods for stream restoration design, two types of equations are typically utilized: 1) hydraulic resistance equations; and 2) sediment transport equations (NRCS 2007a). Manning's equation (1) and the continuity equation (2) were used together for the hydraulic resistance equations, defined as:

$$V = \frac{1}{n} R_h^{2/3} S^{1/2} \quad (1)$$

$$Q = VA \quad (2)$$

where V is the channel velocity (m/s), n is Manning's coefficient, R_h is the hydraulic radius (m), S is the slope (0.004 m/m), Q is the discharge (m^3/s) and A is the cross-sectional area (m^2).

Sediment transport was modeled by comparing the critical shear stress from Shield's entrainment function (3) and the average shear stress (4). Sediment moves if $\tau_{average}$ is greater than $\tau_{critical}$, so the design solution was iteratively solved until $\tau_{average} = \tau_{critical}$. One of the objectives of this restoration project was to design a threshold channel: sediment smaller than the D_{84} would be moved by the average shear stress at both stage flows while larger sediment would remain stationary. Shield's entrainment function was defined as:

$$\tau_{critical} = (\rho_{sediment} - \rho_{water}) g D_{84} \tau^* \quad (3)$$

where $\tau_{critical}$ is the critical shear stress (Pa), $\rho_{sediment}$ is the density of the bed sediment (2850 kg/m^3), ρ_{water} is the density of water (1000 kg/m^3), g is gravity (9.8 m/s^2), D_{84} is the 84th quantile of the grain size distribution, and τ^* is the critical Shield's number or dimensionless shear stress number (Stewardson and Rutherfurd 2008). The average shear stress of the stream was calculated from the equation:

$$\tau_{average} = \rho_{water} g R_h S \quad (4)$$

where $\tau_{critical}$ is the average shear stress (Pa), ρ_{water} is the density of water (1000 kg/m^3), R_h is the hydraulic radius (m), and S is the slope (0.004 m/m).

The dimensions of both channels in the two-stage design (the Q_{bfn} channel and the Q_{bfu} channel) were defined based on the process shown in Fig. 4.3. The two channels were designed sequentially: first the Q_{bfn} channel and then the Q_{bfu} channel. A value for channel-forming discharge was selected and the initial Q_{bfn} channel dimensions (channel width) were set. We then solved for channel depth using the hydraulic resistance equations (1 and 2). Once depth was determined, the values for both critical and average shear stress were calculated using the sediment transport equations (3 and 4) and then compared. If the difference between the two shear stress values was above a minimum threshold (0.1 Pa), then the channel width was incremented or decremented by a small amount (0.05 m) and the process repeated with the hydraulic resistance equations to resolve for depth. The process finished when the critical and average shear stresses were approximately equal, and the final values for depth and width were used for the design channel dimensions.

Once the dimensions for the Q_{bfn} channel were optimized, the design process continued to solve for the dimensions of the Q_{bfu} channel. The channel width and depth for the first stage were held constant using the median values calculated from the stage one uncertainty analysis. Bench width and bench flow depth for the second stage were optimized using the same method as the first stage (Fig. 4.3). Once the final channel dimensions were determined the last objective was tested by comparing the floodplain height to the sum of channel depth and bench flow depth.

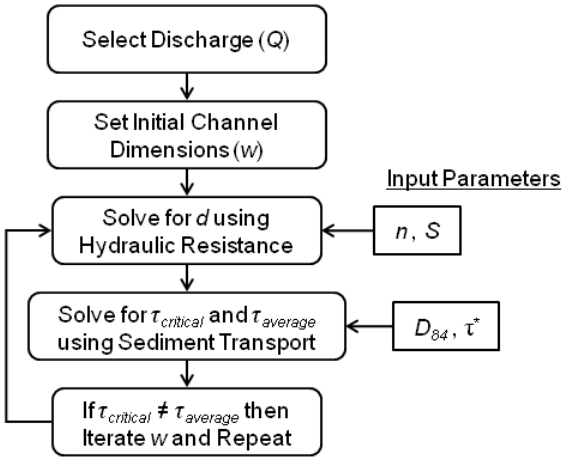

Figure 4.3. Flowchart of the stream restoration design process, culminating with the design outcomes: width and depth. This process was applied to both channel stages in the two-stage design.

Uncertainty Analysis

MCS was used for quantifying the uncertainty in the calculations for channel width, channel depth, bench width, and bench flow depth. A two-phase MCS was implemented based on the methods used by Hession and Storm (2000) (Fig. 4.4). The primary purpose of the two-phase analysis was to explore the variability associated with both types of uncertainty (stochastic variability and knowledge error) separately, since knowledge error can be reduced, but stochasticity is a property of the natural world (Hession and Storm 2000). A nested, two-step iteration was performed. A set of values from the stochastically variable parameters were selected from their respective distributions. This was followed by selecting m = 1000 sets of values at random from the knowledge uncertain parameters (n and τ^*). For each iteration the design process was performed with the selected values. This method was repeated for n = 100 iterations of different stochastically variable parameters (Q and D_{84}). The resulting output from the design calculations was a distribution of complementary cumulative distribution functions (CCDFs) for the design outcomes. CCDFs are functions that define the probability that a certain value will be exceeded (Helton and Shiver 2007).

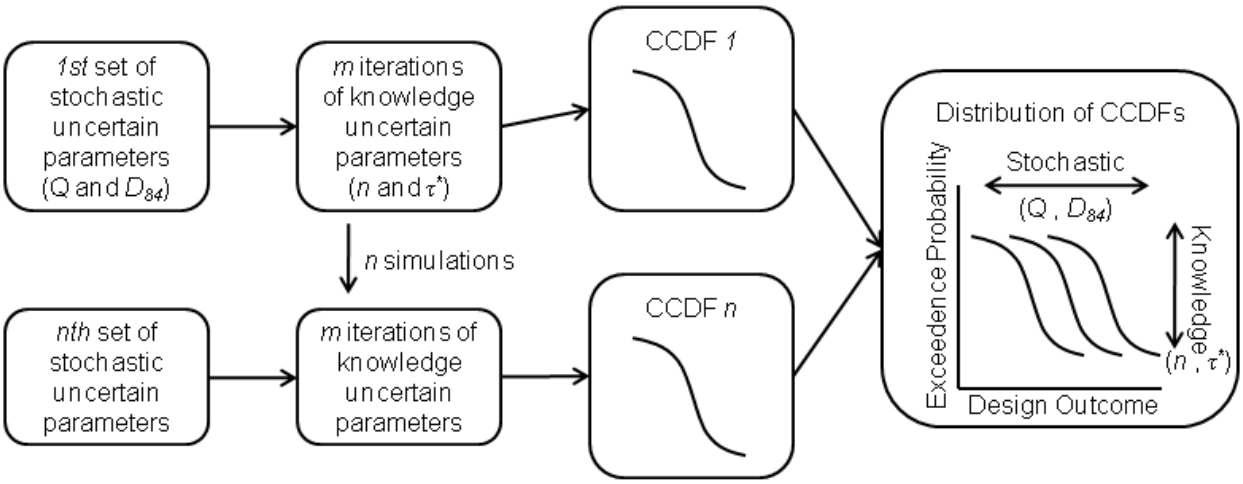

Figure 4.4. The two-phase MCS uncertainty process separating stochastic variability and knowledge error resulting in a distribution of complementary cumulative distribution functions (CCDFs), adapted from Hession et al. (1996).

The distribution of potential values for each input parameter was used for performing the multiple simulations of the design process. Latin hypercube sampling (LHS) was used to select a value for each input parameter during each simulation. LHS divides the probability distribution

function of each input parameter into *n* equal probability intervals and then selects a value at random from each interval.

Stochastic Variability

While there are numerous design parameters that could be considered stochastic in nature (spatially and temporally), we chose to include only bed particle size and design flows for this analysis (Table 4.1). Other obviously varying parameters such as stream cross-section and slope were assumed constant or deterministic.

Grain size distribution is a parameter commonly measured in the field using a method such as the Wolman pebble count (Wolman 1954). The researcher in the field selects 100 random grains from the stream bed and measures the diameter based on the intermediate axis. This is a parameter that can exhibit both stochastic variability (since the grain distribution varies over the length of the stream) and measurement error (due to bias and errors made by the researcher) (Stewardson and Rutherfurd 2008). For this study, a Wolman pebble count was implemented within a riffle of Stroubles Creek. A lognormal distribution was fit to the measured values of grain size. For each run of the MCS, a sample of 100 grain sizes was generated from this distribution randomly. The 84th quantile of grain size (D_{84}) was then calculated and used as an input parameter for the design process.

The selection of a value for bankfull, or channel-forming, discharge is particularly difficult due to the uncertainty involved in defining the parameter, as discussed earlier. There are also many different methods for approximating the bankfull discharge for a stream restoration design, such as using regional curves, hydrologic frequency analysis, hydraulic modeling with Manning's equation, applying stage-discharge rating curves, comparing with a reference reach, etc. For this study, the distribution of possible values for channel-forming discharge was based on the 95% CI of bankfull discharge values from the regional curves developed for the Valley and Ridge Physiographic region (Keaton et al. 2005).

Table 4.1. Input parameters and associated distributions used for Monte Carlo Simulations. Histograms for each distribution can be found in Appendix C.

Input Parameter	Distributions for Q_{bfn} Channel (Stage 1)	Distributions for Q_{bfu} Channel (Stage 2)
Stochastic Variability		
Bed Grain Size (D_{84}) (mm)	Lognormal (2.5, 0.52) [a]	
Event Discharge (Q) (m^3/s)	Triangular (1.8, 5.6, 15.6) [b]	Triangular (4.7, 8.5, 18.5) [b]
Knowledge Error		
Critical Shield's Number, τ^*	Triangular (0.03, 0.045, 0.06) [b]	
Manning's n	Normal (0.023, 0.00025) [c]	Uniform (0.025, 0.160) [d]

[a] Lognormal Distribution (mean, standard deviation)

[b] Triangular Distribution (min, mode, max)

[c] Normal Distribution (mean, standard deviation)

[d] Uniform Distribution (min, max)

Knowledge Error

There are numerous examples of knowledge error in stream restoration design that range from pure measurement error (slopes, cross-sectional parameters, bed grain size distributions) and parameters estimated for the hydraulic and sediment transport equations that are difficult to directly measure (such as Manning's n and critical Shield's number). For this analysis, we chose to focus on errors associated with estimating Manning's n and critical Shield's number (Table 4.1). Calibration of these parameters is possible with intensive field measurements and calculations, but these methods are either not feasible or simply not performed for most restoration designs. These parameters can also exhibit a degree of stochastic variability within the stream reach (both spatial and temporal). As a result, Manning's n and critical Shield's number are generally estimated for most applications. For this study, the distribution of the critical Shield's number was based on the range of values discussed by Buffington and Montgomery (1997).

Manning's n was defined for the surfaces of both channel stages. For the natural bankfull discharge channel, the distribution of n was calculated using Strickler's equation (5), defined as:

$$n = \frac{1}{21.1} D_{50}^{1/6} \quad (5)$$

where D_{50} is the 50th quantile of the grain size distribution (Ghani et al. 2007). The distribution of n was estimated by fitting a normal curve to the median value of 1000 randomly generated samples of 100 particles using the grain size distribution from Table 4.1. For the floodplain

bench and bank, values for n were primarily a function of vegetation. A uniform distribution was used based on the min and max values selected from Chow (1959), ranging from short grass to dense brush. Manning's n for the entire floodplain discharge channel was calculated as a weighted average of n's from both sections using Pavlovskii's equation (6):

$$n_e = \left(\frac{\sum_i^N (P_i n_i^2)}{P}\right)^{1/2} \quad (6)$$

where n_e is the equivalent Manning's n for the channel, P_i is the wetted perimeter of section i, n_i is the Manning's roughness value for section i, and P is the total wetted perimeter of the channel (Djajadi 2009).

4.3 Results and Discussion

Deterministic Design Solutions

The deterministic solution for the stream restoration design was calculated using the expected values for each of the input parameters (Q, D_{84}, n, and τ^*) (Table 4.2). The final two-stage channel dimensions meet all of the objectives of the restoration project. However, there is no consideration for the natural variability of hydrologic or hydraulic parameters, and no information is provided to allow for selecting design variables based on a level of risk the engineer or manager is willing to take (Hession and Storm 2000).

Table 4.2. The design solutions for channel dimensions based on the expected value of the input parameters.

	Input Parameters				Deterministic Design Solutions		
	Q (m^3/s)	D_{84} (mm)	n	τ^*	w (m)	d (m)	τ_{ave} (Pa)
Stage 1 (Q_{bfn})	5.6	21	0.023	0.045	9.0	0.47	17.05
Stage 2 (Q_{bfu})	8.5	21	0.086	0.045	19.6	0.33	17.22

Uncertainty Design Solutions

Natural Bankfull Discharge Channel (Stage 1)

Both the width and depth outcomes for the first channel stage exhibited a wide range of values over the 100,000 simulations performed by MCS (Figs. 4.5 and 4.6). Approximately 7% of the simulations failed to find a solution for width and depth due to the particular combination of input parameters generally occurring at very low discharges. Based on the combined CCDF for all simulations, the 95% CIs for width and depth were 6.0 to 30.6 m and 0.29 to 0.69 m, respectively. The sizes of the 95% CIs were approximately 2.7 times the width and 1.2 times the

depth of the deterministic solution. The variability in possible design outcomes represents a significant amount of uncertainty in the design process.

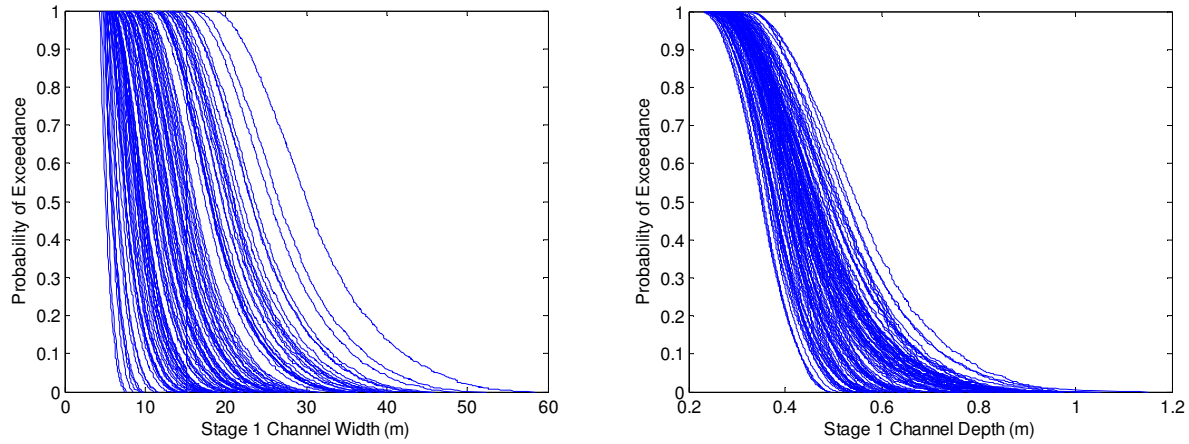

Figure 4.5. Distribution of CCDFs for the Q_{bfn} channel dimensions of a) width and b) depth.

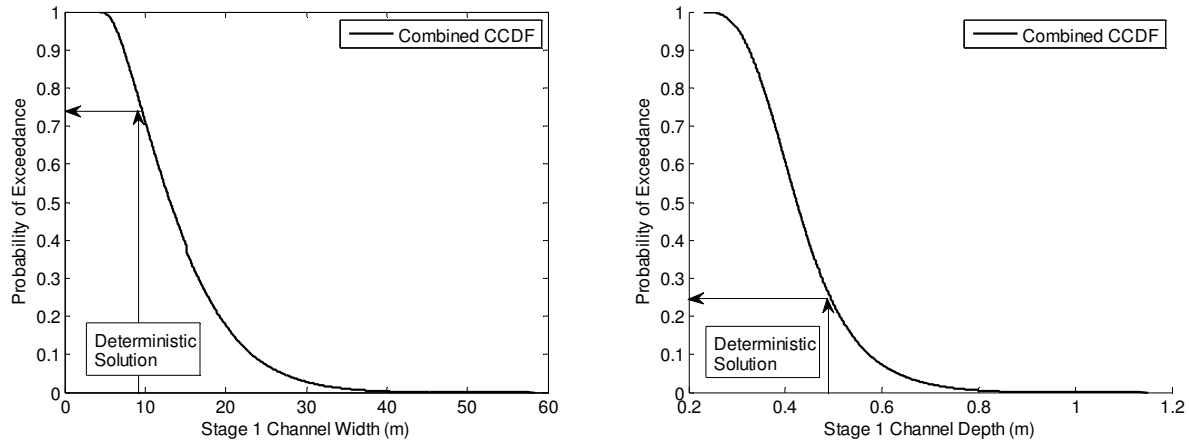

Figure 4.6. Combined CCDFs for the Q_{bfn} channel dimensions of a) width and b) depth.

The uncertainty due to stochastic variability (Q and D_{84}) based on the median value from each CCDF curve had a 95% CI size of 19.8 m for width and 0.17 m for depth (Fig. 4.7). The uncertainty from the knowledge error parameters (n and τ^*) can be determined by taking the median values of the min, max, and CI for each CCDF. For the knowledge uncertainty parameters, the magnitude of the 95% CI was 12.0 m for width and 0.30 m for depth. These results demonstrate that both sources of uncertainty contribute to the overall variability in the design. There is greater stochastic uncertainty in channel width calculations and greater

knowledge uncertainty in channel depth calculations. Also, the overall variability due to all sources of uncertainty (a 95% CI size of 24.6 m for width and 0.40 m for depth) is much more than each source individually, representing how the errors propagate to the total uncertainty.

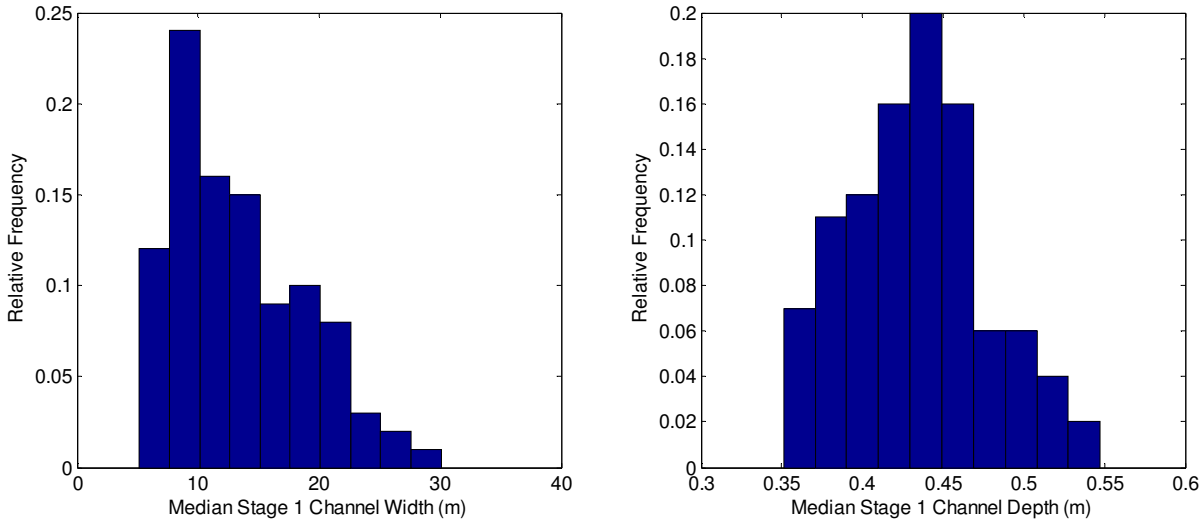

Figure 4.7. Histogram of median values from each CCDF curve, representing the uncertainty in stochastic variability, for the Q_{bfn} channel dimensions of a) width and b) depth.

Urban Bankfull Discharge Channel (Stage 2)

The second stage channel dimensions were determined assuming the median values for the first stage channel dimensions (width = 12.3 m and depth = 0.43 m). Similar to the first stage MCS, 5% of the simulations failed to solve for a design solution, typically for low flows. All of the simulations for the second stage met the design objective of having the total channel height less than the floodplain height (estimated as 1.17 m from nine measured cross sections). Once again, the simulated design solutions from MCS show a wide range in possible values for both bench width and bench flow depth (Figs. 4.8 and 4.9). The 95% CIs for bench width and bench flow depth are 1.7 to 84.1 m and 0.11 m to 0.43 m, respectively. The range of possible design bench width outcomes is 4.2 times greater than the expected deterministic solution. This magnitude is more significant when one considers that the bench width accounts for only one bench and must be multiplied by two for the width of both benches in the two-stage channel. Similarly, the size of the 95% CI for bench flow depth is 97% of the deterministic bench flow depth solution.

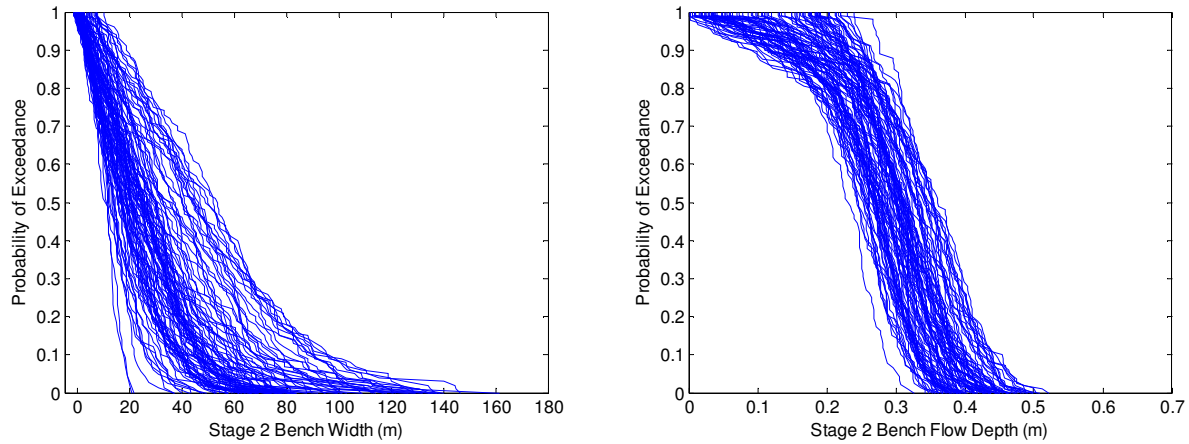

Figure 4.8. Distribution of CCDFs for the Q_{bfu} channel dimensions of a) bench width and b) bench flow depth. (Note: These results include only 10,000 simulations of MCS.)

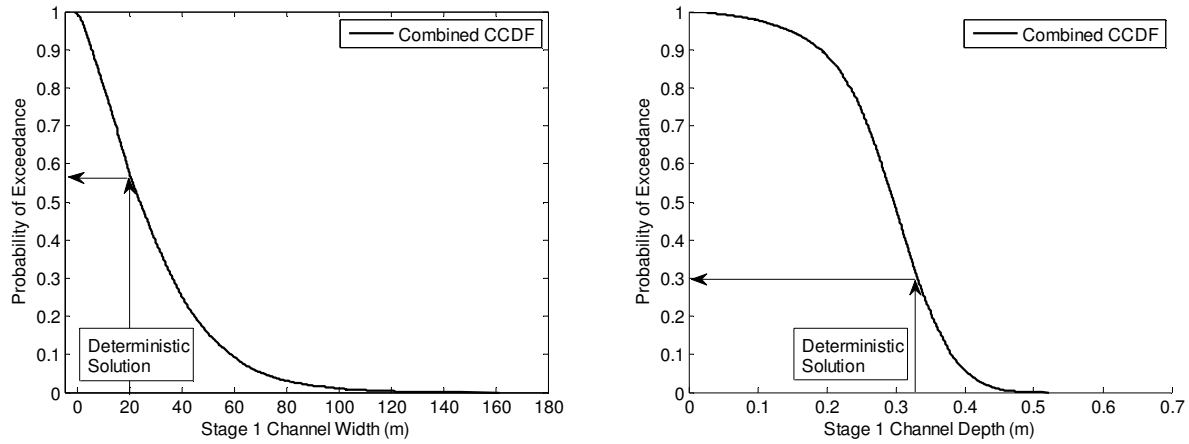

Figure 4.9. Combined CCDFs for the Q_{bfu} channel dimensions of a) bench width and b) bench flow depth.

The distribution of median values from each of the CCDF curves is shown in Fig. 4.10, representing the uncertainty in stochastic variability. For the stochastically variable parameters, the length of the 95% CI was 38.8 m for bench width and 0.11 m for bench flow depth. For the knowledge uncertain parameters the length of the 95% CI was 60.7 m for bench width and 0.26 m for bench flow depth. In both cases the uncertainty due to the knowledge parameters (n and τ^*) is greater than the stochastically variable parameters. This is likely a result of the larger variability allowed for Manning's roughness on the channel bench due to the effect of vegetation.

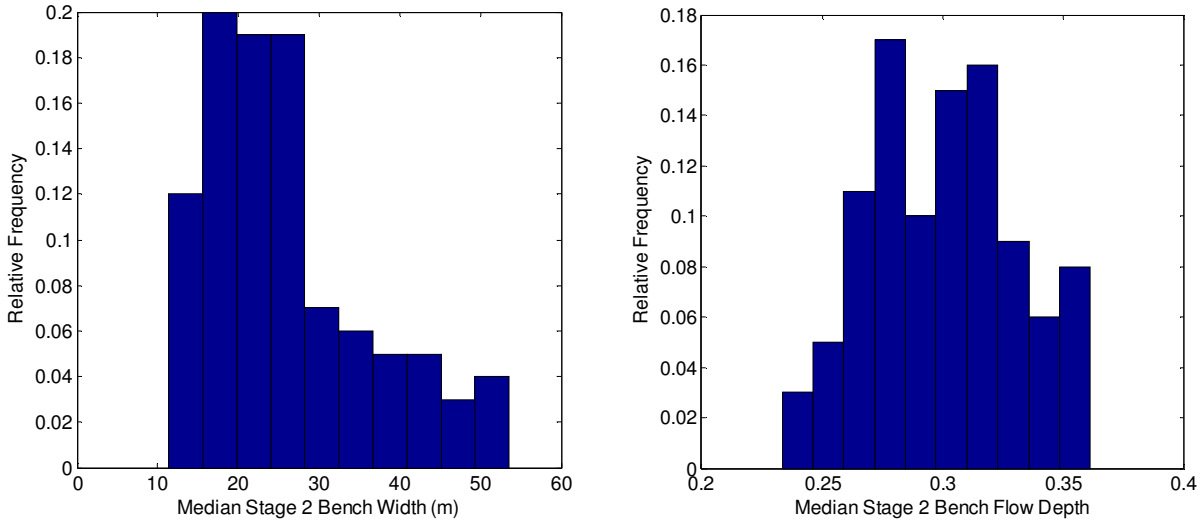

Figure 4.10. Histogram of median values from each CCDF curve, representing the uncertainty in stochastic variability, for the Q_{bfu} channel dimensions of a) bench width and b) bench flow depth.

The wide range of possible design solutions for both channel stages has serious implications for stream restoration designers. For example, one of the criteria for this stream restoration design is that sediment larger than the D_{84} grain size is not transported by either discharge event. The deterministic design model calculated a critical shear stress for this threshold of 17.22 Pa. However, based on the MCS performed, 40% of the design solutions had average shear stress values that exceeded this amount. A greater average shear stress leads to more bed sediment transported by the channel and a possible failure of the design over time.

For another example, assume that the stream restoration designer sets the bench width to 20 m, similar to the deterministic solution. In this case the simulated results show that 57% of the time the project should call for a longer bench width and lead to a design failure (Fig. 4.9). There could be other factors that might influence how long the bench width is made, such as the existing stream topography, property boundaries, and the cost allowances of the restoration project. By performing uncertainty analysis along with the stream restoration design, one can have a better understanding of the confidence in the final design and calculate the risk involved.

Other Sources of Uncertainty

Only four uncertain parameters were investigated for this study: discharge, grain size distribution, Manning's *n*, and critical Shield's number. Many parameters that experience measurement errors, such as longitudinal slope and stream cross-sections, were all neglected for this study. This type of uncertainty can also include the interpolation errors inherent to creating a complete cross-section of the stream topography from a limited number of measured points. Future research should focus on developing a better understanding of these errors so they can be applied to uncertainty analyses. One potential area of research is to use a high-resolution surveying tool, such as TLS, as a reference dataset to compare with traditional methods such as total station surveying and Wolman pebble counts. Another factor that was not investigated by this research was the effect on uncertainty of temporally stochastic parameters, such as Manning's *n* varying over time as a stream restoration develops with riparian vegetation. These uncertainties, as well as others not mentioned here, should be researched further to more fully quantify the uncertainty involved with stream restoration design projects.

4.4 Summary and Conclusions

In this study we demonstrated how uncertainty principles can be applied to a two-stage channel stream restoration design. The uncertainties associated with four of the input parameters involved with the design process (Q, D_{84}, n, and τ^*) were used to develop a distribution of statistically possible channel dimension design outcomes. The uncertainty analysis described and implemented for a case study involving a restoration on Stroubles Creek in Blacksburg, VA could easily be applied to any stream restoration design project.

There is a significant level of uncertainty involved in developing design options for stream restoration activities. For all design parameters (channel width, channel depth, bench width and bench flow depth) the size of the 95% CI was greater than the value calculated by the deterministic solution by at least one order of magnitude. This demonstrates that a sizeable amount of uncertainty exists when determining channel dimensions for a stream restoration design. It is important for design engineers and managers to "honestly" acknowledge the inherent uncertainties in design, perform uncertainty analyses when possible, and utilize the stochastic results to apply levels of risk to their design choices.

Acknowledgements

Special thanks to everyone involved with the Stroubles Creek restoration project at Virginia Tech, including both those involved with the pre-restoration field work and those involved with the restoration process.

4.5 References

Benham, B., Brannan, K., Dillaha, T., Mostaghimi, S., Wagner, R., Wynn, J., Yagow, G., and Zeckoski, R. (2003). "Benthic TMDL for Stroubles Creek in Montgomery County, Virginia." *Virginia Departments of Environmental Quality, and Conservation and Recreation*, Richmond, Virginia.

Bernhardt, E. S., Palmer, M. A., Allan, J. D., Alexander, G., Barnas, K., Brooks, S., Carr, J., Clayton, S., Dahm, C., Follstad-Shah, J., Galat, D., Gloss, S., Goodwin, P., Hart, D., Hassett, B., Jenkinson, R., Katz, S., Kondolf, G. M., Lake, P. S., Lave, R., Meyer, J. L., and O'Don, T. K. (2005). "Synthesizing U. S. River Restoration Efforts." *Science*, 308, 636-637.

Buffington, J. M., and Montgomery, D. R. (1997). "A Systematic Analysis of Eight Decades of Incipient Motion Studies, with Special Reference to Gravel-bedded Rivers." *Water Resources Research*, 33(8), 1993-2029.

Chow, V. T. (1959). *Open-channel Hydraulics*, McGraw- Hill Book Co., New York.

Djajadi, R. (2009). "Comparative Study of Equivalent Manning Roughness Coefficient for Channel with Composite Roughness." *Civil Engineering Dimension*, 11(2), 113-118.

Doyle, M., Shields, D., Boyd, K. F., Skidmore, P. B., and Dominick, D. (2007). "Channel-forming Discharge Selection in River Restoration Design." *Journal of Hydraulic Engineering*, 133(7), 831-837.

Ghani, A. A., Zakaria, N. A., Kiat, C. C., Ariffin, J., Hasan, Z. A., and Ghaffar, A. B. A. (2007). "Revised Equations for Manning's Coefficient for Sand-bed Rivers." *International Journal of River Basin Management*, 5(4), 329-346.

Graf, W. L. (2008). "Sources of Uncertainty in River Restoration Research." River Restoration: Managing the Uncertainty in Restoring Physical Habitat, S. Darby and D. Sear, eds., John Wiley & Sons, Ltd., Chichester, 15-19.

Helton, J. C., and Shiver, A. W. (2007). "A Monte Carlo Procedure for the Construction of Complementary Cumulative Distribution Functions for Comparison with the EPA Release Limits for Radioactive Waste Disposal." *Risk Analysis*, 16(1), 43-55.

Hession, W. C., and Storm, D. E. (2000). "Watershed-level Uncertainties: Implications for Phosphorus Management and Eutrophication." *Journal of Environmental Quality*, 29(4), 1172-1179.

Hession, W. C., Storm, D. E., and Haan, C. T. (1996). "Two-phase Uncertainty Analysis: An Example Using the Universal Soil Loss Equation." *The Transactions of the ASAE*, 39(4), 1309-1319.

Johnson, P. A., and Brown, E. R. (2001). "Incorporating Uncertainty in the Design of Stream Channel Modifications." *Journal of the American Water Resources Association*, 37(5), 1225-1236.

Kauffman, J. B., Beschta, R. L., Otting, N., and Lytjen, D. (1997). "An Ecological Perspective of Riparian and Stream Restoration in the Western United States." *Fisheries*, 22, 12-24.

Keaton, J. N., Messinger, T., and Doheny, E. J. (2005). "Development and Analysis of Regional Curves for Streams in the Non-Urban Valley and Ridge Physiographic Province, Maryland, Virginia, and West Virginia." *Scientific Investigations Report 2005-5076*, USGS.

Kondolf, G. M. (1995). "Five Elements for Effective Evaluation of Stream Restoration." *Restoration Ecology*, 3(2), 133-136.

Kondolf, G. M. (1996). "A Cross Section of Stream Channel Restoration." *Journal of Soil and Water Conservation*, 51(2), 119-125.

Lemons, J., and Victor, R. (2008). "Uncertainty in River Restoration." River Restoration: Managing the Uncertainty in Restoring Physical Habitat, S. Darby and D. Sear, eds., John Wiley & Sons, Ltd., Chichester, 3-13.

MacIntosh, D. L., II, G. W. S., and Hoffman, F. O. (1994). "Uses of Probablistic Exposure Models in Ecological Risk Assessments of Contaminated Sites." *Risk Analysis*, 14, 405-419.

Niezgoda, S. L., and Johnson, P. A. (2007). "Case Study in Cost-based Risk Assessment for Selecting a Stream Restoration Design Method for a Channel Relocation Project." *Journal of Hydraulic Engineering*, 133(5), 468-481.

NRCS. (2007a). "Alluvial Channel Design." *Part 654 Stream Restoration Design National Engineering Handbook, 210-VI-NEH*, United States Department of Agriculture.

NRCS. (2007b). "Two-stage Channel Design." *Part 654 Stream Restoration Design National Engineering Handbook, 210-VI-NEH*, United States Department of Agriculture.

Resop, J. P., and Hession, W. C. (In Press). "Terrestrial Laser Scanning for Monitoring Streambank Retreat: A Comparison with Traditional Surveying Techniques." *Journal of Hydraulic Engineering*.

Shields, F. D., Copeland, R. R., Klingeman, P. C., Doyle, M. W., and Simon, A. (2003). "Design for Stream Restoration." *Journal of Hydraulic Engineering*, 129(8), 575-584.

Shirmohammadi, A., Chaubey, I., Harmel, R. D., Bosch, D. D., Munoz-Carpena, R., Dharmasri, C., Sexton, A., Arabi, M., Wolfe, M. L., Frankenberger, J., Graff, C., and Sohrabi, T. M. (2006). "Uncertainty in TMDL Models." *Transactions of the ASABE*, 49(4), 1033-1049.

Skarpaas, O., Shea, K., and Bullock, J. M. (2005). "Optimizing Dispersal Study Design by Monte Carlo Simulation." *Journal of Applied Ecology*, 42, 731-739.

Smith, F. M. (2009). "Stroubles Creek Restoration Project," Virginia Tech, Blacksburg, VA.

Stewardson, G. M., and Rutherfurd, I. (2008). "Conceptual and Mathematical Modelling in River Restoration: Do We Have Unreasonable Confidence?" River Restoration: Managing the Uncertainty in Restoring Physical Habitat, S. Darby and D. Sear, eds., John Wiley & Sons, Ltd., Chichester, 61-78.

Utley, B. C., and Wynn, T. M. (2008). "Spatial and Temporal Changes in Bank Retreat Rates in a Small Headwater Stream." *American Geophysical Union*, Fall Meeting.

Wheaton, J. M., Darby, S. E., and Sear, D. A. (2008). "The Scope of Uncertainties in River Restoration." River Restoration: Managing the Uncertainty in Restoring Physical Habitat, S. Darby and D. Sear, eds., John Wiley & Sons, Ltd., Chichester, 21-39.

Wilcock, P. R. (2004). "Sediment Transport in the Restoration of Gravel-bed Rivers." *Proceedings of the 2004 ASCE-EWRI World Water and Environmental Resources Congress, Critical Transactions in Water and Environmental Resource Management*, Salt Lake City, Utah, 1-11.

Wolman, M. G. (1954). "A Method of Sampling Coarse River-bed Material." *Transactions of the American Geophysical Union*, 35(6), 951-956.

Wynn, T. M., Henderson, M. B., and Vaughan, D. H. (2008). "Changes in Streambank Erodibility and Critical Shear Stress due to Subaerial Processes along a Headwater Stream, Southwestern Virginia, USA." *Geomorphology*, 97, 260-273.

Yagow, G., Benham, B., Wynn, T., and Younos, T. (2006). "Upper Stroubles Creek Watershed Draft TMDL Implementation Plan, Montgomery County, Virginia." *Virginia Department of Environmental Quality and the Virginia Department of Conservation and Recreation*, Richmond, Virginia.

5.0 Conclusions and Future Research

5.1 Conclusions

Terrestrial Laser Scanning for Fluvial Applications

TLS has been applied to two fluvial applications: monitoring streambank retreat and quantifying habitat complexity. These applications highlight the ability of TLS to provide accurate, precise measurements of topography for creating high-resolution DEMs. The main limitations of this technology are its inability to measure underwater surfaces and the post-processing involved with the massive datasets TLS produces. However, these limitations can be reduced by proper field methods and continued research in the area of developing algorithms to automate the processing of TLS data, such as the streambank retreat measurements and rock delineation algorithm investigated in this research.

Based on the studies presented here involving these two fluvial applications, the following conclusions can be made about the advantages of TLS over traditional field methods such as total station surveying: 1) TLS can measure a higher density of points in a shorter amount of field time than total station surveying; 2) TLS can be used for measuring small-scale topographic processes, such as monitoring retreat and advance over an entire streambank surface; and 3) TLS can be used for qualitative, unbiased measures in an automated manner for metrics that are normally qualitatively defined in the field, such as percent in-stream rock cover. These advantages make TLS an ideal tool for developing accurate DEMs for geomorphologic and hydraulic models. The high-resolution abilities of TLS also open up the possibility for new models to be developed, such as predicting streambank erosion using TLS data.

Terrestrial Laser Scanning for Uncertainty Analysis

For both applications studied in this research, monitoring streambank retreat and measuring habitat complexity, TLS was used as reference dataset for quantifying the uncertainty in traditional topographic measurements. As a note, the DEMs produced using TLS data are not infallible representations of reality and further research is needed to quantify the error and uncertainty associated with using this technology. However, based on the unparalleled point density that TLS provides, one can use TLS data for investigating and quantifying the measurement and interpolation errors inherent when surveying a limited number of points using a traditional method. Although not fully explored by this research, once these uncertainties have

been quantified, the results can be used to propagate error through reach-level calculations and models.

Initial conclusions can be made about the uncertainty related to applying traditional surveying methods to the geomorphologic calculations used in the applications of monitoring streambank retreat and measuring habitat complexity. In general, point measurements from total station surveying greatly simplified topographic surfaces. In some cases this simplification and the resulting interpolation errors led to an overestimation of volumetric streambank retreat due to an undercut bank and in other cases this led to an underestimation of in-stream rock volume. More work is needed to determine the significance of propagating these errors in larger-scale fluvial applications, such as sediment load calculation and habitat or hydraulic modeling.

Uncertainty Analysis for Fluvial Applications

The last objective of this research involved applying uncertainty analysis to stream restoration design. For this study, different sources of uncertainty (both stochastic variability and knowledge uncertainty) were implemented into a MCS for determining possible design outcomes for a two-stage channel stream restoration. The results show that the channel dimension variability ranged from one to four orders of magnitude compared to the deterministic solution. This variability makes it difficult for a researcher or engineer to decide on the "correct" design. However, through uncertainty analysis one can quantify the level of confidence in a selected design outcome and perform risk analysis that accounts for the probability of design failure.

5.2 Future Research

Terrestrial Laser Scanning for Fluvial Applications

- Further develop post-processing methods for using TLS for fluvial applications. More work is needed in classifying points in datasets as either vegetation or surface. This would aid in the automated development of bare-earth DEMs. This would also support research in deriving habitat complexity metrics such as vegetation density.
- Combine TLS with other remote sensing tools, such as bathymetric scanners, to develop DEMs for complete stream topography. This would help offset one of the primary limitations of TLS (surveying below the water surface) and enhance studies involved with channel change and stream bed complexity.

- Find ways and methods to take advantage of the ability of TLS to create truly 3-D surface models (like TINs) as opposed to simpler 2.5-D surface models (like DEMs) and investigate applications to fluvial systems.
- Develop new models that utilize the high-resolution spatial data capacity of TLS, such as erosion prediction models. TLS data should also be applied to existing models, such as 2-D and 3-D hydraulic models, to determine its feasibility as a data source.

Terrestrial Laser Scanning for Uncertainty Analysis

- Explore and quantify the uncertainty that exists for TLS due to errors associated with surface reflectivity.
- Investigate the use of TLS for creating reference datasets to quantify the measurement and interpolation errors of other surveying methods.
- Research the relationship between point density and model error for various fluvial applications, such as measuring streambank retreat, quantifying habitat complexity, or hydraulic modeling. It would be beneficial to quantify the uncertainty associated with taking limited point measurements and help researchers determine exactly how much resolution is needed for the accuracy they desire.
- Quantify the measurement and interpolation errors that result from using limited point measurements for fluvial applications such as streambank retreat and propagate that error to larger scales. This information can be used to estimate the uncertainty involved with calculations such as reach-level sediment load.
- Apply the research performed here to larger studies, such as measuring streambank retreat along an entire stream reach, to better quantify the statistical significance of measurement and interpolation errors.

Uncertainty Analysis for Fluvial Applications

- Further quantify the uncertainty associated with fluvial applications and apply that knowledge to specific examples. In terms of measurement and interpolation errors, the reality is that people will continue to use traditional method of surveying due to the high cost of TLS. The uncertainties due to these errors, and others, need to be applied to models and designs so researchers can determine levels of confidence in model results.

- Further investigate the uncertainties involved with stream restoration design. The study performed here only looked at four parameters as sources of uncertainty in design outcomes. However, many other sources of uncertainty have been identified in the literature. These uncertainties need to be quantified and applied to the design process.

Appendix A - Erosion Pin Streambank Retreat Measurements

A.1 Background

This is an addendum to Chapter 2, "Terrestrial Laser Scanning for Monitoring Streambank Retreat: A Comparison with Traditional Surveying Techniques", which is in press to be published in the Journal of Hydraulic Engineering.

Erosion pins were inserted along a 400-m length of Stroubles Creek for a separate research study (Utley and Wynn 2008). They were inserted into eroding banks on the outside curve of meander bends, approximately 2 m between pins down the length of the stream and 0.3 m between pins from the top of bank to the edge of water at baseflow. The pins were assessed monthly from August 2005 to May 2007 by measuring the length of pin exposed from the bank. Stainless steel rods with a diameter of 6 mm and a length of 50 cm were used for the erosion pins.

The data from the erosion pins was originally intended to be added to the paper that was submitted to the Journal of Hydraulic Engineering, but we did not have time to add the analysis to the final accepted paper. The following is a brief summary of the methods and results.

A.2 Methods

Seven cross sections of erosion pins were installed in the streambank used for this study with on average four pins per cross section and a total of 28 pins over the entire bank face. The erosion pins were measured six times between May 2007 and May 2009 (05/07, 06/07, 01/08, 07/08, 02/09, and 05/09). In general, if a pin was exposed out of the streambank by more than approximately 15 cm, it was reset to 4 cm. Due to the fact that the erosion pin measurements were not performed on the same day as the total station survey and TLS, SBR was compared between the three methods over the entire two year period of the study.

For each cross section of erosion pins, the median SBR value was determined. Total volume change over the entire bank was calculated as a weighted multiplication of the lateral SBR at each cross section, the average bank height, and the distance between cross sections.

A.3 Results and Discussion

Out of the 28 total pins in the streambank, nine were lost or buried over the course of study, leaving 19 pins with values for SBR. For each cross section at least one pin had data.

The median SBR values of the remaining pins generally agreed with the overall measurements made by the total station survey and TLS (Table 1). The largest error between the erosion pins and TLS occurred at cross section 7, where the erosion pins had difficult measuring the simultaneous retreat and advance of the bank at that section. The erosion pins estimated a similar SBR rate for the entire bank as TLS, approximately -0.15 m/yr, compared to the total station survey that overestimated retreat at -0.18 m/yr. When calculating the volumetric retreat over the entire bank, both the erosion pins and total station overestimated the retreat rate compared to TLS (-1.87, -2.10, and -1.60 m^3/yr, respectively). This demonstrates how interpolation errors from a sparse number of point measurements can propagate to errors in calculations such as volume change. These errors can potentially propagate further when making reach- and watershed-scale sediment load calculations.

Table A.1. Measured SBR and volume change over the entire stream bank between May 2007 and May 2009 (Negative = Retreat).

Median SBR (m)			
Cross Section	Erosion Pins	Total Station	TLS
1	-0.24	-0.25	-0.29
2	-0.40	-0.34	-0.39
3	-0.27	No Data	No Data
4	-0.34	-0.40	-0.32
5	-0.37	-0.44	-0.32
6	-0.11	No Data	No Data
7	-0.31	-0.22	-0.08
Volume Change (m^3)			
	-3.73	-4.20	-3.19

A.4 References

Utley, B. C., and Wynn, T. M. (2008). "Spatial and Temporal Changes in Bank Retreat Rates in a Small Headwater Stream." *American Geophysical Union*, Fall Meeting.

Appendix B - MATLAB Code

B.1 Streambank Retreat Measurement

```
%Calculates SBR for each of the total station cross sections.
function [retreat ret_area bank_ret] = bank_ret_xsec(xsec,b,eow)
   %Calculates retreat at cross section b for each of the five time diffs
   %xsec = total station data, eow = edge of water index for each cross section
   %retreat = median SBR, ret_area = cross sectional area of retreat, bank_ret = interpolated retreat values

   %Extract each of six dates from xsec data matrix
   curr = 1;
   i = 4;
   xs = 1;
   while i <= max(size(xsec))
      if (xsec(i,3) < 100)
         i = i + 1;
      else
         bank{xs} = xsec(curr:i-1,:);
         curr = i;
         i = i + 3;
         xs = xs + 1;
      end
   end
   bank{xs} = xsec(curr:max(size(xsec)),:);

   %Convert from xyz coords to dist-elev coords, use 500-500 as ref
   for i = 1:6
      for j = 1:max(size(bank{i}))
         bank{i}(j,4) = sqrt((bank{i}(j,1) - 500)^2 + (bank{i}(j,2) - 500)^2);
      end
   end

   %Loop through 2-1, 3-2, 4-3, 5-4, 6-5 time diffs, calculate retreat
   for i = 1:5
      %Set up banks to be used
      bank_old = [bank{i}(:,4), bank{i}(:,3)];
      bank_old = bank_old(2:eow(b,i),:);
      bank_old = sortrows(bank_old,2); %Should already be sorted high to low
      bank_new = [bank{i+1}(:,4), bank{i+1}(:,3)];
      bank_new = bank_new(2:eow(b,i+1),:);
      bank_new = sortrows(bank_new,2);

      %Iterate y from edge of water to top of bank, use min and max values
      start = max(min(bank_new(:,2)),min(bank_old(:,2)));
      stop = min(max(bank_new(:,2)),max(bank_old(:,2)));
      step = 0.02; %2-cm interval
      j = 1;
      for yi = start:step:stop
         %Interpolate to find values of x
         bank_ret(j,2*i) = yi;
         x_old = linterp(bank_old(:,2),bank_old(:,1),yi); %Interpolate old value
         x_new = linterp(bank_new(:,2),bank_new(:,1),yi); %Interpolate new value
         bank_ret(j,2*i-1) = x_old - x_new;
```

```
        j = j + 1;
    end

    bank_ret(:,2*i) = zero2nan(bank_ret(:,2*i));
    bank_ret(:,2*i-1) = zero2nan(bank_ret(:,2*i-1));

    retreat(i,1) = median(igNan(bank_ret(:,2*i-1)));
    ret_area(i,1) = sum(igNan(bank_ret(:,2*i-1)) * step);
end

%Calculate 6-1, overall retreat
%Set up banks to be used
bank_old = [bank{1}(:,4), bank{1}(:,3)];
bank_old = bank_old(2:eow(b,1),:);
bank_old = sortrows(bank_old,2); %Should already be sorted high to low
bank_new = [bank{6}(:,4), bank{6}(:,3)];
bank_new = bank_new(2:eow(b,6),:);
bank_new = sortrows(bank_new,2);

%Iterate y from edge of water to top of bank, use min and max values
start = max(min(bank_new(:,2)),min(bank_old(:,2)));
stop = min(max(bank_new(:,2)),max(bank_old(:,2)));
step = 0.02; %2-cm interval
i = 6;
j = 1;
for yi = start:step:stop
    %Interpolate to find values of x
    bank_ret(j,2*i) = yi;
    x_old = linterp(bank_old(:,2),bank_old(:,1),yi); %Interpolate old value
    x_new = linterp(bank_new(:,2),bank_new(:,1),yi); %Interpolate new value
    bank_ret(j,2*i-1) = x_old - x_new;
    j = j + 1;
end

bank_ret(:,2*i) = zero2nan(bank_ret(:,2*i));
bank_ret(:,2*i-1) = zero2nan(bank_ret(:,2*i-1));

retreat(i,1) = median(igNan(bank_ret(:,2*i-1)));
ret_area(i,1) = sum(igNan(bank_ret(:,2*i-1)) * step);

retreat = retreat';
ret_area = ret_area';
bank_ret = zero2nan(bank_ret);
end
```

%Projects the raw TLS data into two planes parallel to the streamflow.

```
function [s1 s2] = gridNorm_two(points,breaks)
    %points = TLS data
    %breaks = divides the TLS into two projections, breaks(1,:) = y data, breaks(2,:) = x data

    %Set up tangents
    for i = 1:2
        ct(i,1:2) = [breaks(i:i+1,1) ones(2,1)] \ [breaks(i:i+1,2)];
    end

    %Set up normals
```

```
    for i = 1:2
        cn(i,1) = -1 / ct(i,1);
        cn(i,2) = breaks(i,2) - cn(i,1) * breaks(i,1);

        cnb(i,1) = cn(i,1);
        cnb(i,2) = breaks(i+1,2) - cn(i,1) * breaks(i+1,1);
    end

    %Set up dividers
    for i = 1:1
        cd(i,1) = -1 / tan((atan(-1/ct(i,1)) + atan(-1/ct(i+1,1))) / 2);
        cd(i,2) = breaks(i+1,2) - cd(i,1) * breaks(i+1,1);
    end

    n = length(points);
    s1 = [];
    s2 = [];

    for i = 1:n
        if (points(i,1) > cd(1,1)*points(i,2)+cd(1,2)) %Point in section 1
            %Create new x value based on dist from new ref tan line
            %Calculate shortest distance between point and tan line
            xn = point_to_line([points(i,2),points(i,1)],breaks(1,:),breaks(2,:));
            %Create new y value as projection to tan line
            %m = cn(1,1); %b = xg(i,j)-m*yg(i,j);
            ynxn = [-1*ct(1,1) 1; -1*cn(1,1) 1] \ [ct(1,2);points(i,1)-cn(1,1)*points(i,2)];
            yn = ynxn(1);
            %Correct x value if behind reference line
            if (points(i,1) < ynxn(2))
                xn = -xn;
            end
            %Use same z value
            zn = points(i,3);
            %Create new x-y-z grid for this section
            s = size(s1);
            s1(s(1)+1,:) = [xn,yn,zn];
        else %Point in section 2
            xn = point_to_line([points(i,2),points(i,1)],breaks(2,:),breaks(3,:));
            ynxn = [-1*ct(2,1) 1; -1*cn(2,1) 1] \ [ct(2,2);points(i,1)-cn(2,1)*points(i,2)];
            yn = ynxn(1);
            if (points(i,1) < ynxn(2))
                xn = -xn;
            end
            zn = points(i,3);
            s = size(s2);
            s2(s(1)+1,:) = [xn,yn,zn];
        end
    end

end

%Code from Mathworks website 02/03/09
function d = point_to_line(pt, v1, v2)
    a = [v1 - v2, 0];
    b = [pt - v2, 0];
    d = norm(cross(a,b)) / norm(a);
```

```
end

%Converts the projected TLS data to a 2 cm grid, using the minimum point in each grid.
function [xg] = gridBank_min(data,delta,y,z)
   z_delta = 0.02;
   X = data(:,1);
   Y = data(:,2);
   Z = data(:,3);
   %Calculate min x for delta-cm grid, filter out vegetation
   for i = 1:length(y)
      for j = 1:length(z)
         temp = min(X((y(i) - delta/2 < Y) & (y(i) + delta/2 > Y) & (z(j) - z_delta/2 < Z) & (z(j) + z_delta/2 > Z)));
         if (isempty(temp))
            xg(j,i) = nan;
         else
            xg(j,i) = min(X((y(i) - delta/2 < Y) & (y(i) + delta/2 > Y) & (z(j) - z_delta/2 < Z) & (z(j) + z_delta/2 >
Z)));
         end
      end
   end
end

%Fill in the small data gaps within the TLS DEM using the average value of surrounding cells.
function grid = gridFillin(grid)
   n = size(grid);
   %Fill in holes using the average
   for i = 1:n(1)
      for j = 1:n(2)
         if (isnan(grid(i,j)) && (i~=1) && (j~=1) && (i~=n(1)) && (j~=n(2)))
            b = [grid(i-1,j-1) grid(i-1,j) grid(i-1,j+1) grid(i,j-1) grid(i,j+1) grid(i+1,j-1) grid(i+1,j) grid(i+1,j+1)];
            if (sum(isnan(b)) < 4)
               grid(i,j) = mean(ignan(b));
            else
               %Do nothing, likely a boundary
            end
         else
            %Do nothing, use old value
         end
      end
   end
end
```

B.2 Habitat Complexity

%Main code for converting TLS data to a DEM and performing rock delineation.

```
%Load raw TLS data and convert to 2-cm DEM with min elevation for each point
ins = load('instream.csv');
delta = 0.02;
for i = 160710:length(ins)
insg(round((ins(i,1) - min(ins(:,1))) / delta + 1),round((ins(i,2) - min(ins(:,2))) / delta + 1)) = ins(i,3);
end

%Convert to binary grid, fill in small data gaps with average value of surrounding cells
insg_bw = not(isnan(insg));
insg_fill = falsePosNeg(insg_bw,1);
insg_1 = bwmorph(insg_fill,'clean',Inf);
insg_1 = bwmorph(insg_1,'fill',Inf);
insg_1 = bwmorph(insg_1,'hbreak',Inf);
insg_1 = bwmorph(insg_1,'spur',Inf);
insg_1 = bwareaopen(insg_1, 26, 4);
[bt,tt1,nt] = bwboundaries(insg_1,4);
tt2 = bwareaopen(tt1>nt, 26, 4);
insg_2 = insg_1 + (tt1>insg_1) - tt2;
insg_2 = imopen(insg_2,strel('disk',3));
insg_2 = bwareaopen(insg_2, 26);
[insg_f] = fillIn(insg,insg_2);
insg_m = insg_f;
temp = isnan(insg_f);
insg_m(temp) = 0;
insg_m = insg_m .* insg_2; %Final TLS 2-cm DEM

%Define the boundary between rock surface and water surface
insg_temp = insg_m;
temp = (insg_m == 0);
insg_temp(temp) = Inf;
insg_rwb = bwmorph(insg_temp==Inf,'remove'); %Grid of rock/water boundary

%Smooth surface with average filter
meanfilt = fspecial('average',[5 5]);
insg_mean = imfilter(insg_m,meanfilt);

%Use local minima filter to define boundary between individual rocks
insg_min = findMin(insg_mean,3);
insg_mer = (insg_min>0 | insg_rwb);
insg_val = closeGaps(insg_mer);
insg_dead = deadEnds(insg_val);
insg_val_1 = not(insg_dead);
insg_val_1(insg_temp == Inf) = 0;
insg_val_1 = bwareaopen(insg_val_1, 26);
insg_val_1 = imopen(insg_val_1,strel('disk',2));
insg_val_1 = imfill(insg_val_1,8,'holes');
insg_val_2 = insg_val_1;
insg_val_2(insg_temp == Inf) = 0;

%Use smoothed DEM and boundary layer to delineate rocks
[insg_stream_m3 insg_size_m3] = getRocks(insg_mean,insg_val_2);
```

```
%Remove small data gaps in the TLS DEM, uses sub-function "filt."
function [hug_fill] = falsePosNeg(hug,n)
   %Different ways tested to clean up binary image
   %hug = Binary grid of the original TLS DEM
   if (n == 1)
      fun = @filt;
   elseif (n == 2)
      fun = @thresh;
   elseif (n ==3)
      fun = @fillrocks;
   end
   hug_fill = blkproc(hug,[1 1],[2 2],fun);
end

function y = filt(x)
   %So far only method used
   y = x;
   if (sum(sum(x)) > 18)
      y(3,3) = 1;
   elseif (sum(sum(x)) < 7)
      y(3,3) = 0;
   else
      %Keep old value
   end
end

%Fill in small surface data gaps in the DEM with mean filter.
function [hug_fill] = fillIn(hug,huf)
   %Fill in data holes with mean value of surrounding cells
   %Loop until all holes are filled
   %NaN = No Data
   %hug = Original DEM with holes
   %huf = On/Off binary grid of final stream DEM
   hug_fill = hug;
   tofill = huf - not(isnan(hug));
   [n m] = size(tofill);
   total = sum(sum(tofill==1));
   fillvec = cell(1,total);
   c = 1;
   for i = 1:n
      for j = 1:m
         if (tofill(i,j) == 1)
            fillvec{c} = [i,j];
            c = c + 1;
         end
      end
   end
   x = 1;
   old = length(fillvec);
   while (not(isempty(fillvec)))
      k = 1;
      c = 1;
      while c <= length(fillvec)
         i = fillvec{k}(1);
         j = fillvec{k}(2);
         if ((i ~= 1) && (i ~= n) && (j ~= 1) && (j ~= m))
```

```
            mask = [hug_fill(i-1,j-1);hug_fill(i-1,j);hug_fill(i-1,j+1);hug_fill(i,j-1);hug_fill(i,j+1);hug_fill(i+1,j-
1);hug_fill(i+1,j);hug_fill(i+1,j+1)];
         else
            mask = 0;
         end
         if (sum(isnan(mask)) < x)
            mask(isnan(mask)) = [];
         end
         hug_fill(i,j) = mean(mask);
         if (not(isnan(hug_fill(i,j))))
            fillvec(k) = [];
         else
            k = k + 1;
         end
         c = c + 1;
      end
      if (length(fillvec) == old)
         x = x + 1;
      end
      old = length(fillvec);
   end
end

%Performs local minima filter to identify boundary pixels between rocks, uses the sub-function "localMin."
function [hug_min] = findMin(hug,f)
   %hug = Mean filtered DEM with NoData = 0
   %f = Size of min filter: 1, 2, 3, or 4
   fun = @localMin;
   temp = (hug == 0);
   hug(temp) = Inf;
   hug_min = blkproc(hug,[1 1],[f f],fun);
   hug_min(temp) = NaN;
end

function freq = localMin(x)
   %Based on (Culvenor, 2002)
   freq = 0;

   %Get size of matrix: n = 3, 5, 7 or 9
   n = size(x,1);

   if (n == 3)
      mask = [Inf 1 Inf;Inf 1 Inf;Inf 1 Inf];
   elseif (n == 5)
      mask = [Inf Inf 1 Inf Inf;Inf Inf 1 Inf Inf;Inf Inf 1 Inf Inf;Inf Inf 1 Inf Inf;Inf Inf 1 Inf Inf];
   elseif (n == 7)
      mask = [Inf Inf Inf 1 Inf Inf Inf;Inf Inf Inf 1 Inf Inf Inf;Inf Inf Inf 1 Inf Inf Inf;Inf Inf Inf 1 Inf Inf Inf;Inf Inf Inf
1 Inf Inf Inf;Inf Inf Inf 1 Inf Inf Inf;Inf Inf Inf 1 Inf Inf Inf];
   elseif (n == 9)
      mask = [Inf Inf Inf Inf 1 Inf Inf Inf Inf;Inf Inf Inf Inf 1 Inf Inf Inf Inf;Inf Inf Inf Inf 1 Inf Inf Inf Inf;Inf Inf Inf
Inf 1 Inf Inf Inf Inf;Inf Inf Inf Inf 1 Inf Inf Inf Inf;Inf Inf Inf Inf 1 Inf Inf Inf Inf;Inf Inf Inf Inf 1 Inf Inf Inf Inf;Inf Inf
Inf Inf 1 Inf Inf Inf Inf;Inf Inf Inf Inf 1 Inf Inf Inf Inf];
   end
   filt = x .* mask;
   if (x((n+1)/2,(n+1)/2) == min(min(filt)))
      freq = freq + 1;
```

```
    end

    if (n == 3)
        mask = [Inf Inf Inf;1 1 1;Inf Inf Inf];
    elseif (n == 5)
        mask = [Inf Inf Inf Inf Inf;Inf Inf Inf Inf Inf;1 1 1 1 1;Inf Inf Inf Inf Inf;Inf Inf Inf Inf Inf];
    elseif (n == 7)
        mask = [Inf Inf Inf Inf Inf Inf Inf;Inf Inf Inf Inf Inf Inf Inf;Inf Inf Inf Inf Inf Inf Inf;1 1 1 1 1 1 1;Inf Inf Inf Inf
Inf Inf Inf;Inf Inf Inf Inf Inf Inf Inf;Inf Inf Inf Inf Inf Inf Inf];
    elseif (n == 9)
        mask = [Inf Inf Inf Inf Inf Inf Inf Inf Inf;Inf Inf Inf Inf Inf Inf Inf Inf Inf;Inf Inf Inf Inf Inf Inf Inf Inf Inf;Inf Inf
Inf Inf Inf Inf Inf Inf Inf;1 1 1 1 1 1 1 1 1;Inf Inf Inf Inf Inf Inf Inf Inf Inf;Inf Inf Inf Inf Inf Inf Inf Inf Inf;Inf Inf Inf
Inf Inf Inf Inf Inf Inf;Inf Inf Inf Inf Inf Inf Inf Inf Inf];
    end
    filt = x .* mask;
    if (x((n+1)/2,(n+1)/2) == min(min(filt)))
        freq = freq + 1;
    end

    if (n == 3)
        mask = [1 Inf Inf;Inf 1 Inf;Inf Inf 1];
    elseif (n == 5)
        mask = [1 Inf Inf Inf Inf;Inf 1 Inf Inf Inf;Inf Inf 1 Inf Inf;Inf Inf Inf 1 Inf;Inf Inf Inf Inf 1];
    elseif (n == 7)
        mask = [1 Inf Inf Inf Inf Inf Inf;Inf 1 Inf Inf Inf Inf Inf;Inf Inf 1 Inf Inf Inf Inf;Inf Inf Inf 1 Inf Inf Inf;Inf Inf Inf
Inf 1 Inf Inf;Inf Inf Inf Inf Inf 1 Inf;Inf Inf Inf Inf Inf Inf 1];
    elseif (n == 9)
        mask = [1 Inf Inf Inf Inf Inf Inf Inf Inf;Inf 1 Inf Inf Inf Inf Inf Inf Inf;Inf Inf 1 Inf Inf Inf Inf Inf Inf;Inf Inf Inf 1
Inf Inf Inf Inf Inf;Inf Inf Inf Inf 1 Inf Inf Inf Inf;Inf Inf Inf Inf Inf 1 Inf Inf Inf;Inf Inf Inf Inf Inf Inf 1 Inf Inf;Inf Inf
Inf Inf Inf Inf Inf 1 Inf;Inf Inf Inf Inf Inf Inf Inf Inf 1];
    end
    filt = x .* mask;
    if (x((n+1)/2,(n+1)/2) == min(min(filt)))
        freq = freq + 1;
    end

    if (n == 3)
        mask = [Inf Inf 1;Inf 1 Inf;1 Inf Inf];
    elseif (n == 5)
        mask = [Inf Inf Inf Inf 1;Inf Inf Inf 1 Inf;Inf Inf 1 Inf Inf;Inf 1 Inf Inf Inf;1 Inf Inf Inf Inf];
    elseif (n == 7)
        mask = [Inf Inf Inf Inf Inf Inf 1;Inf Inf Inf Inf Inf 1 Inf;Inf Inf Inf Inf 1 Inf Inf;Inf Inf Inf 1 Inf Inf Inf;Inf Inf 1
Inf Inf Inf Inf;Inf 1 Inf Inf Inf Inf Inf;1 Inf Inf Inf Inf Inf Inf];
    elseif (n == 9)
        mask = [Inf Inf Inf Inf Inf Inf Inf Inf 1;Inf Inf Inf Inf Inf Inf Inf 1 Inf;Inf Inf Inf Inf Inf Inf 1 Inf Inf;Inf Inf Inf
Inf Inf Inf 1 Inf Inf Inf;Inf Inf Inf Inf 1 Inf Inf Inf Inf;Inf Inf Inf 1 Inf Inf Inf Inf Inf;Inf Inf 1 Inf Inf Inf Inf Inf Inf;Inf 1
Inf Inf Inf Inf Inf Inf Inf;1 Inf Inf Inf Inf Inf Inf Inf Inf];
    end
    filt = x .* mask;
    if (x((n+1)/2,(n+1)/2) == min(min(filt)))
        freq = freq + 1;
    end
end
```

```
%Close small gaps in the boundary layer raster to make a continuous boundary between rocks.
function [hug_close] = closeGaps(hug)
   %Based on (Culvenor, 2002)
   %hug = rock boundary layer grid

   %Remove gaps
   fun = @ifGap;
   hug_close = blkproc(hug,[1 1],[1 1],fun);

   %Remove small, isolated objects and clean up network
   hug_close = bwareaopen(hug_close, 26, 8);
   hug_close = bwmorph(hug_close,'fill',Inf);
   hug_close = bwmorph(hug_close,'skel',Inf);
end

function y = ifGap(x)
   y = x;
   if (x(2,2) == 0)
      mask = [1 1 1;1 0 1;1 1 1];
      filt = x .* mask;
      m = sum(sum(filt));
      if (m > 1)
         [b,l,n] = bwboundaries(filt,4,'noholes');
         if (n > 1)
            y(2,2) = 1;
         end
      end
   end
end

%Removes parts of the boundary layer that do not create a closed boundary (aka dead ends).
function [hug_dead] = deadEnds(hug)
   %Based on (Culvenor, 2002)
   %Remove dead ends
   %hug = rock boundary layer grid

   repeat = 1;
   while (repeat == 1)
      hug_ends = bwmorph(hug,'endpoints');
      hug_maj = bwmorph(hug,'majority');
      hug_dead = hug - (hug_ends & hug & hug_maj == 0);
      if (sum(sum(hug ~= hug_dead)) == 0)
         repeat = 0;
      end
      hug = hug_dead;
   end
end

%Main rock delineation algorithm, outputs raster with each rock IDed and list of rocks with locations and sizes.
function [stream area] = getRocks(hug_dem,hug_roc)
   %Select rocks from each object area, starting with largest ones
   %hug_dem = DEM, with No Data = 0
   %hug_roc = Binary Grid of rock areas, with Rocks = 1, Water = 0

   stream = zeros(size(hug_dem));
```

```
    c = 1;
    for j = 15:-1:3 %Modify minimum threshold? - 3 looks good, 0.1 m dia
        %Find location of rock tops
        tophat = imtophat(hug_dem .* hug_roc,strel('disk',j));
        thresh = (tophat<1 & tophat>0);
        open = imopen(thresh,strel('disk',j-1));
        open_b = bwboundaries(open);
        open_max = zeros(length(open_b),3);
        for i = 1:length(open_b)
            r = bwselect(open,open_b{i}(:,2),open_b{i}(:,1));
            r = hug_dem .* r;
            open_max(i,3) = max(max(r));
            if (open_max(i,3) > 0)
                [open_max(i,1),open_max(i,2)] = find(r == open_max(i,3));
            else
                open_max(i,:) = [];
            end
        end

        %Smooth rock boundary - Modify method?
        hug_open = imopen(hug_dem .* hug_roc,strel('disk',j)); %Modify?
        hug_open = (hug_open > 0);
        rock_start = c;

        %ID each rock and calculate arae
        for i = 1:size(open_max,1)
            rock_temp = bwselect(hug_open,open_max(i,2),open_max(i,1),4);
            area_temp = sum(sum(rock_temp));
            %Check for multiple rocks in same area - Deal with separately?
            dup = 0;
            for k = rock_start:c-1
                if (sum(sum(rock_temp ~= rock{k,1})) == 0)
                    dup = 1;
                end
            end
            if (area_temp > 0 && dup == 0)
                rock{c,1} = rock_temp;
                area(c,1) = open_max(i,1);
                area(c,2) = open_max(i,2);
                area(c,3) = open_max(i,3);
                area(c,4) = area_temp;
                c = c + 1;
            end
        end
        rock_stop = c - 1;

        %Merge all rocks into grid
        for i = rock_start:rock_stop
            stream = stream + rock{i,1} * i;
            hug_roc = hug_roc - rock{i,1};
        end

        %Remove rocks from binary grid and repeat with smaller filter size
        fprintf('Filter Size = %d, Num Rocks = %d. ',j,size(open_max,1));
    end
end
```

```
%Finds the delineated TLS rocks that are closest to the measured total station rocks.
function [out] = rockFind(ts_roc,tls_roc)
   %ts_roc = x y coordinates of validation rocks
   %tls_roc = x y coordinates of delineated tls rocks
   %Based on distance between center of mass

   out = zeros(length(ts_roc),6);
   for i = 1:length(ts_roc)
      min_dist = Inf;
      index = -1;
      for j = 1:length(tls_roc)
         x1 = ts_roc(i,6);
         x2 = tls_roc(j,5);
         y1 = ts_roc(i,7);
         y2 = tls_roc(j,6);
         curr_dist = sqrt((x1-x2)^2 + (y1-y2)^2);
         if (curr_dist < min_dist)
            min_dist = curr_dist;
            index = j;
         end
      end
      out(i,:) = [tls_roc(index,5:6) tls_roc(index,3) tls_roc(index,7:8) index];
   end
end

%Calculates the volume for each delineated rock in the TLS dataset
function vols = rockVols(dem,rocks,delta)
   %dem = Final TLS DEM before mean smoothing filter
   %rock = list of rocks
   %delta = grid size

   n = max(max(rocks));
   vols = zeros(n,1);
   for i = 1:n
      roc_curr = (rocks == i);
      roc_dem = dem .* roc_curr;
      temp = (roc_dem == 0);
      roc_dem(temp) = 9999;
      roc_min = min(min(roc_dem));
      roc_vol = sum(sum((roc_dem - roc_min) .* not(temp))) * delta^2;
      vols(i,1) = roc_vol;
   end
end

%Performs the cross-sectional analysis (area and heterogeneity) for both TLS and total station data
function [area_ts area_tls het_ts het_tls] = tlsXsec(xsecs,n)
   %Coverts cross section data for xsec n to a discrete grid
   %Calculates for both TLS and total station
   %Then calculates heterogeneity and area under water surface

   %Grabs cross section n
   xs = xsecs(xsecs(:,1) == n,:);
   xs(xs(:,4) == -10000,4) = NaN;
```

```
    %Calcualtes minimum lat and long
    m1 = min(xs(:,2));
    m2 = min(xs(:,3));

    %Calculates distance of each point along cross section
    xs(:,6) = sqrt((xs(:,2)-m1).^2 + (xs(:,3)-m2).^2);
    xs = sortrows(xs,6);
    xst = xs(not(isnan(xs(:,4))),:);

    %Convert data to discrete grid
    delta = 0.02;
    xsd = zeros(round(max(xs(:,6))/delta)+1,3);
    for i = 1:length(xsd)
        xsd(i,1) = (i-1)*delta;
        xsd(i,2) = interp1(xst(:,6),xst(:,4),xsd(i,1)); %TLS data
        xsd(i,3) = interp1(xs(:,6),xs(:,5),xsd(i,1)); %TS data
    end
    xsd(isnan(xsd(:,2)),:) = [];

    %Calculate "area" of water under max total station elevation
    max_ws = min(xsd(:,3)) + 2; %Min depth plus 2 meter of water
    area_ts = (max_ws - xsd(:,3));
    area_ts = sum(area_ts(area_ts > 0)) * delta;
    area_tls = (max_ws - xsd(:,2));
    area_tls = sum(area_tls(area_tls > 0)) * delta;
    area = (area_ts - area_tls) / area_tls * 100;

    %Calculate the "roughness" or heterogeneity based on the std of window
    w = 25; %51 cell or 1 m moving window
    std_ts = zeros(length(xsd)-2*w,1);
    std_tls = zeros(length(xsd)-2*w,1);
    for i = 1:length(xsd)-2*w
        std_ts(i,1) = std(xsd(i:i+2*w,3));
        std_tls(i,1) = std(xsd(i:i+2*w,2));
    end
    het_ts = mean(std_ts);
    het_tls = mean(std_tls);
    het = (mean(std_ts) - mean(std_tls)) / mean(std_tls) * 100;

    %Plot figures to verify
    %figure, plot(xs(:,6),xs(:,5),xs(not(isnan(xs(:,4))),6),xs(not(isnan(xs(:,4))),4)), axis equal
    %figure, plot([min(xsd(:,1)),max(xsd(:,1))],[min(xsd(:,3)) + 2,min(xsd(:,3)) +
2],xsd(:,1),xsd(:,3),xsd(:,1),xsd(:,2)), axis equal
end
```

B.3 Stream Restoration Uncertainty

```
%Runs simulations for the first channel stage
function out = lhs_two()
   %Performs monte carlo simulation on stream restoration design
   %Input ranges of Q, Bankfull Discharge
   Qmin = 1.8;
   Qmax = 15.6;
   Qmode = 5.6;

   %Number of MCS simulations
   its = 100;
   sims = 1000;

   out = cell(sims,its);
   %Pull out input parameters based on LHS
   Q1 = trilhs(Qmin,Qmax,Qmode,its);
   %Two-phase uncertainty analysis for n iterations
   for j = 1:its
      D = normrnd(2.5,0.52,[100 1]);
      D = exp(D);
      D84 = quantile(D,0.84) / 1000;
      %Simulate m times
      n = lhsnorm(0.023,0.00025^2,sims);
      Tcs = trilhs(0.03,0.06,0.045,sims);
      %Run model
      for i = 1:sims
         out{i,j} = mannings(Q1(j),n(i),Tcs(i),D84);
      end
   end
end
```

```
%Solves the first channel stage design dimensions using the input parameters
function out = mannings(Q,n,Tcs,D84)
   %Solve for simple stream restoration design
   %Mannings Equation and Shield's Entrainment Function
   %Assume trapezoidal channel with width and depth

   %Input ranges of Q, w, and d from Regional Curves
   %Qmin = 1.8; %Bankfull Discharge
   %Qmax = 15.6;
   wmin = 4.57; %Stream width
   wmax = 15.24;
   dmin = 0.366; %Stream depth
   dmax = 0.762;

   %Use average Q for channel forming discharge
   %Q = 5.1;
   %Initial value for w and d
   w = wmax;
   d = dmax;

   %Constant parameters, n and S
   %n = 0.03; %Manning's n
   S = 0.004454; %Longitudinal slope
```

```
    %Set up Manning's equation
    %fun = inline('Q - (1/n) * (d*w)^(5/3) * (2*d+w)^(-2/3) * S^(1/2)');
    fun = inline('Q - (1/n) * (d*w-3*d^2)^(5/3) * (w+(2*sqrt(10)-6)*d)^(-2/3) * S^(1/2)');

    %Compare Tmax to Tcrit, stopping when error is below tolerance
    error = Inf;
    while (abs(error) > 0.1)
        %Solve for d with Mannings
        d = fzero(@(d) fun(Q,S,d,n,w),d);

        %Calculate hydraulic radius
        %A = d*w;
        %P = 2*d+w;
        A = d*w-3*d^2;
        P = w+(2*sqrt(10)-6)*d;
        R = A / P;

        %Constant parameters, pw, ps, and g
        pw = 1000;
        ps = 2850;
        g = 9.8;

        %Constant parameters, D84 and Tcs
        %D84 = 21 / 1000; %84th Quantile of Particle Size Distribution
        %Tcs = 0.045; %Shield's number

        %Calculate max shear stress
        Tave = pw * g * R * S;
        %Tmax = pw * g * d * S;

        %Calculate critical shear stress
        Tcrit = (ps - pw) * g * D84 * Tcs;

        %Compare both to determine error, and iterate if needed
        error = Tave - Tcrit;
        if (error > 0.1)
            w = w + 0.05;
        elseif (error < 0.1)
            w = w - 0.05;
        end
    end
    out = [Q n Tcs D84 w d Tave];
end
```

%Runs simulations for the second channel stage

```
function out = lhs_two_dos()
    %Performs monte carlo simulation on stream restoration design
    %Input ranges of Q, Bankfull Discharge
    Qmin = 4.7;
    Qmax = 18.5;
    Qmode = 8.5;

    %Number of MCS simulations
    its = 100;
    sims = 1000;
```

```
    out = cell(sims,its);
    %Pull out input parameters based on LHS
    Q2 = trilhs(Qmin,Qmax,Qmode,its);
    %Two-phase uncertainty analysis for m iterations
    for j = 1:its
        D = normrnd(2.5,0.52,[100 1]);
        D = exp(D);
        D84 = quantile(D,0.84) / 1000;
        %Simulate n times
        n1 = lhsnorm(0.023,0.00025^2,sims);
        n2 = lhsdesign(sims,1)*(0.160 - 0.025) + 0.025;
        Tcs = trilhs(0.03,0.06,0.045,sims);
        %Run model
        for i = 1:sims
            out{i,j} = two_stage_dos(Q2(j),n1(i),n2(i),Tcs(i),D84);
        end
    end
end

%Solves the second channel stage design dimensions using the input parameters
function out = two_stage_dos(Q2,n1,n2,Tcs,D84)
    %Solve for second stage of restoration design
    %Mannings Equation and Shield's Entrainment Function
    %Assume trapezoidal channel with width and depth

    %Fixed values for w1 and d1
    w1 = 12.2900; %Median value of first stage
    d1 = 0.43; %Median value of second stage
    A1 = d1*w1-3*d1^2;
    P1 = w1+(2*sqrt(10)-6)*d1;
    %R1 = A1 / P1;
    %Fixed value for d2
    %h_fp = 1.17; %Height of floodplain
    %d2 = h_fp - d1; %Depth of bench

    %Initial guess for w2
    w2 = 15.24;
    d2 = 0.762;

    %Constant parameters, n and S
    %n = (((P1)*n1^2+(P2)*n2^2)/(P1+P2))^(1/2);
    %n = ((P1*n1^2+(2*w2+(2*sqrt(10))*d2)*n2^2)/(P1+2*w2+(2*sqrt(10))*d2))^(1/2);
    S = 0.004454; %Longitudinal slope

    %Set up Manning's equation
    fun2 = inline('Q2 - (1/(((P1*n1^2+(2*w2+(2*sqrt(10))*d2)*n2^2)/(P1+2*w2+(2*sqrt(10))*d2))^(1/2))) * (A1 +
d2*w1+2*d2*w2+3*d2^2)^(5/3) * (P1 + 2*w2+(2*sqrt(10))*d2)^(-2/3) * S^(1/2)');

    %Compare Tmax to Tcrit, stopping when error is below tolerance
    error = Inf;
    while (abs(error) > 0.1)
        %Solve for d2 with Mannings
        d2 = fzero(@(d2) fun2(A1,P1,Q2,S,d2,n1,n2,w1,w2),d2);

        %Calculate hydraulic radius
```

```
        A2 = A1 + d2*w1+2*d2*w2+3*d2^2;
        P2 = P1 + 2*w2+(2*sqrt(10))*d2;
        R2 = A2 / P2;
        n = (((P1)*n1^2+(P2)*n2^2)/(P1+P2))^(1/2);

        %Constant parameters, pw, ps, and g
        pw = 1000;
        ps = 2850;
        g = 9.8;

        %Constant parameters, D84 and Tcs
        %D84 = 21 / 1000; %84th Quantile of Particle Size Distribution
        %Tcs = 0.045; %Shield's number

        %Calculate max shear stress
        Tave2 = pw * g * R2 * S;

        %Calculate critical shear stress
        Tcrit = (ps - pw) * g * D84 * Tcs;

        %Compare both to determine error, and iterate if needed
        error = Tave2 - Tcrit;
        if (error > 0.1)
            w2 = w2 + 0.05;
        elseif (error < 0.1)
            w2 = w2 - 0.05;
        end
    end
    out = [Q2 n1 n2 n Tcs D84 w2 d2 Tave2 Tcrit];
end

%Outputs n random numbers from a triangular distribution using latin hypercube sampling
function r = trilhs(min,max,mode,n)
    t = lhsdesign(n,1);
    r = zeros(size(t));
    for i = 1:n
        if (t(i) <= (mode-min)/(max-min))
            r(i) = min + sqrt(t(i) * (max-min) * (mode-min));
        else
            r(i) = max - sqrt((1-t(i)) * (max-min) * (max-mode));
        end
    end
end
```

Appendix C - Stream Restoration Design Input Parameter Distributions

C.1 Channel Forming Discharge Channel (Stage 1)

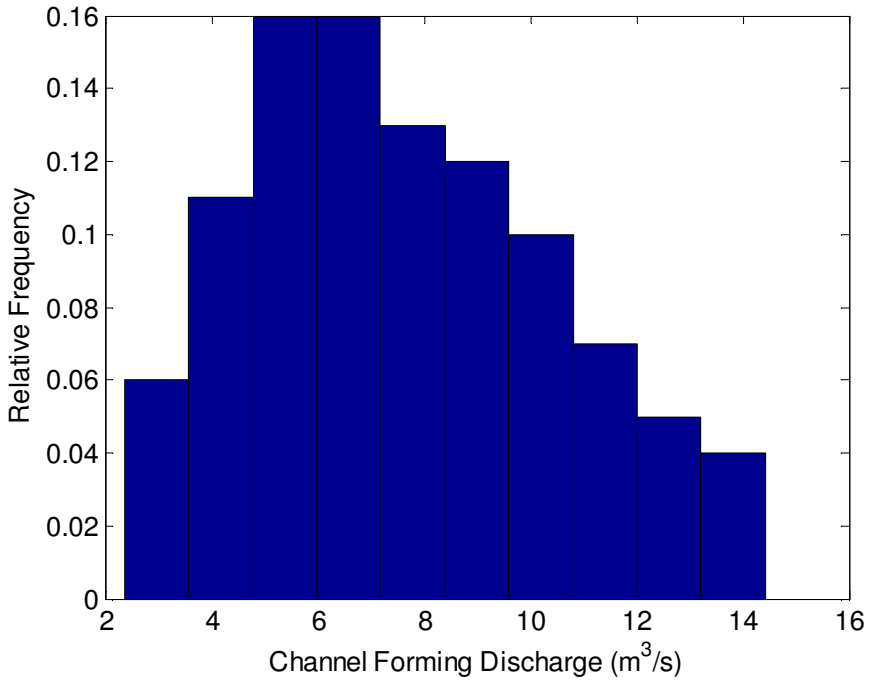

Figure C.1. Channel forming discharge distribution for the first stage.

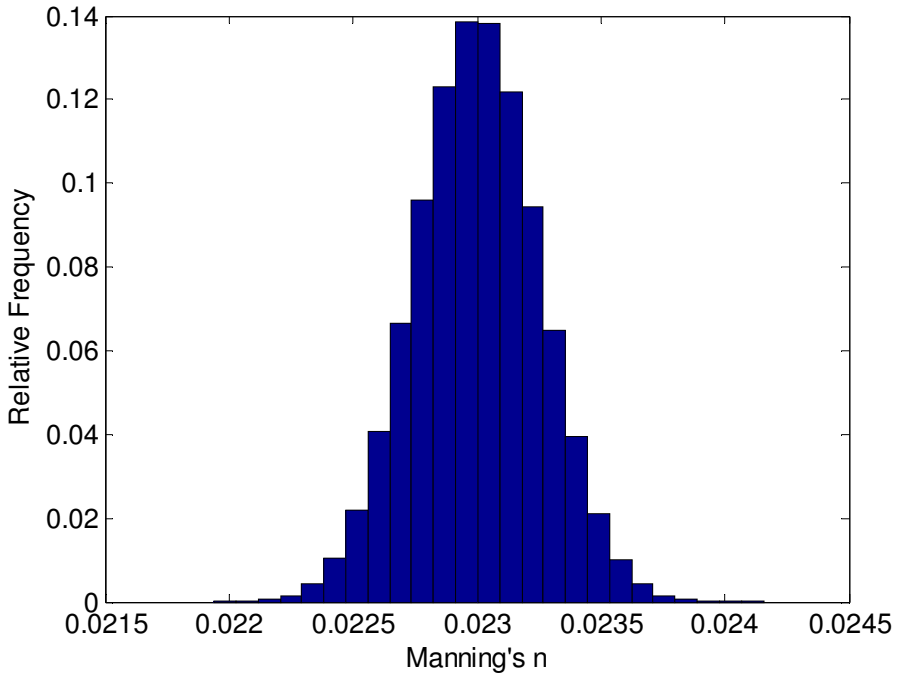

Figure C.2. Manning's roughness *n* distribution for the first stage.

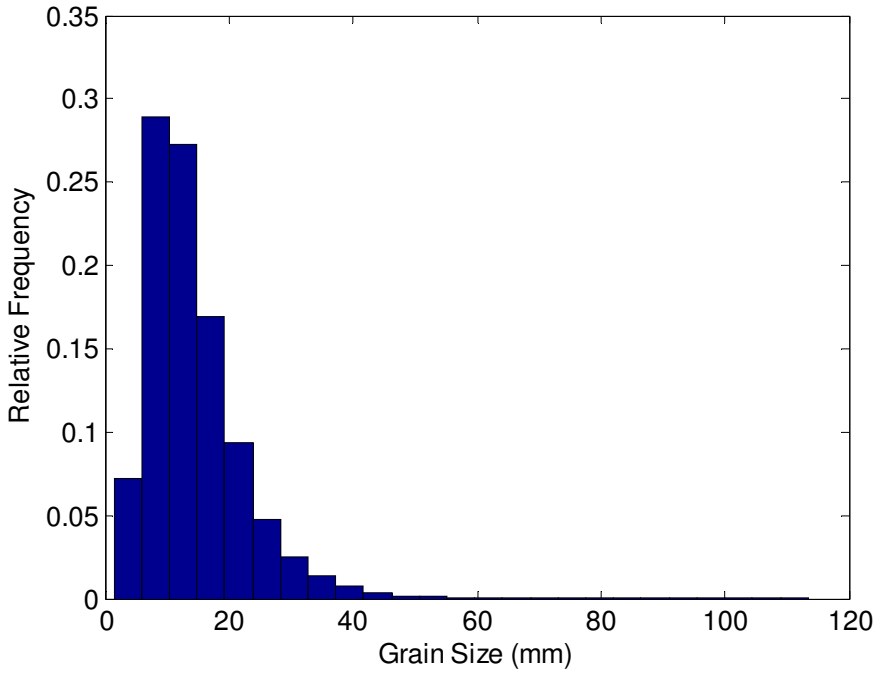

Figure C.3. Stream bed grain size distribution.

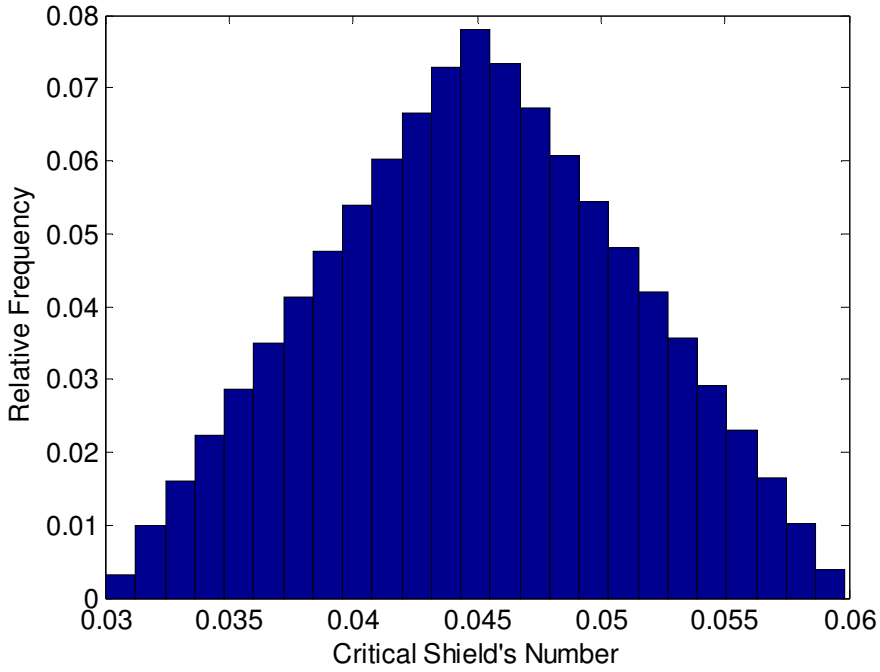

Figure C.4. Critical Shield's number or dimensionless shear stress number distribution.

C.2 Floodplain Discharge Channel (Stage 2)

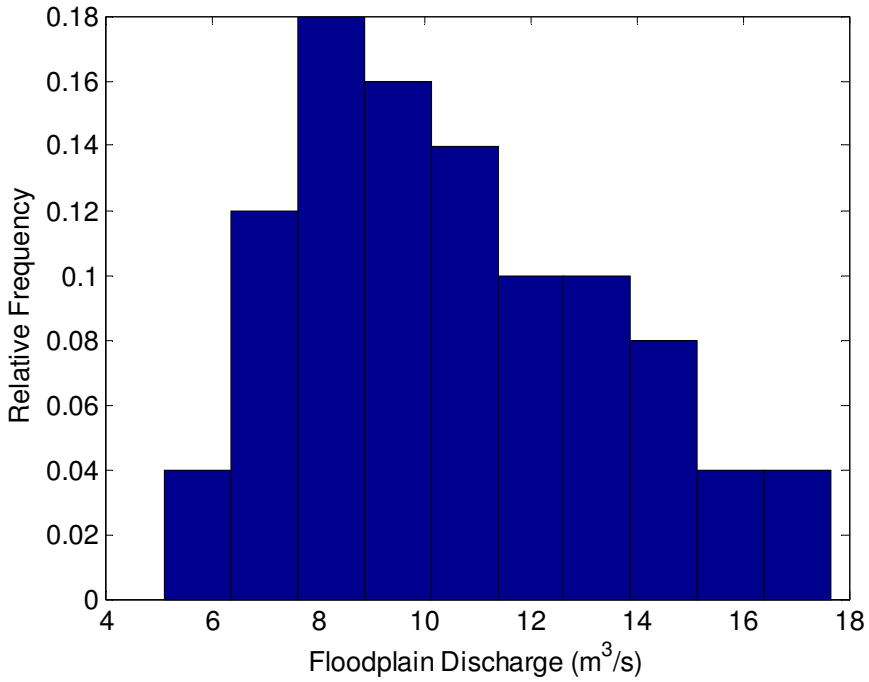

Figure C.5. Floodplain discharge distribution for the second stage.

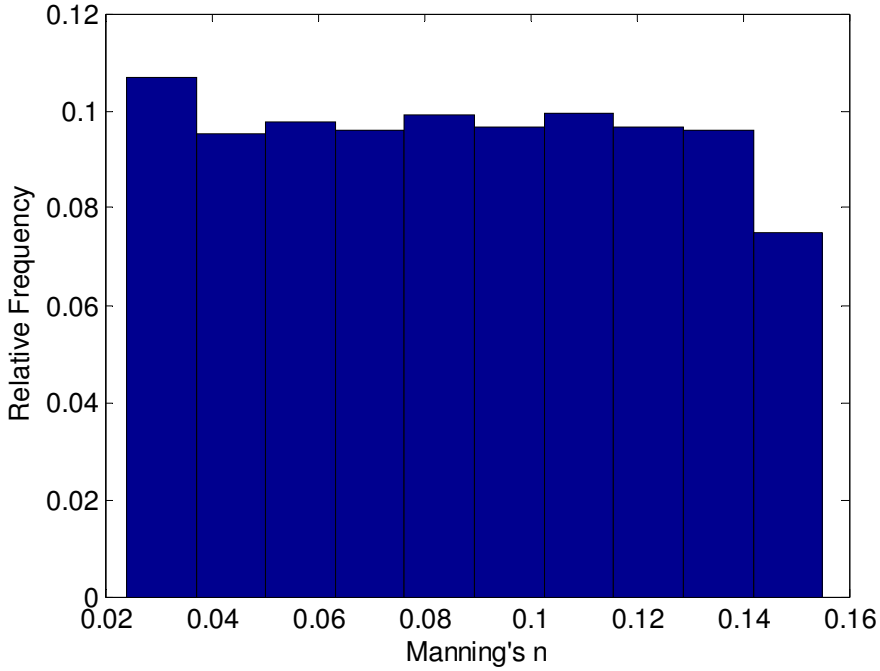

Figure C.6. Manning's roughness *n* distribution for the second stage.

Appendix D - Terrestrial Laser Scanning Streambank Retreat Measurements

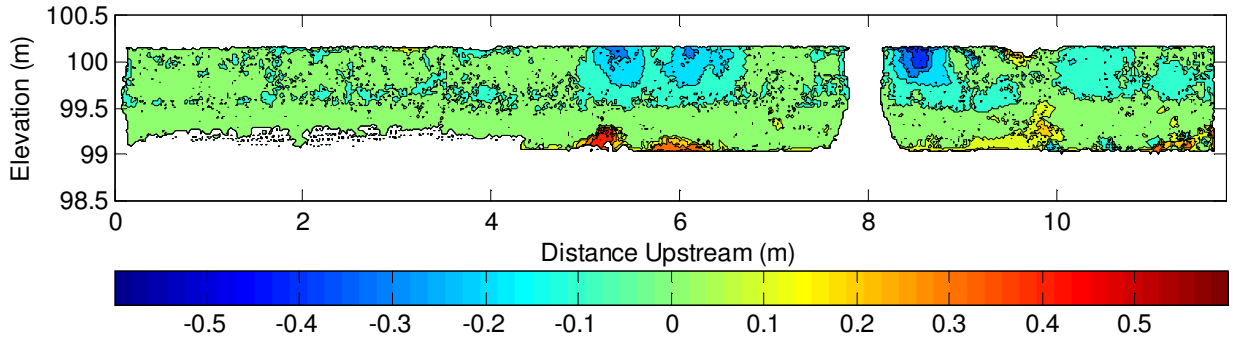

Figure D.1. Streambank retreat measured with TLS from May 2007 to August 2007.

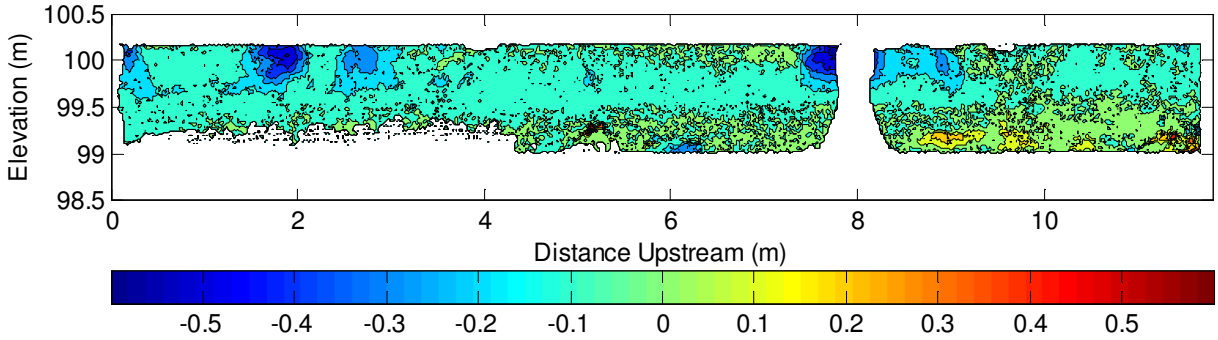

Figure D.2. Streambank retreat measured with TLS from August 2007 to December 2007.

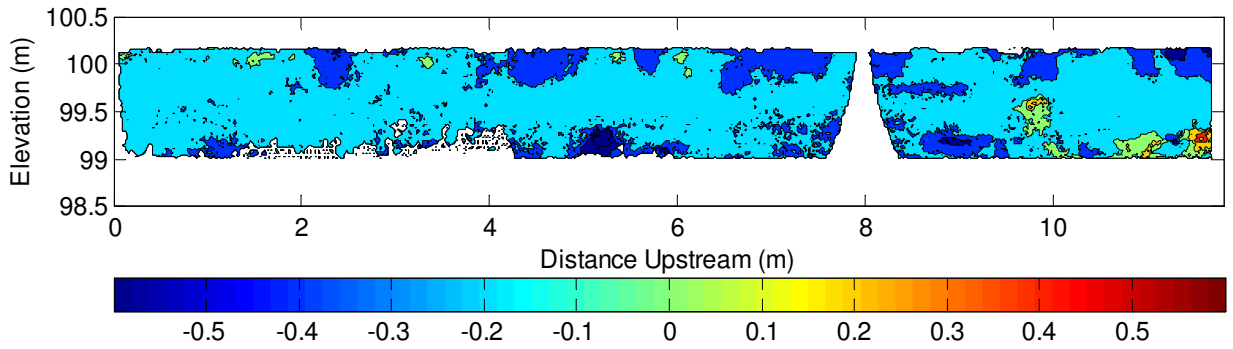

Figure D.3. Streambank retreat measured with TLS from December 2007 to May 2008.

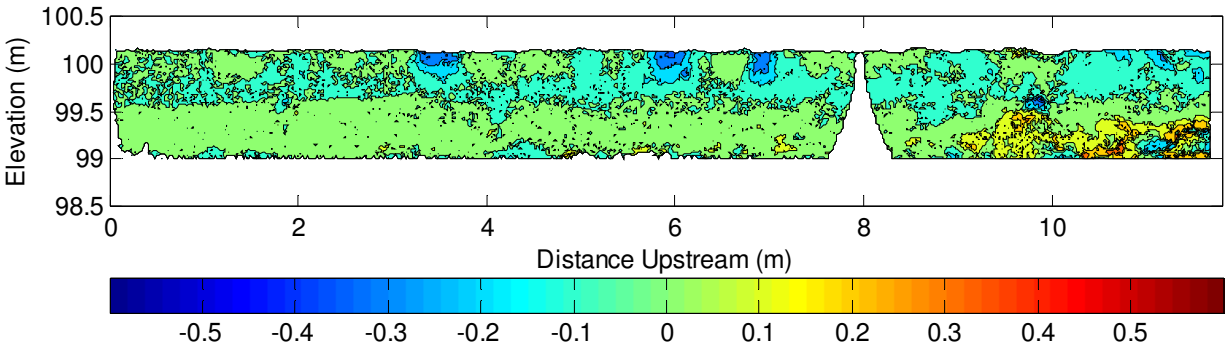

Figure D.4. Streambank retreat measured with TLS from May 2008 to December 2008.

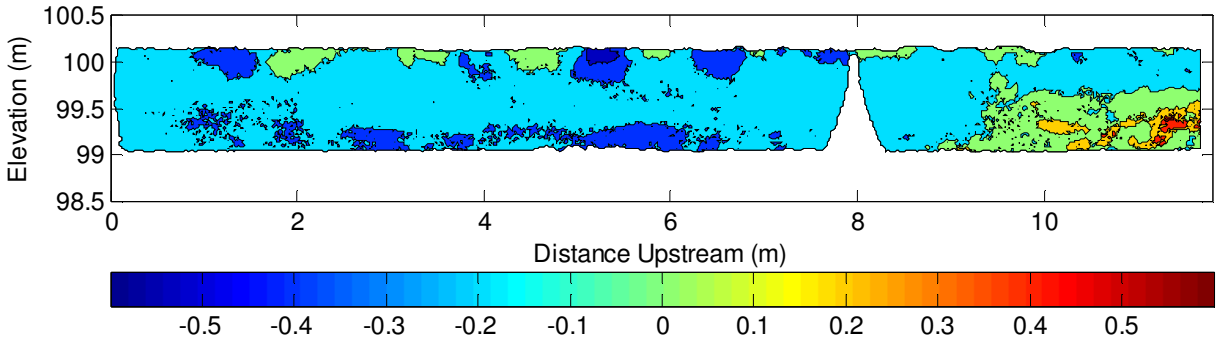

Figure D.5. Streambank retreat measured with TLS from December 2008 to May 2009.